Quantum Microstructure Lasers :

Fabrication Technologies and Device Physics

$$\left(\begin{array}{c} 量子マイクロ構造レーザ \\ －作製技術とデバイス物理－ \end{array} \right)$$

A Thesis Presented to

the Graduate School of the University of Tokyo

in Partial Fulfillment of the Requirements

for the Degree of Doctor of Philosophy

in Electronic Engineering

by

Takuji Takahashi

December 20, 1991

To My Wife

Preface

This thesis describes an essential part of the research work carried out at Research Center for Advanced Science and Technology (RCAST), and Institute of Industrial Science (IIS), University of Tokyo, while the author was working as a graduate student of the Department of Electrical Engineering, University of Tokyo, from 1987 to 1992.

For future applications of quantum microstructures such as quantum well, quantum well wire and quantum well box structures to opto-electronic devices, fabrication technologies of quantum microstructures and theoretical analysis of device physics are significantly required. At the present time, since only quantum well structures can be fabricated with high quality, the device applications are limited within the quantum well devices.

In this thesis, fabrication technologies and theoretical analysis of device physics of quantum microstructure lasers are studied for the purpose of fundamental understandings and future applications to opto-electronic devices.

December 1991   *Takuji Takahashi*

Acknowledgements

The author would like to take this opportunity to thank my dissertation supervisor, Professor Yasuhiko Arakawa, Research Center for Advanced Science and Technology, University of Tokyo, for his constant guidance and encouragement throughout my graduate studies at University of Tokyo. His valuable insights proved a great boon to my work, and being a member of his research group expanded my interests to many new areas of quantum electronics.

The author is grateful to Professor T. Ikoma, Institute of Industrial Science, University of Tokyo, and Professor H. Sakaki, Research Center for Advanced Science and Technology, University of Tokyo, for their suggestions and fruitful discussions. The author wishes to express my special thanks to Professor J. Hamasaki and Professor Y. Fujii, Institute of Industrial Science, University of Tokyo, for their constant guidance and encouragement.

The author is also grateful to Dr. J. N. Schulman, Hughes Research Laboratories, who was a visiting professor in Research Center for Advanced Science and Technology, for fruitful discussions and valuable collaborations.

The author wishes to thank Dr. K. Yoshihara, Dr. J. Fujiwara and Dr. D. Fujita of the National Research Institute for Metals for the measurements of the micro Auger electron spectroscopies.

Abstract

The author has established the understanding of the quantum microstructure lasers from the view points of both fabrication technologies and device physics. The author has addressed following two point as the main purpose.

1) Fundamental study about fabrication technologies for quantum microstructures.

2) Theoretical investigations of the lasing characteristics in quantum microstructure lasers.

With respect to 1), the author has experimentally demonstrated the successful fabrication of GaAs quasi-quantum wire and dot structures by two kinds of selective growth techniques with electron beam irradiation in the metalorganic chemical vapor deposition (MOCVD) system such as the direct growth by the electron beam irradiation and the *in situ* process using contamination resists formed by the electron beam irradiation and conventional MOCVD growth. With respect to 2), the author has theoretically investigated the orientation dependence of lasing properties in quantum well lasers using tight binding method, the lasing characteristics in quantum well wire and quantum well box lasers, and the nonlinear gain effects in quantum microstructure lasers with considering multi-dimensional quantum confinement effects.

Contents

Contents

Contents

Chapter I Introduction

1.1. Background of This Study

Recent progress in the electronics and optics fields has received great attention in order to apply to various kinds of electronics and optical devices. Since the first invention of the transistor by Schockly, the performance of the integral circuits (IC) have been improved with extremely high degree. Though Si substrates are commonly used for IC's, III/V compounds such as GaAs are also used for high speed circuits. By using two-dimensional (2D) electron gas at a hetero-interface of GaAs and AlGaAs, high electron mobility transistor (HEMT) [1] has been realized. Moreover, it is pointed out that performance of transistors can be more improved using one-dimensional (1D) electron gas in quantum well wire (QWW) structures because of reduction of some scattering effects [2].

In the optical fields, on the other hand, semiconductor lasers with III/V compounds have been widely studied and have already been applied to optical communications. At the initial stage, doublehetero (DH) structures are used for semiconductor lasers. Since Dingle *et al.* pointed out the ability of improvements in the optical devices by using of quantum well (QW) structures [3], the application of QW structures to semiconductor lasers [4], [5] has received considerable attention because of physical interest as well as its superior characteristics, such as low threshold current density [6], [7], low temperature dependence of threshold

1

current [8]-[10], lasing wavelength tunability, and excellent dynamic properties [11]-[13]. In addition, QWW and quantum well box (QWB) structures as well as QW structures are received great attention from both physical and technical view points, because it is expected that multi-dimensional quantum confinement effects will improve many lasing characteristics to high extent [12].

It becomes easy to fabricate QW structures by the recent progress of metalorganic chemical vapor deposition (MOCVD) [14]-[17] and molecular beam epitaxy (MBE) [18]-[22] techniques, while it is still difficult to fabricate QWW and QWB structures at present stage. Therefore, fabrication technologies for QWW and QWB structures are extensively studied by using fine pattern lithography techniques such as electron beam lithography or selective growth techniques in the MOCVD or MBE method. Among such fabrication technologies for the selective growth, for instance, light assisted selective growth technique is one of hopeful methods; Ultra violet (UV) lights [23]-[27], excimer lasers [28]-[35] and Ar ion lasers [36]-[52] are used for the light sources. Achievement of atomic layer epitaxy (ALE) growth has also been reported using laser beam irradiation [44]-[47]. However, it is the most serious problem that diameter of laser beam spot is much larger than the size which can realize the quantum confinement effects. As the same way, other methods for the selective growth have their own merits and demerits. Thus, it is the state of things that each technique has some

problems that should be solved before the application to actual technologies for fabrication of QWW and QWB structures. Therefore, an establishment of a new technology for the selective growth enough to realize the multi-dimensional quantum confinement effects is strongly required.

Concerning theoretical analysis of lasing properties in QW lasers, we can understand some properties qualitatively to a great extent by using various approximations. It becomes usual that theoretical results and experimental results agree with each other. However, there still exist many unknown factors in actual operations of QW lasers such as band nonparabolicity effect [53]-[56] and nonlinear gain effect [57], [58] on lasing properties. More precise analysis is needed in order to discuss them.

Regarding QWW and QWB lasers, it is very difficult to fabricate them with high quality [59]-[66]. Therefore, there are very few reports to succeed in examination of the theory and the experiments simultaneously at present stage [67], [68]. However, since knowing the achievable limits of quantum microstructure lasers is quite important, theoretical investigation of the lasing characteristics in QWW and QWB lasers is one of important subjects [69]-[73].

1. 2. Motivation and Objectives of This Study

Applications of QWW and QWB structures to opto-electronics devices will give us stronger impact than that the applications of QW structures gave: Transistors will operate faster, and semiconductor lasers will operate with lower injection current, wider modulation bandwidth and higher coherency.

Though fabrication of quantum microstructures such as QWW and QWB is almost impossible in present stage, it is a quite important subject to be solved in order to apply them to actual devices. Therefore, we have proposed and investigated an electron beam induced metalorganic chemical vapor deposition (EBI-MOCVD) method as one of selective growth technologies for fabrication of quantum microstructures. Since electron beam can be focused as narrow as < 100 Å, it is expected that we can successfully fabricate quantum microstructures by this method.

On the other hand, theoretical analysis of lasing properties in QW lasers is still important to understand actual behavior of fabricated QW lasers precisely and to design QW laser structures for improvements of the lasing properties. Since material parameters of semiconductors have asymmetries concerning substrate orientations, one possibility to improve the lasing characteristics is a choice of the substrate orientation on which the QW structure is grown. Therefore, we have investigated the lasing properties in two kinds of QW lasers grown on different substrate orientation by using tight binding method. In addition, nonlinear gain effects such as gain saturation are also very

important characteristics to operate semiconductor lasers, because nonlinear gain effects increase threshold current and reduce both modulation dynamics and spectral coherency. Therefore, the nonlinear gain effects due to spectral hole burning have been investigated theoretically, indicating that the quantum confinement affects the nonlinear gain properties.

Taking account of possibility to realize QWW and QWB structures in near future, it is needed to analyze the lasing properties such as gain property, modulation dynamics and spectral properties in QWW and QWB lasers theoretically in order to clarify how extent we can expect to improve the lasing properties by using QWW and QWB laser structures. In addition, the conditions which is required to fabrication technologies in order to realize the QWW and QWB structures with high quality should be clarified. Therefore, the lasing properties in QWW and QWB lasers have been investigated theoretically, indicating improvements of the lasing properties by the multi-dimensional quantum confinement effects and the importance to fabricate uniform QWW or QWB structures.

1. 3. Synopses of This Thesis

In this thesis, fabrication technologies and device physics of quantum microstructure lasers are investigated in order to realize quantum microstructure lasers and understand lasing properties of those lasers. This thesis is organized as follows.

Chapter I is the introduction. The back ground of this study is mentioned.

In Part I, the successful fabrication of GaAs wire structures by an electron beam induced selective growth technique in a metalorganic chemical vapor deposition (MOCVD) system is described.

Chapter II is the introduction of Part I.

In Chapter III, we describe the experimental system named as electron beam induced metalorganic chemical vapor deposition (EBI-MOCVD) system.

In Chapter IV, selective growth for the purpose to fabricate the quantum microstructures using *in situ* irradiation of the electron beam in the EBI-MOCVD system is provided, demonstrating successful fabrication of GaAs quasi-quantum wire and dot structures. In addition, we discuss the growth mechanisms of this selective growth.

In Chapter V, an *in situ* processes for the fabrication technology of semiconductor microstructures combining the contamination resists formed by the electron beam irradiation and MOCVD method is demonstrated.

Chapter VI is the summary of Part I.

In Part II, the theoretical analysis of lasing characteristics in quantum microstructure lasers such as quantum well (QW), quantum well wire (QWW), and quantum well box (QWB) lasers are described.

Chapter VII is the introduction of Part I.

In Chapter VIII, theoretical analysis of effects of the substrate-orientation on lasing properties of QW lasers using the tight binding method is provided, indicating importance to choose the substrate-orientation while considering which lasing property should be improved for a given application.

In Chapter IX, lasing characteristics of GaAs/AlGaAs semiconductor lasers having QWB structures are theoretically analyzed in order to clarify achievable limits of lasing characteristics in quantum microstructure lasers.

In Chapter X, nonlinear gain effects in GaAs/AlGaAs and InGaAsP/InP QW, QWW, and QWB lasers are theoretically analyzed, indicating that the nonlinear gain significantly affects these lasing characteristics.

Chapter XI is the summary of Part I.

Chapter XII is the conclusions of this work.

Part I Fabrication Technologies of Quantum Microstructures

Abstract

We report the successful fabrication of GaAs wire structures by an electron beam induced selective growth technique in a metalorganic chemical vapor deposition (MOCVD) system.

We have demonstrated selective formation of a GaAs quasi-quantum wire structure as narrow as 300 nm using *in situ* irradiation of the electron beam. Selective formation of a GaAs quasi-quantum dot structure is also achieved. Auger Analysis and growth condition dependence suggest that this selective growth results from the decomposition of tri-methyl-gallium (TMG) by the electron beam irradiation.

We have also demonstrated a novel *in situ* process for fabrication of semiconductor quantum wire structures, combining contamination resists and selective growth in MOCVD, showing successful formations of a GaAs quasi-quantum wire with the width as narrow as 700 nm. Auger Analysis confirmed that the contamination resists are resulting from adsorption of carbon material.

Chapter II Introduction of Part I

In recent years, various kinds of fabrication techniques have been intensively investigated to fabricate quantum wire and quantum box structures. These include laser assisted atomic layer epitaxy (ALE) [44]-[47], fractional layer superlattice (FLS) growth [74]-[89], and facet wire growth [90], [91]. The laser assisted ALE technology has high degree of freedom for designing structures. However, the dimension of the grown structures can not be reduced enough to realize the quantum wire effects, because the laser beam diameter is much larger than the electron wavelength. Although the dimension of structures in the FLS growth can be reduced enough to realize the quantum confinement effects, the FLS growth has lower degree of freedom for designing structures. This is due to the fact that the dimension and the direction of structures is definitely determined by terrace width and step direction, respectively. On the other hand, the facet wire growth using SiO_2 masks has high degrees of freedom. Moreover, the dimension of structures can be smaller than the limit of lithography. However, it needs several independent processes such as deposition of SiO_2 film, lithography, etching and re-growth. Therefore, it is useful to develop a new type of growth technique which can form the quantum wires and quantum boxes using *in situ* process with high degree of freedom for designing.

In Part I, we report the successful fabrication of GaAs wire structures by an electron beam induced selective growth technique in a metalorganic chemical vapor deposition (MOCVD) system.

In Chapter III, we describe an experimental system named as an electron beam induced MOCVD (EBI-MOCVD).

In Chapter IV, selective formation of a GaAs quasi-quantum wire structure as narrow as 300 nm using *in situ* irradiation of the electron beam with simultaneous supply of tri-methyl-gallium (TMG) and cracked AsH_3 is reported. Selective formation of a GaAs quasi-quantum dot structure is also achieved. Auger Analysis and dependence of the growth on source materials and types of the substrate suggest that the selective growth results from the decomposition of TMG by the electron beam irradiation. By using this technique high degree of freedom for designing structures and possibility to reduce the dimension of grown structures are preserved, because the electron beam diameter can be reduced less than 10 nm.

In Chapter V, we report an another novel *in situ* process for fabrication of semiconductor quantum wire structures, combining contamination resists and selective growth in metalorganic chemical vapor deposition (MOCVD). The results show successful formations of a GaAs quasi-quantum wire with the width as narrow as 700 nm. In addition, use of micro Auger electron spectroscopy analysis confirmed that the contamination resists are resulting from adsorption of carbon material.

Chapter III Electron Beam Induced Metalorganic Chemical Vapor Deposition System

Schematic illustration of the experimental system (EBI-MOCVD system) is shown in Fig. 3. 1. A modified scanning electron microscopy (SEM) system, in which electron beam is irradiated on a substrate during the flow of source gases, is connected to an MOCVD gas system. Source materials are 10 % AsH_3 in H_2, tri-methyl-gallium (TMG) and tri-methyl-aluminium (TMA) carried by H_2 gas flows whose pressure is 2 atm. The gas flows are controlled by the mass flow controllers. Typical flow rates of AsH_3 and H_2 for bubbling TMG are 1.0 sccm and 3.0 sccm, respectively. Temperature of a TMG bubbler is set at -10 °C. In this condition, V/III ratio is about 1.2. We can crack AsH_3 in a cracking cell up to 1200 °C. The growth chamber and the electron beam gun are evacuated separately by the differential exhaust systems which consist of diffusion pumps and rotary pumps. The background pressure in the chamber is about 10^{-7} torr and the pressure during growth is in the range of 10^{-5} - 10^{-4} torr. As regards the pressure, the growth mode in this method should be similar to that in a metalorganic molecular beam epitaxy (MOMBE) method. Substrates can be heated up to 700 °C by a radiation heater. The electron beam current density varies from 1 to 100 A/cm^2 depending on the acceleration voltage of the electron beam. A generally used acceleration voltage of electron beam is 25 keV, though we can vary it of 5, 15, or 25 keV.
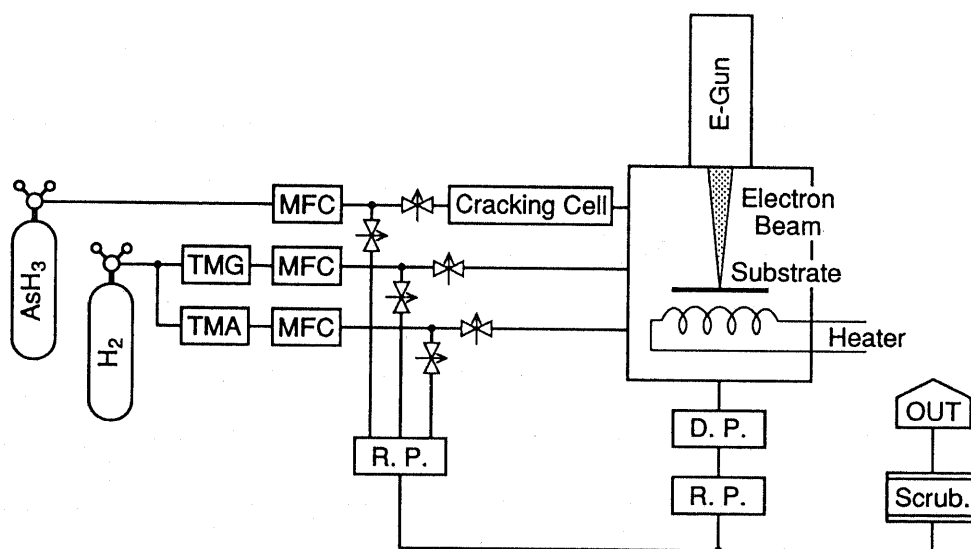
Fig. 3. 1　Schematic illustration of the experimental system (EBI-MOCVD system). As shown in this figure, a modified scanning electron microscopy system, in which the electron beam is irradiated on the substrate during flowing source gases, is connected to an MOCVD gas system.

Chapter IV Selective Growth by Electron Beam Irradiation

4. 1. Fabrication of Wire and Dot Structures

In this chapter, we report the selective growth by electron beam irradiation in EBI-MOCVD system. Fig. 4. 1 shows a scanning electron microscope (SEM) photograph of selective growth achieved by this technique. The source materials supplied are AsH_3 cracked at 1000 °C and TMG. The substrate temperature is room temperature and growth time is 1 hour. The electron beam is irradiated by a line scanning mode. Fig. 4. 1 indicates that the wire shaped material is grown where the electron beam is irradiated. The elements of which this grown material consists is discussed in the next section. The dimension of this wire structure is as narrow as 300 nm. We consider that this dimension is determined by not the electron beam diameter but some vibration problems existing in this system. Therefore, it is expected that, if these vibration problems are solved, the dimension of grown structures can be reduced as narrow as 10 nm which is equal to the electron beam diameter. We can also fabricate a dot structure as shown in Fig. 4. 2. In this case, the electron beam is irradiated at one point during the growth and the other conditions are same as above. Diameter of this grown dot structure is about 1 μm.
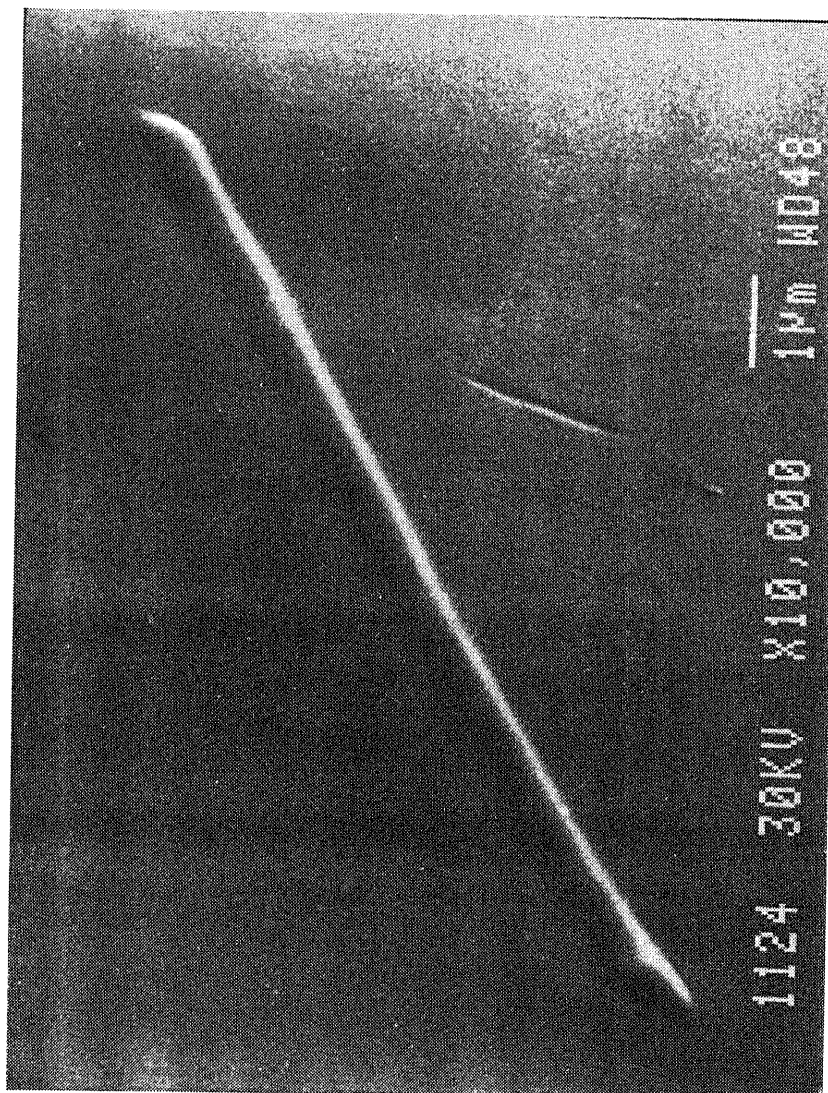
Fig. 4. 1   A SEM photograph of a GaAs wire formed by the electron irradiation by a line scanning mode when AsH$_3$ cracked at 1000 °C and TMG are supplied at room temperature.
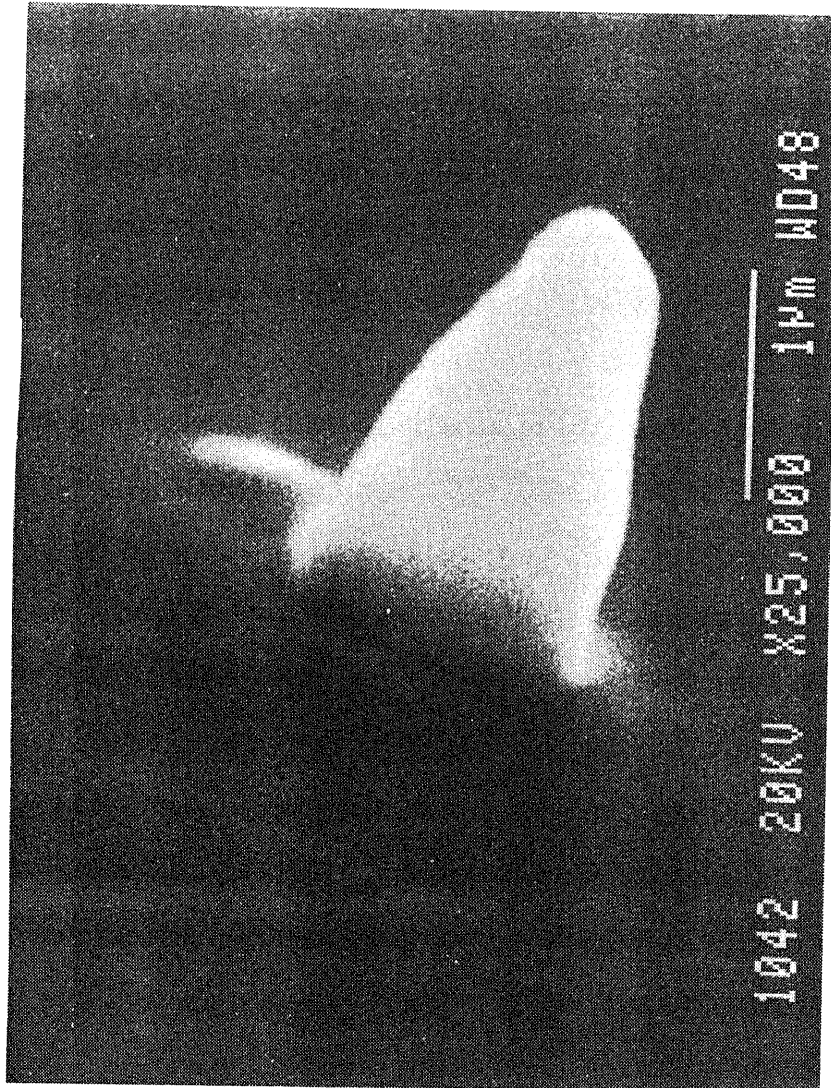
Fig. 4. 2 A SEM photograph of a GaAs dot formed when the
electron is irradiated at one point during the growth.
The other conditions are same as those in the case of
Fig. 4. 1.

4. 2. Elemental Analysis

To analyze the elements of which the grown material consists, we investigated micro Auger electron spectroscopy (AES) measurement. Fig. 4. 3 shows measured AES's from the selectively grown micro-structures when we supplied (a) AsH_3, (b) TMG, and (c) both AsH_3 and TMG, respectively. In this experiment, Si substrates are used in order to avoid the detection of Ga and As peaks from the substrates. Figs. 4. 3 (a) and (b) show clear peaks of As and Ga, respectively, and both Ga and As peaks are observed in Fig. 4. 3 (c). As shown in Fig. 4. 3 (b), As peak is also observed when only TMG is supplied, which is probably due to the fact that little amount of As remained in the growth chamber due to previous growth experiments. Table IV. I shows a summary of atomic concentrations of each structures. When cracked AsH_3 and TMG are supplied, almost the same amount of Ga and As are contained in the grown structure, which is clearly different from the other structures. This result confirms that GaAs wire and dot structures are successfully fabricated by this selective growth technique. On the other hand, AES revealed that all structures contain a large amount of carbon. We consider that this incorporation of carbon results from complete decomposition of TMG by the electron beam. Reduction of carbon is very important issue in applying this technique to device fabrications.

(a)

$\dfrac{dN}{dE}$

O

C

Ga

As

0   340   680   1020   1360   1700

Kinetic Energy (eV)

(b)

$\dfrac{dN}{dE}$

As

C   O   Ga

0   340   680   1020   1360   1700

Kinetic Energy (eV)

(c)

$\dfrac{dN}{dE}$

O

C   Ga   As

0   340   680   1020   1360   1700

Kinetic Energy (eV)
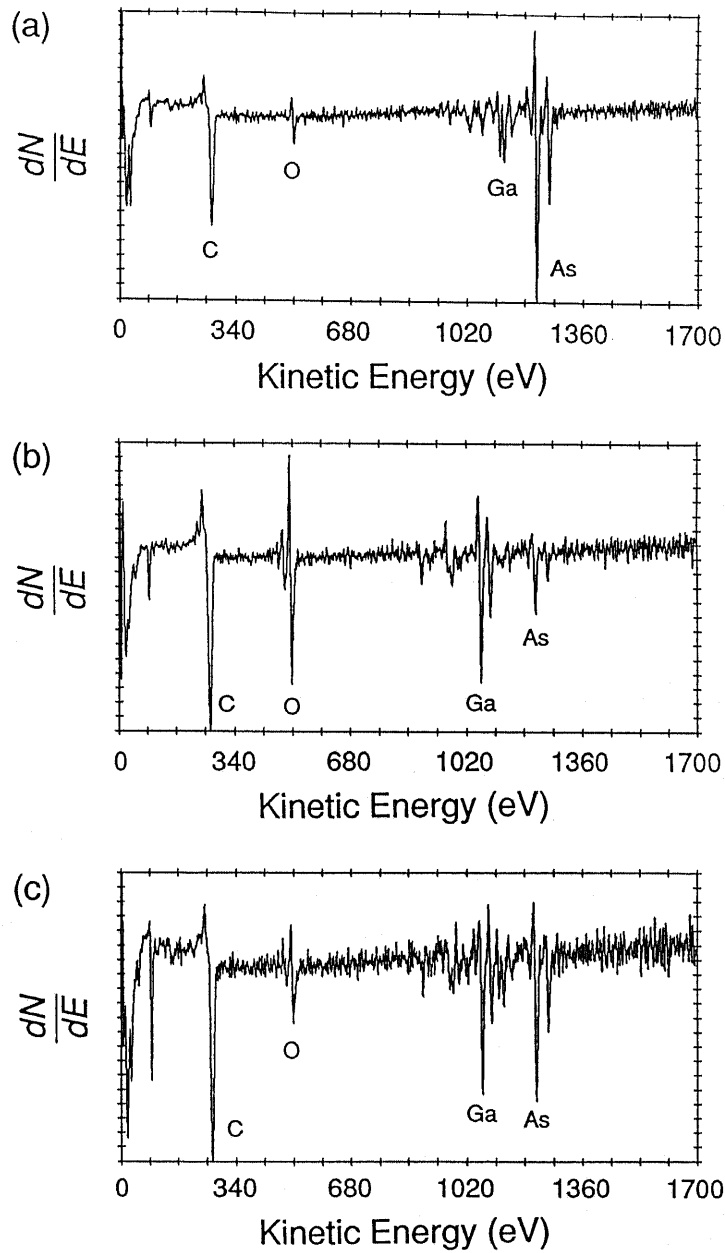
Fig. 4. 3 Measured Auger electron spectroscopies (AES's) from the selectively grown micro-structures when we supplied (a) AsH_3, (b) TMG, and (c) both AsH_3 and TMG, respectively.

	Ga	As	C	O (%)
AsH$_3$ (1000°C)	8	65	22	5
TMG	29	22	37	12
{ AsH$_3$ (1000°C) { TMG	30	39	25	6

Table IV. I Atomic concentrations (%) of three types of structures: the source materials are only AsH$_3$, only TMG, and both AsH$_3$ and TMG.

4. 3. Dependence on Growth Conditions

4. 3. 1. Substrate Temperature

We have investigated the substrate temperature dependence of this selective growth. Fig. 4. 4 shows a wire structure successfully achieved when only TMA is supplied at 300 °C. When we supply only TMG or TMA, selective growth similar to Fig. 4. 4 is realized at the electron beam irradiated area in the temperature range of room temperature (R. T.) ~ 300 °C or R. T. ~ 700 °C, respectively. However, the growth rate at high temperature becomes very low in each case supplying TMG or TMA compared to the growth rate at R. T. On the other hand, when we supply TMG and cracked AsH_3 at 1000 °C, the selective growth at the electron beam irradiated area is realized in the temperature range of R. T. ~ 400 °C and above 450 °C the GaAs crystal is grown everywhere place on the substrate thermally.

These changes of the substrate temperature dependence with changing supplying source materials clearly indicate that the grown material in each case consists of the elements generated by decomposition of source materials or reactions among them.
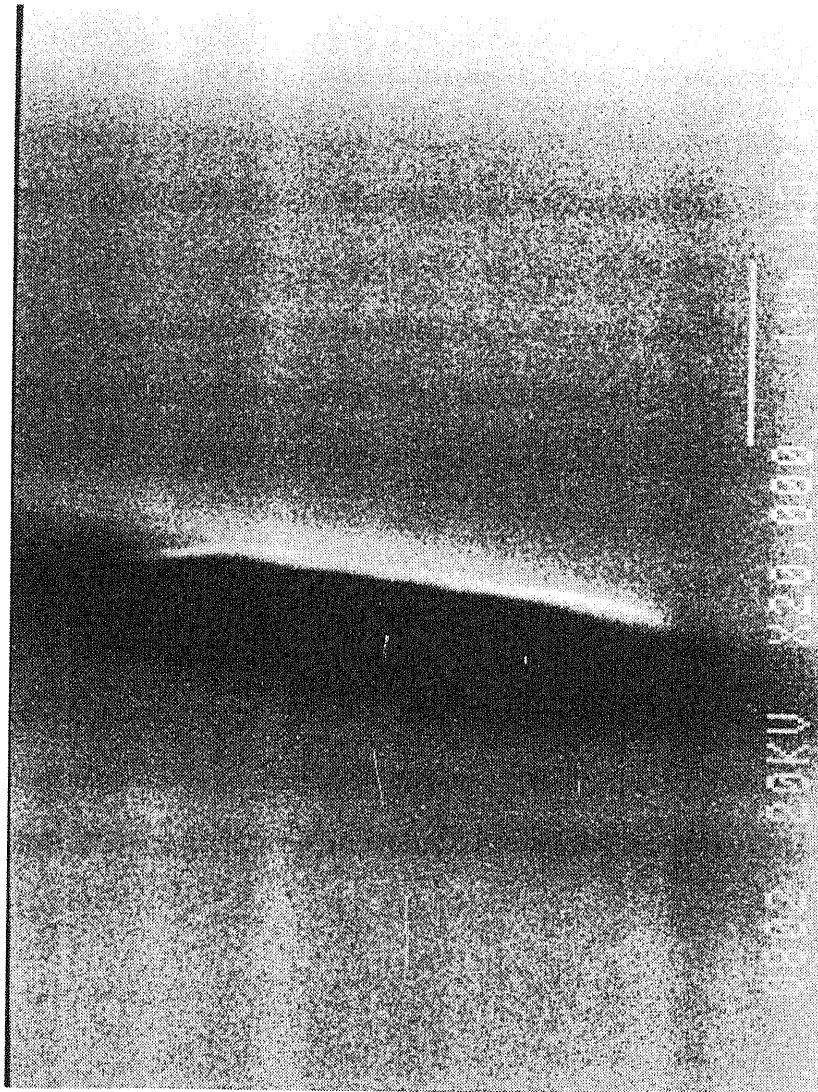
Fig. 4. 4   A SEM photograph of a wire structure achieved when
only TMA is supplied at 300 °C.

4. 3. 2. Source Materials

Next we have investigated dependence of growth rate on source materials at room temperature when the electron beam is irradiated at a spot. The results are summarized in Table IV. II. Fig. 4. 5 shows the mixtures grown selectively by the electron beam irradiation when we supply only cracked AsH_3, only TMG, or both of them. As shown in this photograph, the growth rate with supplying both AsH_3 cracked at 1000 °C and TMG is much higher compared to the growth rate under the other conditions. Thus, the existence of both AsH_3 and TMG enhances the growth rate. On the other hand, when no materials are supplied, formation of a structure due to accumulation of carbon (i.e., contamination resist) is not observed. This result confirms that carbon incorporated in the GaAs: C mixture is generated from TMG.

Contamination Resist	$\sim 0\ \mu m/h$
AsH_3 (R.T.)	$0.1\ \mu m/h$
AsH_3 (1000°C)	$0.4\ \mu m/h$
TMG	$1.3\ \mu m/h$
$\begin{cases} AsH_3\ (R.T.) \\ TMG \end{cases}$	$0.3\ \mu m/h$
$\begin{cases} AsH_3\ (1000°C) \\ TMG \end{cases}$	$2.0\ \mu m/h$

Table IV. II Source materials dependence of the growth rate.

TMG   AsH₃ (1000°C)   { AsH₃ (1000°C)
                                   { TMG

10 μm
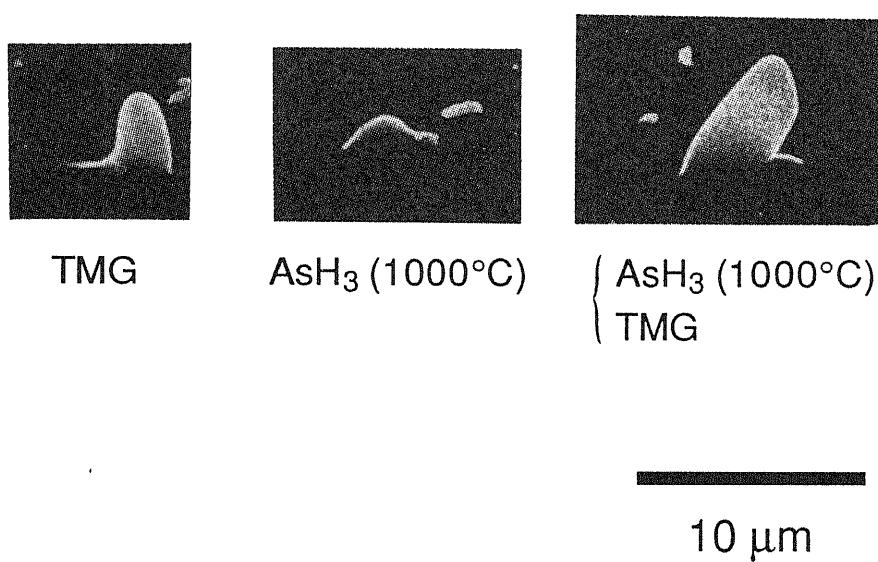
Fig. 4. 5   A SEM photograph of the mixtures grown selectively
            by the electron beam irradiation when we supply only
            TMG, only cracked AsH₃, or both of them.

4. 3. 3. Supplying Rate of Source Materials

The growth rate with supplying both cracked AsH_3 and TMG increases with the increase of TMG flow rate, while the growth rate decreases with the increase of AsH_3 flow rate. A SEM photograph of grown mixtures is shown in Fig. 4. 6 and the growth rate in each condition is summarized in Table IV. III. These results indicate that this reaction velocity is determined by the supplying rate of III-group materials. We can understand the fact that the growth rate decreases with the increase of AsH_3 flow rate by considering the equivalent decrease of TMG pressure in the chamber.

AsH$_3$ Flow Rates (sccm)

0.4   2.0

Fig. 4. 6 A SEM photograph of grown mixtures when the flow
rates of AsH$_3$ is 0.4 or 2.0 sccm and the flow rates of H$_2$
bubbling TMG is 0.6 or 3.0 sccm.

		AsH$_3$ Flow (sccm)	
		0.4	2.0
TMG Flow (sccm)	3.0	2.0 μm/h (2.7)	1.3 μm/h (1.7)
	0.6	1.2 μm/h (1.6)	0.75 μm/h (1)

Table IV. III Growth rates of GaAs: C mixtures when the flow rates of AsH$_3$ is 0.4 or 2.0 sccm and the flow rates of H$_2$ bubbling TMG is 0.6 or 3.0 sccm.

4. 3. 4. Electron Beam Current (Electron Beam Diameter)

In our electron beam gun system, electron beam current density is a almost constant regardless of electron beam diameter when we fix the acceleration voltage. Therefore, in order to change total electron beam current, it is needed to change the electron beam diameter. Fig. 4. 7 shows the grown mixtures with various electron beam diameter, that is, various total electron beam current. As shown in this figure, size of grown mixture becomes large with the increase of the total electron beam current. This result confirms that the decomposition of source materials are enhanced by the electron beam.

4. 3. 5. Kind of Substrates

This selective growth has no substrates dependence; GaAs: C mixtures are grown on regardless of kind of substrates such as semi-insulated GaAs substrate, epitaxial grown GaAs layer, n-type Si substrate and SiO_2 film deposited on GaAs substrate. This fact suggests that generation of electrons or holes by the electron beam irradiation inside the substrates is not a dominant mechanism for the growth and, in addition, that the grown crystal is not mono-crystalline but polycrystalline or amorphous.
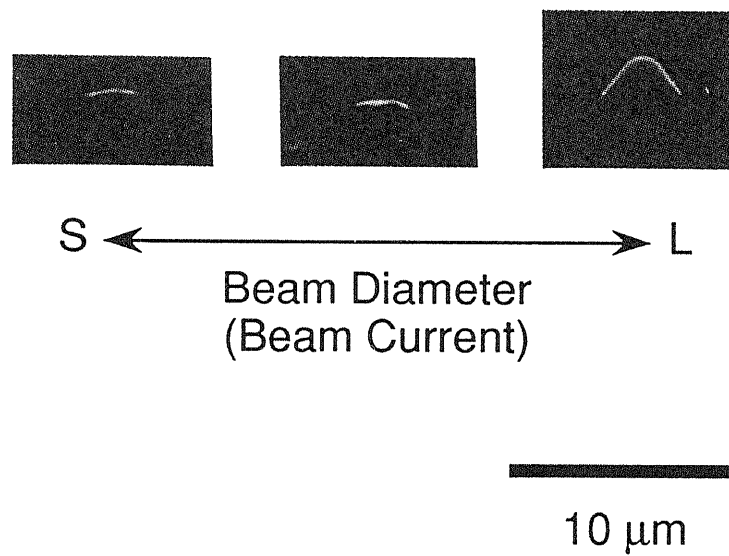
Fig. 4. 7　A SEM photograph of the grown mixtures with various electron beam diameter, that is, various total electron beam current.

4. 4. Growth Mechanisms

On the basis of our experimental results, we investigate growth mechanisms of this selective growth [92]-[95].

First, we discuss a thermal effect due to the electron beam irradiation. We consider that the thermal effect is not dominant because of three following reasons: (1) If the thermal effect is dominant, the size of grown mixtures should be larger than that obtained in our experiments because of thermal conduction of the substrate. (2) The growth rate at high temperature should be higher than that at low temperature if the thermal effect is dominant, however, our experimental results show the opposite tendency. (3) We have also achieved the selective growth when we irradiate the electron beam by the pulse mode whose duty ratio is about 25 %. Therefore, we need to investigate other mechanisms for this selective growth.

In our experiments, supplied AsH_3 onto the substrate has been already decomposed into As atoms or molecules in the cracking cell. Therefore, it is reasonable to assume that the role of the electron beam irradiation is to decompose TMG into Ga atoms. Now, three kinds of effects of the electron beam for decomposition of TMG are possible: (1) TMG adsorbed onto the substrate is decomposed by the irradiated electrons, (2) TMG adsorbed onto the substrate is decomposed by the electrons or holes generated in the substrate by the electron beam irradiation, and (3) TMG in the vapor phase is decomposed by the electron beam. The second mechanism is excluded because the selective

growth occurs regardless of kind of substrates. If the third one is dominant, size of the grown structure should be much larger than that obtained in our experiments because decomposed Ga atoms are diffused in vapor phase with long diffusion length. Consequently, the first effect is the most possible mechanism for the decomposition of TMG. This mechanism is illustrated in Fig. 4. 8: First, supplied TMG is absorbed onto the substrate surface, then adsorbed TMG is decomposed by the irradiated electron beam and, finally, Ga atoms generated from TMG decomposition reacts to As atoms or molecules generated by the cracking of AsH_3, resulting in the formation of GaAs mixture. In the process of decomposition, carbon is generated due to the completely decomposition of TMG and this carbon is incorporated into the GaAs mixture.
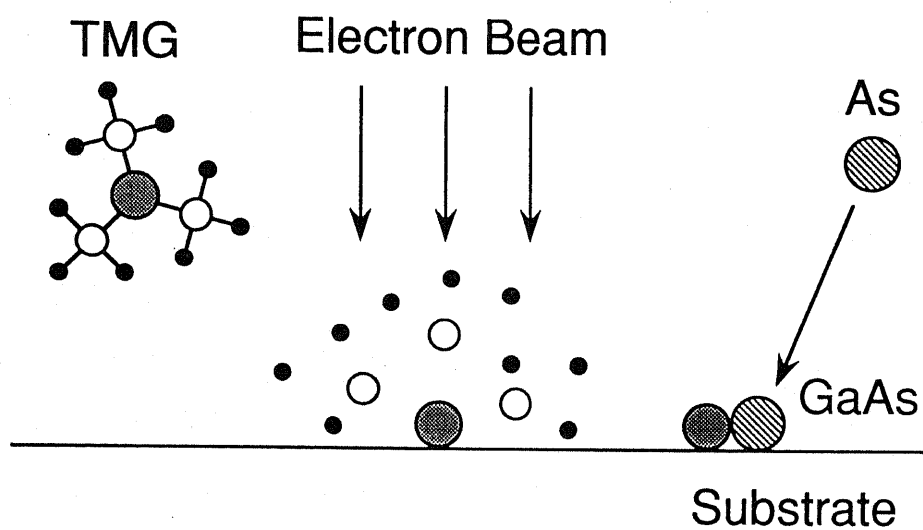
Fig. 4. 8   The illustration of the growth mechanisms. First, supplied TMG is absorbed onto the substrate surface, then adsorbed TMG is decomposed by the irradiated electron beam and, finally, Ga atoms generated from TMG decomposition reacts to As atoms or molecules generated by the cracking of AsH_3, resulting in the formation of GaAs mixture.

4. 5. Selective Growth by Pulse Mode Supply of Source Materials

We have also demonstrated selective growth by pulse mode supply of source materials [42]-[47]. In these experiments we supply the source materials with time sequences shown in Figs. 4. 9 (a), (b) and (c), while the electron beam is continuously irradiated at a spot. Between the supplying source materials such as AsH_3 and TMG, we supply H_2 gas in order to purge AsH_3 or TMG from the chamber. Substrate temperature is 300 °C and AsH_3 is cracked at 1000 °C. Fig. 4. 10 shows a grown dot structure in the case of (a). On the other hand, in the cases of (b) and (c) no growth is achieved. These results indicate that this selective growth can be achieved, only when we supply both AsH_3 and TMG, but even when the time interval exists between AsH_3 supply and TMG supply. On the basis of our results, desorption time of Ga or TMG from the substrate surface can be considered to be longer than 15 sec. Our results suggest potentiality for applying this selective growth technique to atomic layer epitaxy (ALE) growth.
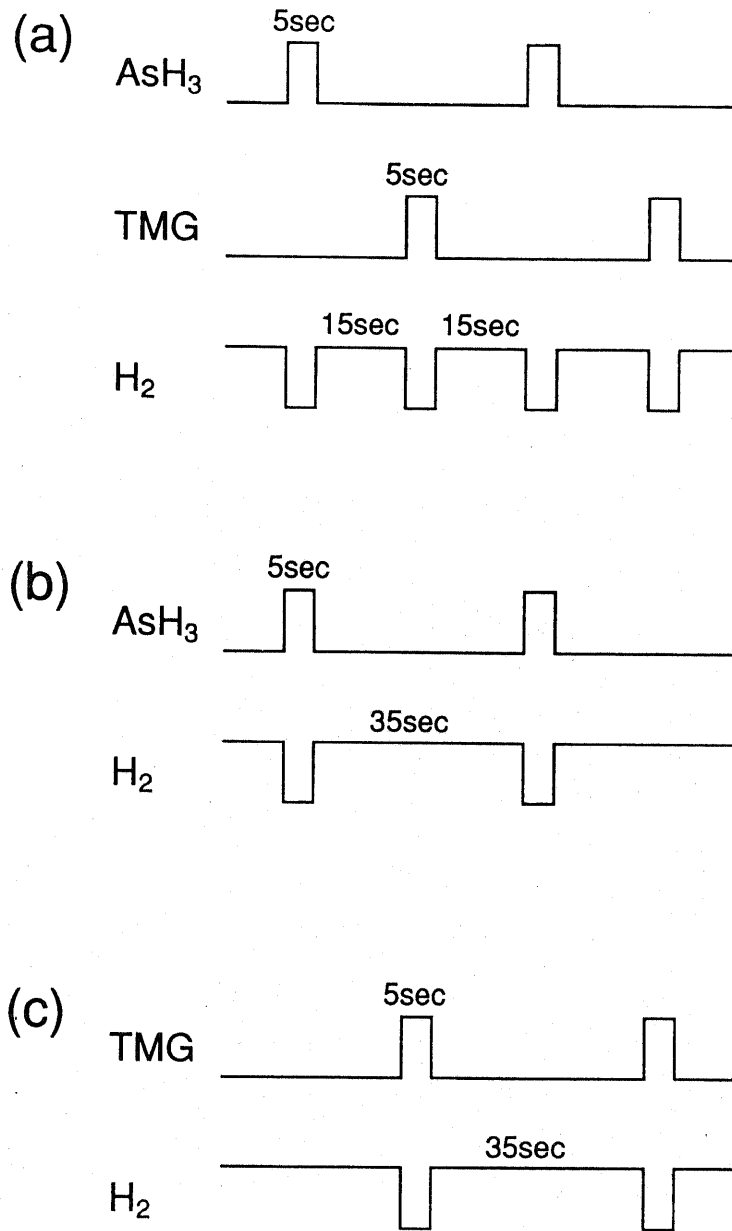
Fig. 4. 9 Time sequences of the pulse mode supply of source materials. Between the supplying source materials such as AsH_3 and TMG, we supply H_2 gas in order to purge AsH_3 or TMG. The electron beam is irradiated continuously at a spot.
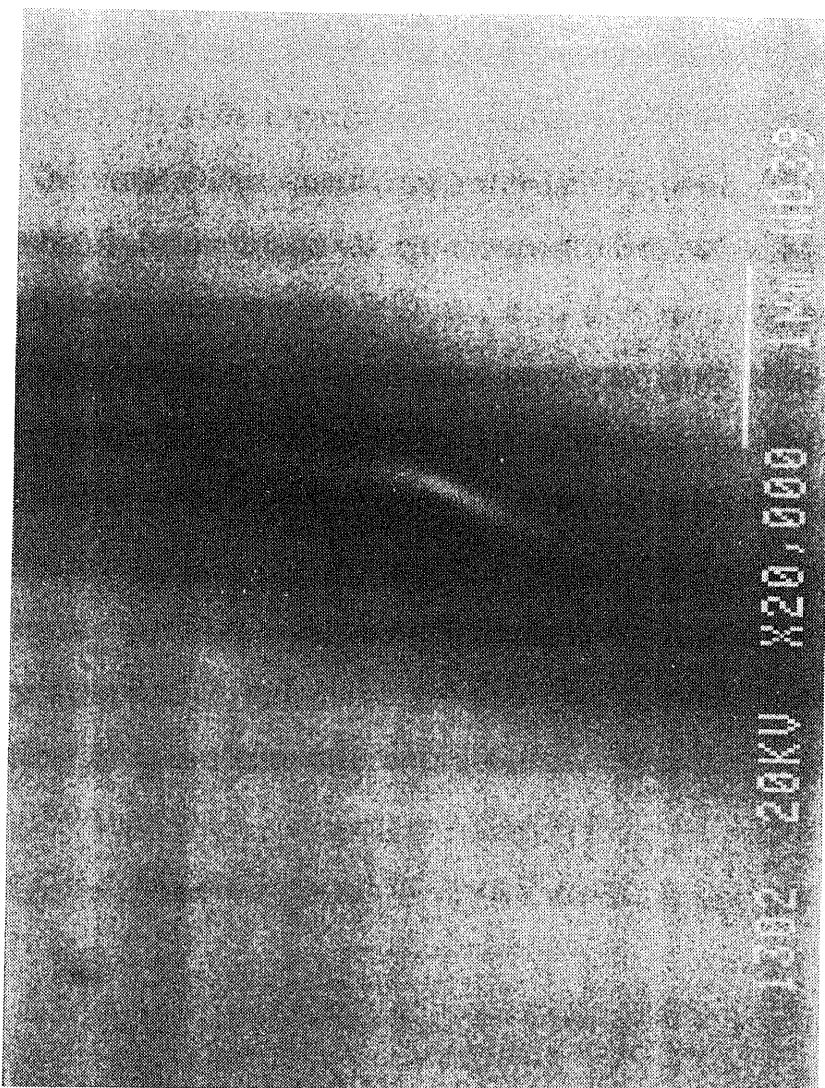
Fig. 4. 10 A SEM photograph of a grown dot structure in the case of Fig. 4. 9 (a). In this case, AsH_3 is cracked at 1000 °C and substrate temperature is 300 °C.

4. 6. Concluding Remarks

In Chapter IV, we demonstrated a novel selective growth technique using *in situ* irradiation of the electron beam for the purpose to fabricate the quantum microstructures. The results show successful fabrication of quasi-quantum wire structures whose width is as narrow as 300 nm and dot structures. Auger electron spectroscopy measurements confirm that these grown structures are GaAs: C mixtures. We also discuss the growth mechanisms of this selective growth, showing that the electron beam irradiation affects the decomposition of TMG adsorbed onto the substrate surface. Although our results are still at preliminary stage, this selective growth has various potentiality for fabrication of quantum microstructures.

Chapter V *In situ* Selective Growth Using Contamination Resists

5. 1. Growth Processes

In this chapter, we report the *in situ* selective growth using contamination resists [96], [97] in EBI-MOCVD system. The time sequence for this growth is shown in Fig. 5. 1; they are (1) electron beam irradiation onto the substrate surface to form contamination resists at room temperature, (2) heating the substrate up to 700 °C for thermal cleaning for a few minutes, (3) setting the growth temperature, (4) supplying the source materials and crystal growth, and (5) cooling down to room temperature. We continuously supply AsH_3 cracked at 1000°C during heating to avoid the desorption of As atoms from the substrate surface. Using this procedure, semiconductor crystals are selectively fabricated after forming contamination resist without exposing the sample to the air. This method is one of the *in situ* selective growth processes.
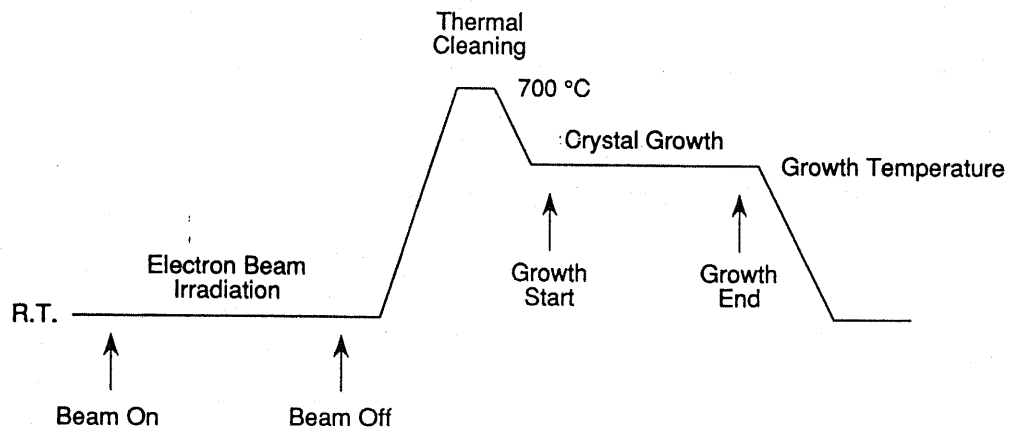
Fig. 5. 1 Time sequence for *in situ* selective growth using contamination resists.

5. 2. Formation of Contamination Resists by Electron Beam

Fig. 5. 2 shows a selective growth achieved by this process sequence. The electron beam irradiated area is about 20 μm × 20 μm. The source materials used are AsH_3 cracked at 1000 °C and TMG. The substrate temperature is 500 °C and growth time is 1 hour. As shown in this scanning electron microscope (SEM) photograph, the GaAs crystal is grown outside of the electron beam irradiated area. The grown crystal formed outside of the region where the electron beam is irradiated is confirmed to be the *mono*-crystalline by means of the observation of the electron channeling pattern.

(a)
(b)
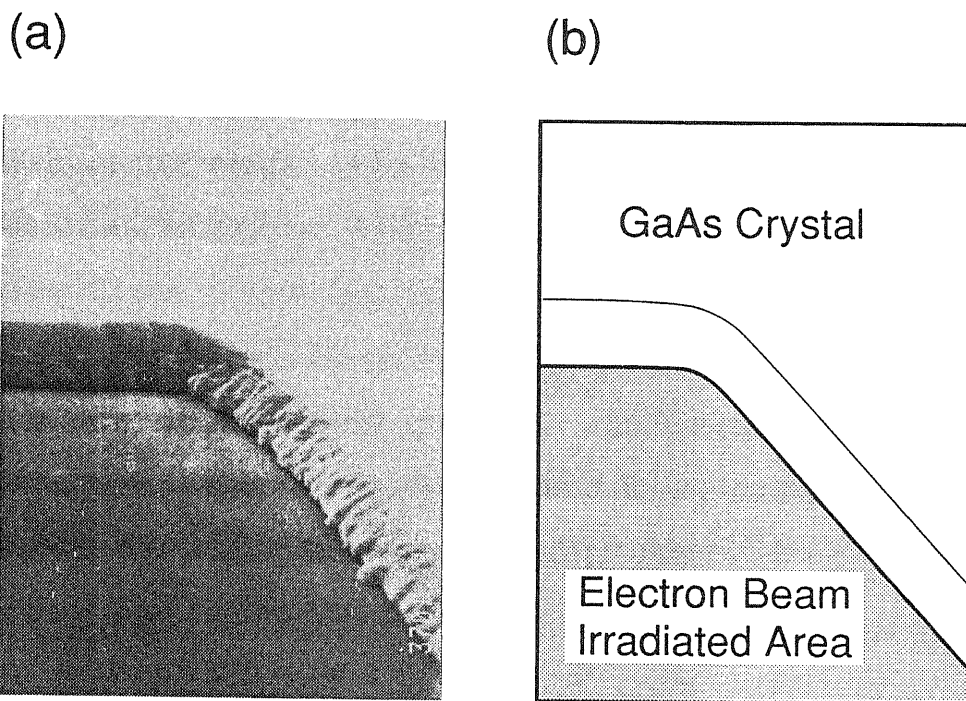
Fig. 5. 2   (a) A SEM photograph and (b) an illustration of the
electron irradiated area in the selective ungrowth
when AsH$_3$ cracked at 1000 °C and TMG are supplied
at 500 °C substrate temperature.

5. 3. Fabrication of GaAs Wire Structures

This selective growth technique is applied to fabricate quantum wire structures using the method illustrated in Fig. 5. 3. First, we irradiate the electron beam onto separated regions of the substrate surface in order to form contamination resists without supplying source materials, then the crystal growth is performed. Fig. 5. 4 shows a successfully fabricated GaAs quasi-quantum wire structure using this technique. The wire width is as narrow as 700 nm. The dimension of the wire demonstrated here is still large compared to the dimensions which can achieve real quantum confinement. However, we believe that this technology has the potential for forming quantum wires and boxes by scanning the electron beam on the substrate just before the growth.

Electron Beam Irradiation

Substrate

Crystal Growth
of Microstructures
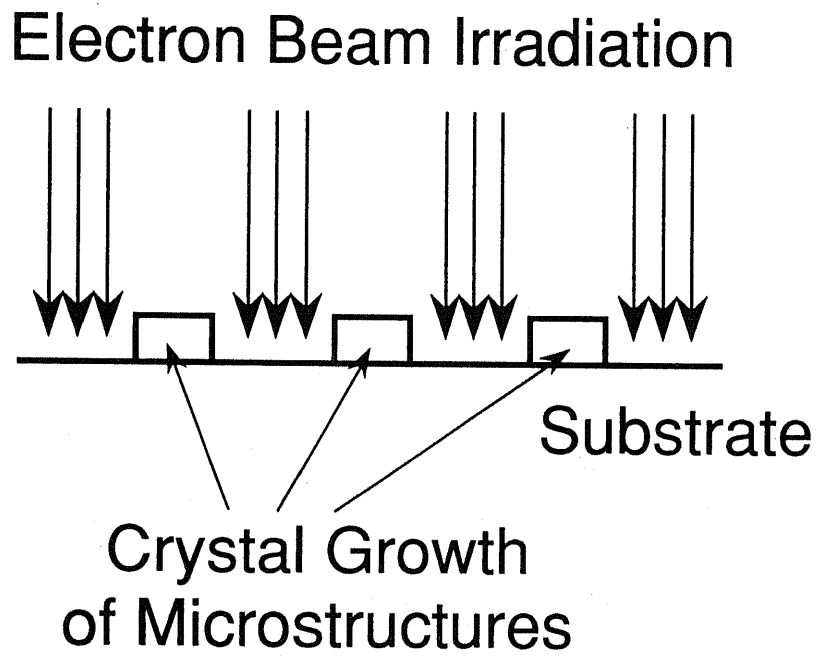
Fig. 5. 3   Fabrication method using *in situ* patterning before the
growth method for quantum wires.
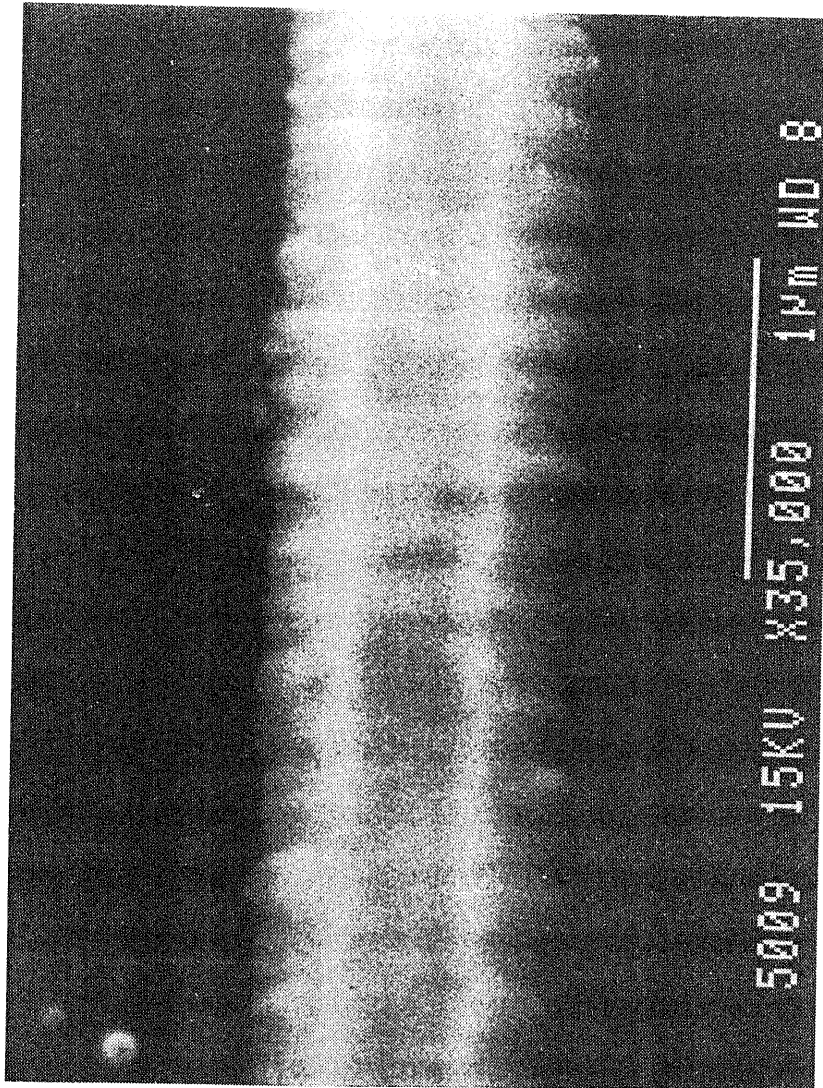
Fig. 5. 4   A SEM photograph of the GaAs quasi-quantum wire
structure   fabricated   by   this   selective   growth
technique. The wire width is as narrow as 700 nm.

5. 4. Elemental Analysis of Contamination Resists

To analyze elements of the contamination resists, we used a micro Auger electron spectroscopy technique. Fig. 5. 5 shows Auger electron spectroscopies from the substrate surface in (a) the ungrown area and (b) the crystal growth area. The vertical axis is normalized by a peak value in each figure. As shown in these figures, a strong carbon peak is observed from the ungrown area surface compared to the crystal growth area. In addition, it is observed that in the depth profile of each area as shown in Fig. 5. 6 or Fig. 5. 7, carbon only exists within 10 Å which corresponds to a few mono-layers from the substrate surface. The oxygen peak is also observed in both surfaces with the same intensities. They decrease within the range of 10 Å, which is similar to the carbon peaks. On the other hand, in the spectroscopy after sputtering about 200 Å from the surface, both carbon and oxygen peaks completely disappear and only gallium and arsenic peaks are observed (Fig. 5. 8). Therefore, we can conclude that the selective ungrowth in the region where the electron beam is irradiated results from the contamination resists consisting of carbon whose thickness is thinner than 10 Å.
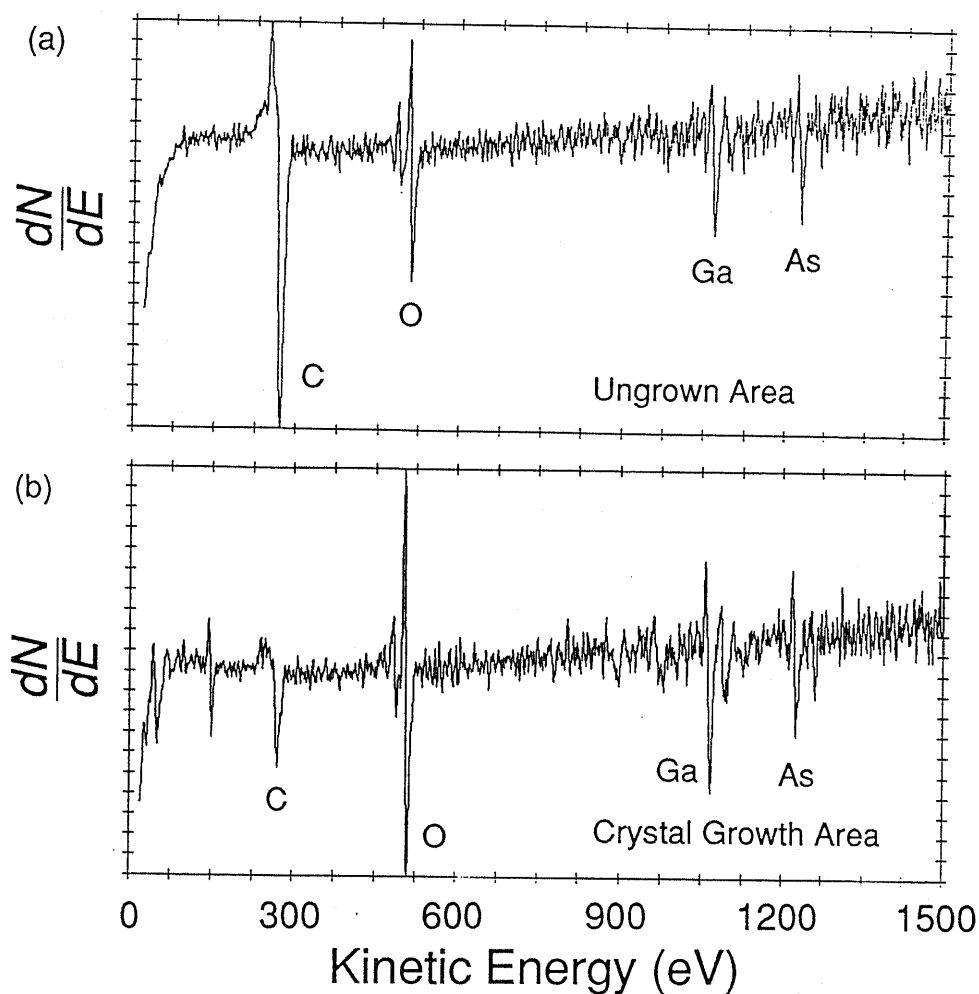
Fig. 5. 5   AES's from the substrate surface in (a) the ungrown
area and (b) crystal growth area. A vertical axis is
normalized by a peak value in each figure. As shown
in these figures, a strong carbon peak is observed from
the ungrown area surface compared with the crystal
growth area.
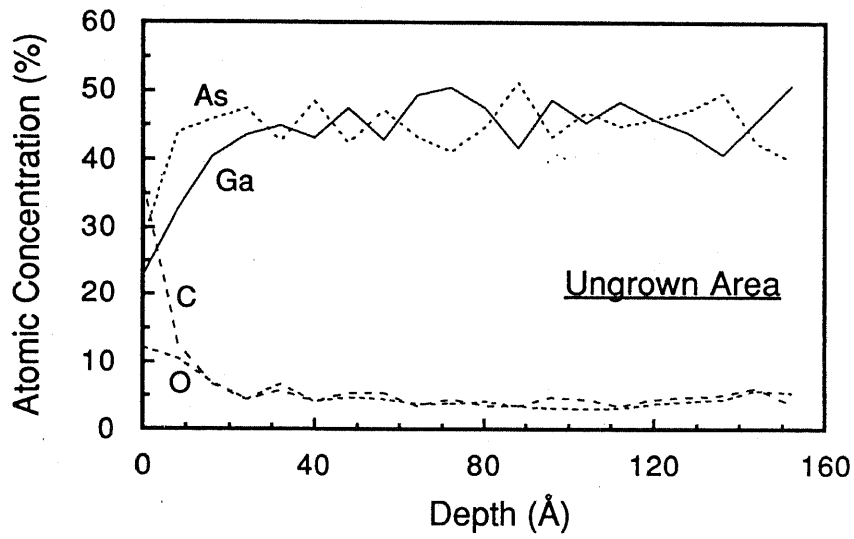
Fig. 5. 6   Depth profile of the ungrown area.
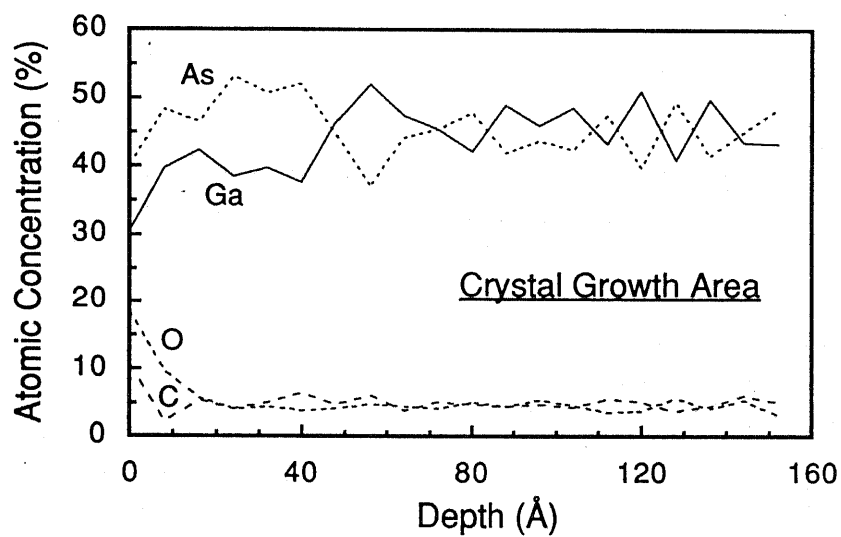
Fig. 5. 7   Depth profile of the crystal growth area.
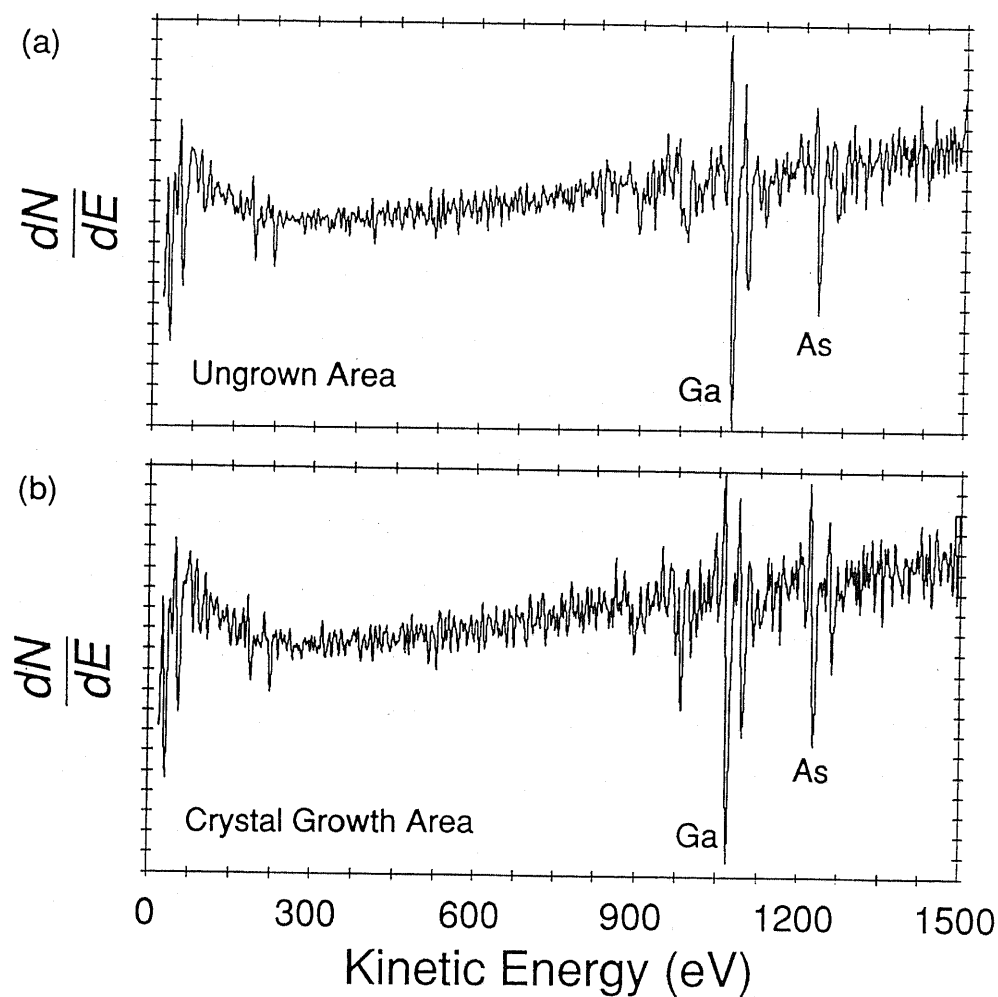
Fig. 5. 8   AES's from the substrate after sputtering about 200 Å
in (a) the ungrown area and (b) crystal growth area.
As shown in these figures, both carbon and oxygen
peaks completely disappear and only gallium and
arsenic peaks are observed.

5. 5. Formation Mechanisms of Contamination Resists

The ungrown area width is plotted as a function of the acceleration voltage is shown in Fig. 5. 9, when the electron beam is scanned by the line scanning mode. As shown in this figure, the ungrown area width becomes narrower with the decrease of the acceleration voltage. On the other hand, the electron beam diameter should be much smaller than 0.1 μm and it becomes smaller with the increase of the acceleration voltage. Therefore, this ungrown area width is not determined by the electron beam diameter. A possible mechanism that opposes the acceleration voltage like Fig. 5. 9 is the back scattering effects of electrons or generated electron-hole pairs. Therefore, our result suggests that a possible factor which forms this carbon contamination resist is these back scattering effects of electron or generated electron-hole pairs.
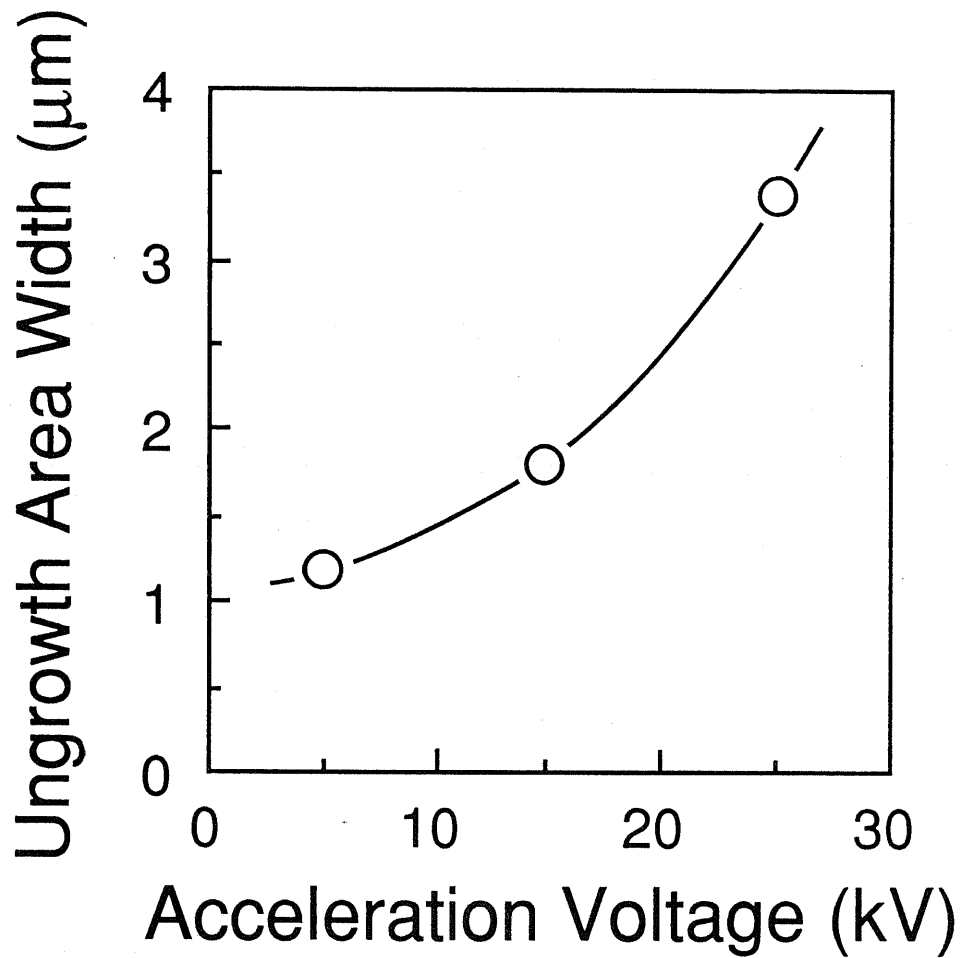
Fig. 5. 9 The ungrown area width as a function of the acceleration voltage when the electron beam is scanned by the line scanning mode.

5. 6. Concluding Remarks

In Chapter V, we demonstrated an *in situ* processes for the fabrication technology of semiconductor microstructures combining the contamination resists formed by the electron beam irradiation and MOCVD method. The results show successful fabrication of a GaAs quasi-quantum wire structure whose width is as narrow as 700 nm. These techniques lead to potential applications to the fabrication of semiconductor structures with real multi-quantum confinement effects.

Chapter VI Summary of Part I

In Part I, we reported the successful fabrication of GaAs wire structures by an electron beam induced selective growth technique in a metalorganic chemical vapor deposition (MOCVD) system.

We demonstrated a novel selective growth technique using *in situ* irradiation of the electron beam in the EBI-MOCVD system for the purpose to fabricate the quantum microstructures. The results show successful fabrication of GaAs quasi-quantum wire structures whose width is as narrow as 300 nm. In addition, we discuss the growth mechanisms of this selective growth, showing that the electron beam irradiation affects the decomposition of TMG adsorbed onto the substrate surface.

We also demonstrated an *in situ* processes for the fabrication technology of semiconductor microstructures combining the contamination resists formed by the electron beam irradiation and MOCVD method. The results show successful fabrication of GaAs quasi-quantum wire structures whose width is as narrow as 700 nm.

Although our results are still at preliminary stage, these techniques lead to potential applications to the fabrication of semiconductor quantum microstructures with real multi-confinements effects.

Part II   Theoretical Analysis of Lasing Characteristics in Quantum Microstructure Lasers

Abstract

Theoretical analysis of lasing characteristics in quantum microstructure lasers such as QW, QWW, and QWB lasers are investigated.

We discuss the substrate-orientation on lasing properties of QW lasers using the tight binding method, showing the importance to choose the substrate-orientation while considering which lasing property should be improved for a given application.

We also discuss lasing characteristics of quantum wel box (QWB) lasers theoretically. The results indicate that many lasing properties are significantly improved by using QWB structures but that the size fluctuation of the QWB structures affects the reduction of the lasing characteristics.

In addition, we discuss nonlinear gain effects in quantum microstructure lasers theoretically. The results indicate the nonlinear gain is enhanced with the increase of the dimensionality of quantum confinement.

Chapter VII Introduction of Part II

The ability to fabricate quantum well (QW) devices has given rise to new optical and electronics devices as well as to new physical phenomena [98]. Since the first investigation of optical properties in quantum wells by Dingle *et al.* [3], the application of quantum well structures to semiconductor laser diodes [4], [5] has received considerable attention because of physical interest as well as its superior characteristics, such as low threshold current density [6], [7], low temperature dependence of threshold current [8]-[10], lasing wavelength tunability, and excellent dynamic properties [11]-[13]. By controlling the width of the quantum wells, one can modify the electron and hole wavefunctions, which leads to the modulation of material parameters. The choice of substrate-orientation on which the quantum well structures are grown also leads the modulation of material parameters such as electron or hole effective mass. This results in improvements of the laser characteristics, as well as introduction of new concepts to semiconductor optical devices.

In addition, quantum well wire (QWW) and quantum well box (QWB) structures as well as quantum well structures are received great attention from both physical and technical view points [12], though it is difficult to fabricate QWW and QWB structures at present stage [59]-[66]. Moreover, these quantum microstructure devices are expected to be nonlinear optical devices [57], [58].

In Part II, the theoretical analysis of lasing characteristics in quantum microstructure lasers such as QW, QWW, and QWB lasers are investigated.

In Chapter VII the orientation dependence of lasing characteristics in quantum well lasers are discussed using tight binding method to calculate band structures.

In Chapter VII, the lasing characteristics in QWB lasers are described to clarify the achievable limits of semiconductor lasers.

In Chapter X, optical nonlinear effects in quantum microstructure lasers are discussed.

Chapter VIII Orientation Dependence of Lasing Characteristics in Quantum Well Lasers

8.1. Introduction

In semiconductor lasers, threshold current, relaxation frequency, and α-parameter are important parameters for practical applications. To improve these parameters, modifications of the material using quantum well (QW) structures have been proposed [11] and experimentally demonstrated [99]. In these structures, the change in the density of states from parabolic to step-like is significant. As an ultimate structure, use of quantum wire or box structures was also discussed [11]. In addition for modifying the density of states, changing the effective mass as well as the nonparabolicity of the dispersion curve has been discused using strained-layer structures [100]-[108]. There is, on the other hand, another way to change the dispersion curve, including the effective mass by choosing the substrate-orientation [109]-[121]. In fact, it is well known in a zinc-blende type crystal like GaAs that there exists an asymmetry in the energy bands, especially in the heavy-hole band.

There is experimental work [109]-[119] by Hayakawa, *et al.* showing improved optical properties of excitons in GaAs QWs grown on (111)-substrates as well as the achievement of lower threshold currents in (111)-QW lasers compared with (100) QW

lasers. The theoretical discussion about the valence band structure and optical gain of (111)-QW lasers based on $k \cdot p$ perturbation theory is reported by Batty, et al. [120], and it is indicated that a reduction of threshold carrier density can be achieved in (111)-QW lasers.

In this chapter, we theoretically discuss the asymmetry of the energy band structures in the (100)- and (111)-QW planes in terms of the tight binding method [122]-[130] in order to analyze the band structures more carefully. We also discuss the orientation dependence of several lasing properties. The results indicate that the in-plane effective masses are reduced in (111)-QW lasers, which leads to a reduction of threshold current. These results are consistent with the previous works [109]-[121]. On the other hand, the modulation dynamics and spectral properties are degraded in (111)-QW lasers compared to (100)-QW lasers. The discussion here will reveal the importance of choosing the substrate-orientation carefully considering which lasing property is to be emphasized.

8. 2. Tight Binding Theory

In tight binding theory, we assume that electrons or holes are strongly bound to each atom which consists of crystal lattice [122]-[130]. Therefore, electron (or hole) wave functions are assumed to be expressed by linear combination of atomic orbitals of each atoms such as s-, p_x-, p_y- or p_z- orbitals. By using this assumption, the electron wave function ψ can be expressed as

$$\psi = \sum_n \sum_j C_j^n \, \psi_j^n , \qquad (8\text{-}1)$$

where n and j are labels indicating position of atom and atomic orbitals of each atom, respectively, and ψ_j^n is a wave function of an atomic orbital labeled by n and j. C_j^n is a constant of the linear combination. In the tight binding theory, finding these C_j^n 's is main issue in order to determine ψ and a procedure using Hamiltonian matrix formula is very useful. Eigen vectors and eigen values of Hamiltonian matrix whose elements are expressed by $<\psi_j^n \mid H \mid \psi_k^m>$ and so on correspond to C_j^n 's of the wave functions and energies of electrons, respectively. $<\psi_j^n \mid H \mid \psi_k^m>$ is determined by parameter fitting for the bulk band structures considering the place of each atom and interactions between the orbitals of atoms. Here, we use first

neighborhood approximation, in which one orbital only interacts with orbitals of its neighboring atoms.

8. 3. Energy Band Structures

Fig. 8. 1 and Fig. 8. 2 show the conduction and valence band structures near the Γ point, respectively, of (100)- and (111)-QWs calculated by the tight binding method. In this calculation, a GaAs QW sandwiched by AlGaAs layers grown on (100) or (111) planes is assumed. Note that the in-plane wave vector $k_{//}$ is normalized by $2\pi/a$, where the lattice constant a of GaAs (100) or (111) is 5.66 Å or 6.53 Å, respectively. We assume that the GaAs QW thickness is 50 Å, which corresponds to 18 or 15 atomic layers for (100) or (111)-orientation, respectively. As shown in Fig. 8. 1 and Fig. 8. 2, there is strong dependence of the dispersion curves on the substrate-orientation especially in the valence band, which leads to a difference in the in-plane effective mass.

We summarize the estimated effective masses in Table VIII. I. In Table VIII. I, $m_{\perp}$ is the normal effective mass which is estimated from the quantum energy level by fitting with a simple particle-in-a-box model, $m_{//}$ is the in-plane effective mass estimated from the E-$k_{//}$ dispersion curve and m_0 is the mass of an electron in vacuum. As indicated in this table, concerning the normal effective masses only the heavy hole has a significant dependence on the substrate-orientation. However, this difference in the normal effective masses only causes a change in the band gap energy, (i.e., the lasing wavelength). On the other hand, the change in the in-plane effective mass $m_{//}$ directly influences the band-to-band transition properties. Since there is a strong dependence of $m_{//}$ on the substrate-orientation,

showing all three in-plane effective masses are reduced in the QWs on (111)-orientated substrates, the densities of states of (111)-QWs become smaller than that of (100)-QWs, which leads to significant changes in lasing properties such as threshold current and modulation dynamics.
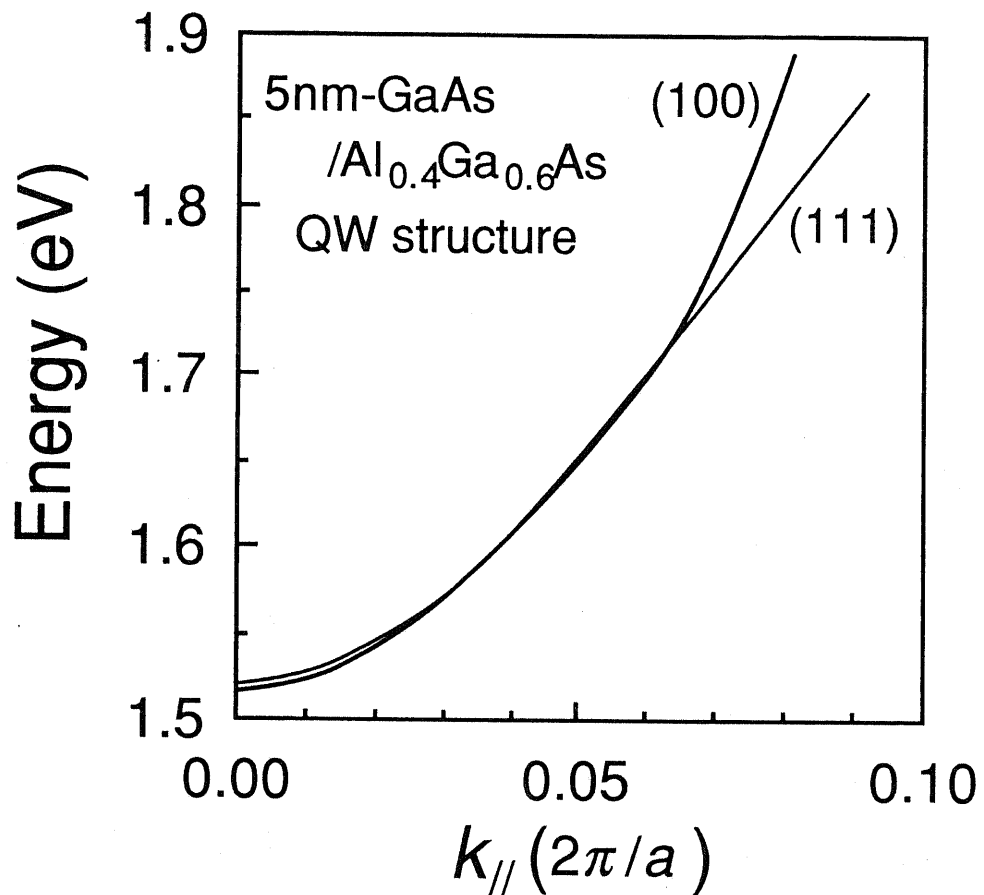
Fig. 8. 1 Conduction band structure near Γ point in (100)- and (111)-QWs.
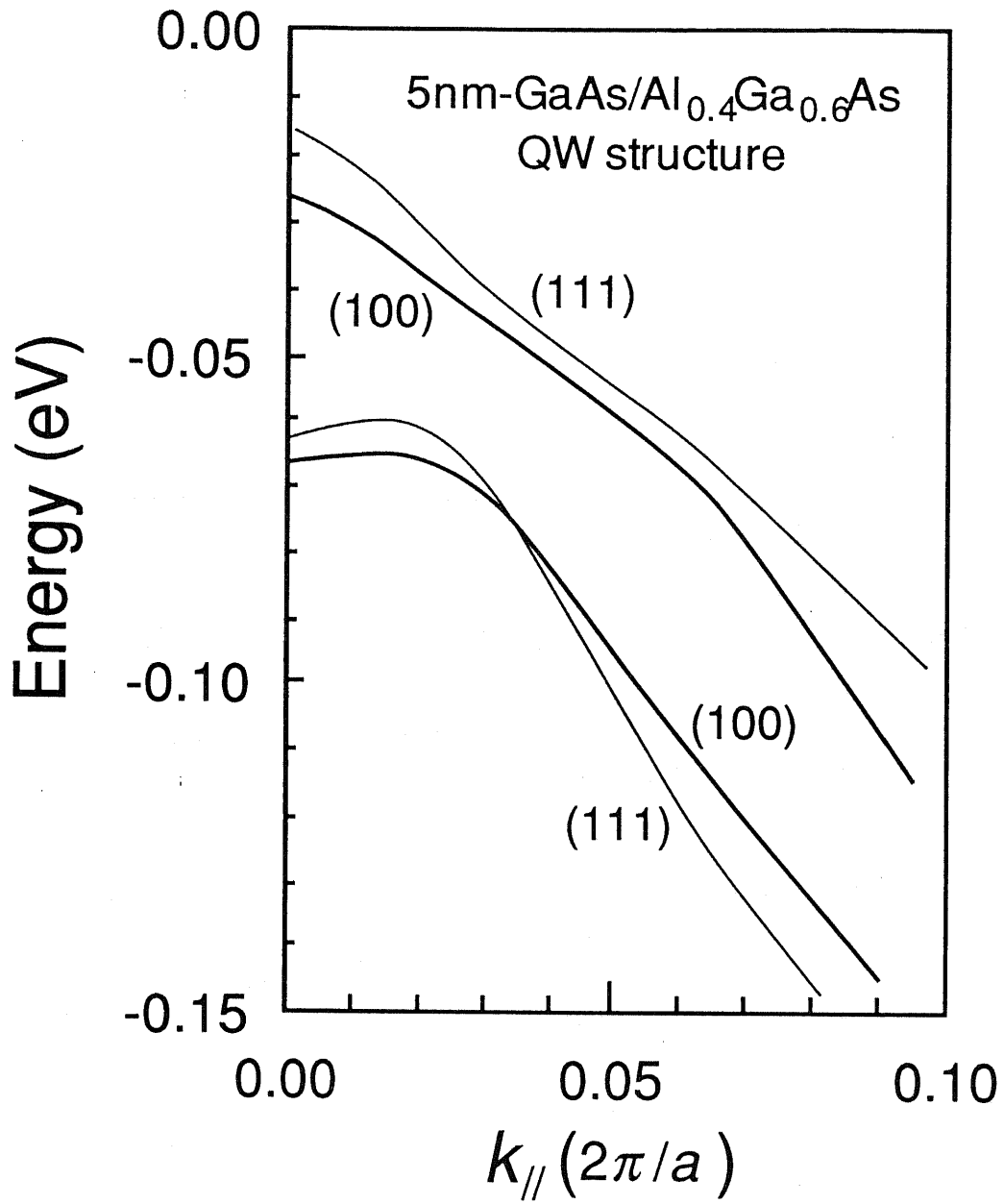
Fig. 8. 2   Valence band structure near Γ point for (100)- and (111)-QWs.

	$m_\perp/m_0$			$m_{/\!/}/m_0$		
	e	h.h.	l.h.	e	h.h.	l.h.
(100)	0.053	0.30	0.070	0.081	0.097	0.83
(111)	0.050	0.59	0.078	0.060	0.060	0.45

Table VIII. I Estimated effective masses for both conduction
and valence bands using the curves in Figs. 8. 1
and 8. 2.

8. 4. Orientation Dependence of Gain Properties

Lasing properties of (100)- and (111)-QW lasers are calculated using the energy band structures shown in Fig. 8. 1 and Fig. 8. 2. The modal gain as a function of the injected carrier density in a single QW (SQW) laser grown on (100) or (111) oriented substrate is shown in Fig. 8. 3. As shown in this figure, the (111)-SQW laser has higher modal gain than the (100)-SQW laser with the same carrier density, which results in lower threshold carrier density in the (111)-SQW laser than in the (100)-SQW laser. This is due to the smaller in-plane effective mass, that is, smaller density of states in the (111)-SQW structure.

Fig. 8. 4 shows the modal gain of a SQW laser as a function of the injected current. The results indicate lower injected current can achieve the same modal gain in the (111)-SQW laser compared to the (100)-SQW laser due to the smaller density of states caused by the smaller in-plane effective mass, which is consistent with previous work [109]-[121]. Since (111)-QW lasers have a smaller density of states, the gain flattening effect, which causes an increase of the threshold current, is more significant than in (100)-QW lasers. However, this problem can be solved by using multi-QW structures, which suggests that it is important to control the number of QWs in conjunction with the substrate-orientation.
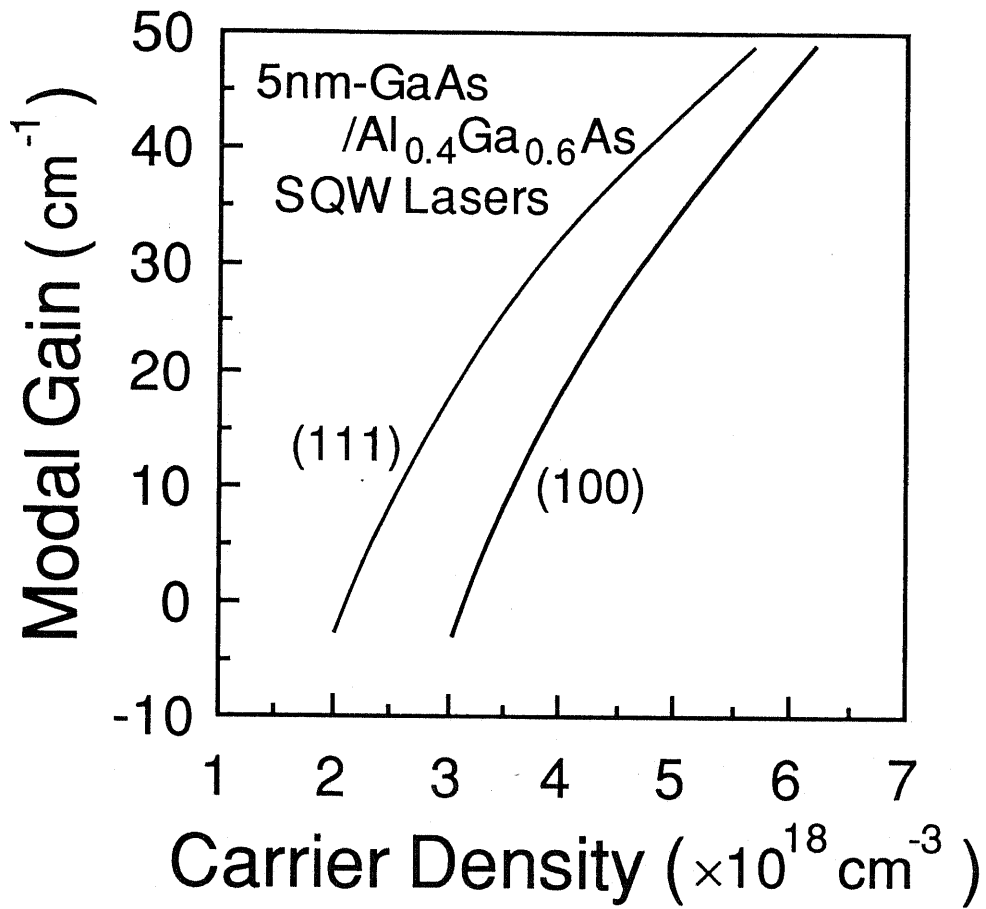
Fig. 8. 3 Modal gain as a function of the injected carrier density in (100)- and (111)-SQW lasers
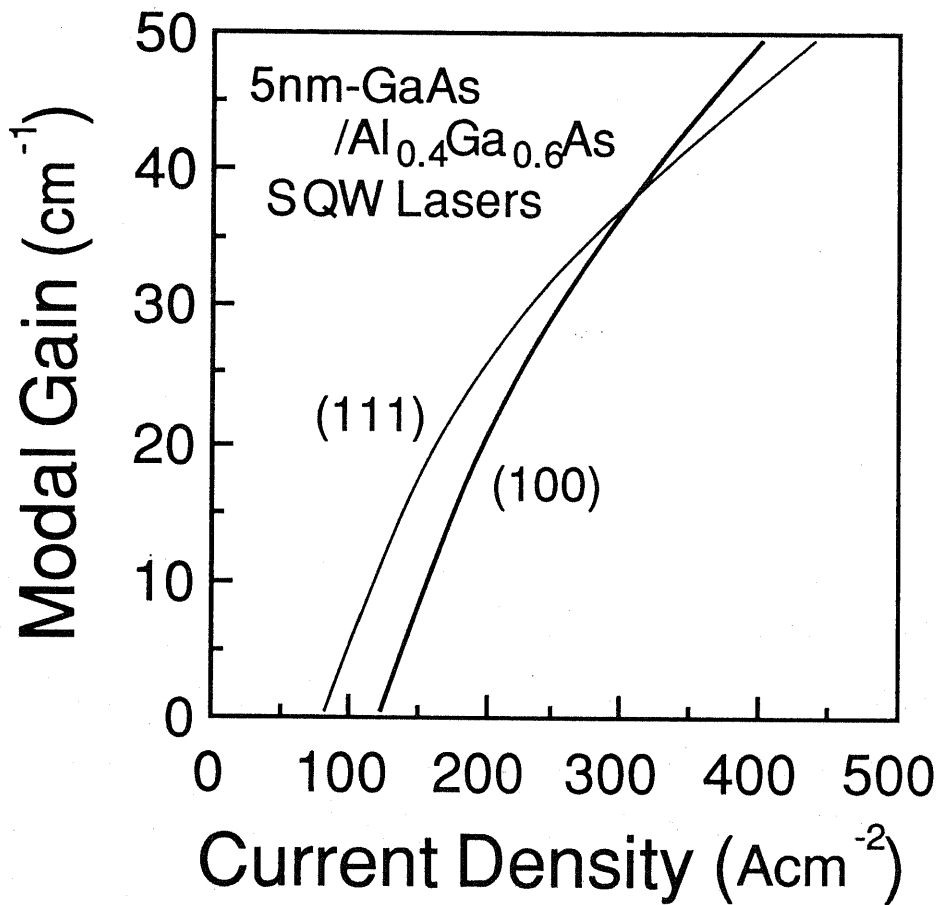
Fig. 8. 4 Modal gain as a function of the injected current
density in (100)- and (111)-SQW lasers

8. 5. Differential Gain Properties

In this section, we discuss the differential gain properties which is very important parameter to determine modulation dynamics. Fig. 8. 5 shows the differential gain as a function of the modal gain in (100) and (111) SQW lasers. The differential gain g' is defined as the derivative of the gain g with respect to carrier concentration n as following equation:

$$g' = \frac{\partial g}{\partial n}. \tag{8-2}$$

Higher differential gain leads to an improvement of the modulation dynamics. As shown in the figure, the differential gain of the (111)-SQW laser is smaller compared to that of the (100)-SQW laser. This is also due to the reduced in-plane effective masses of (111)-SQW lasers. This result indicates that QW structures grown on (111)-substrates are not as effective compared to QW lasers on (100) substrates in order to enhance the modulation bandwidth.
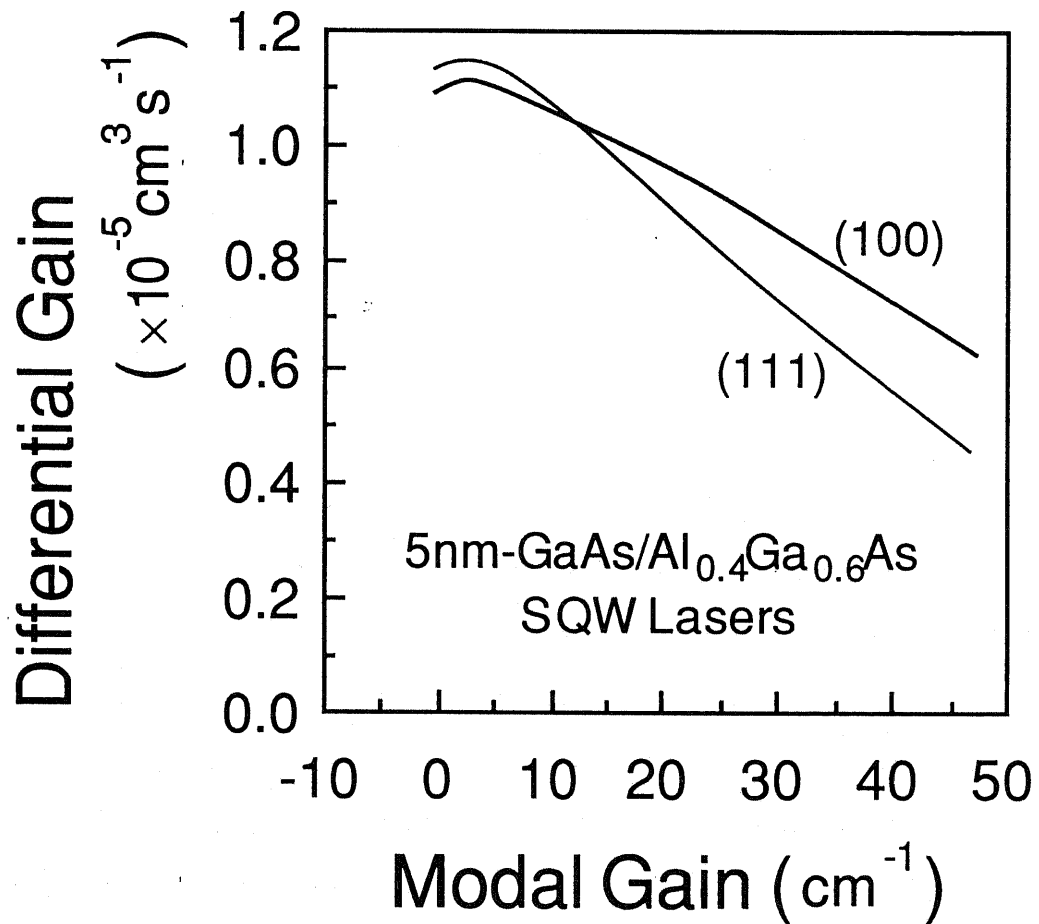
Fig. 8. 5   Differential gain as a function of the modal gain of
(100)- and (111)-SQW lasers.

8. 6. Spectral Properties

In semiconductor lasers, the spectral linewidth Δv is enhanced by a factor $(1+\alpha^2)$ as compared to the Schawlow-Townes linewidth Δv_{ST}, which expresses the spectral linewidth in conventional gas or solid state lasers. α is referred to as the linewidth enhancement factor defined as following equation:

$$\alpha = \frac{\partial \chi_R / \partial n}{\partial \chi_I / \partial n}, \qquad (8\text{-}3)$$

where χ_R and χ_I are the real and imaginary part of the complex susceptibility, respectively, and n is the carrier density. Fig. 8. 6 shows the substrate-orientation dependence of the linewidth enhancement factor α as a function of the modal gain in the (100)- and (111)-SQW lasers. Unless a quite low total loss is achieved, or a large number of QWs is used, the α of the (111)-SQW laser is worse than that of the (100)-SQW laser. This result is also due to the reduction of the in-plane effective masses of the (111)-SQW laser.
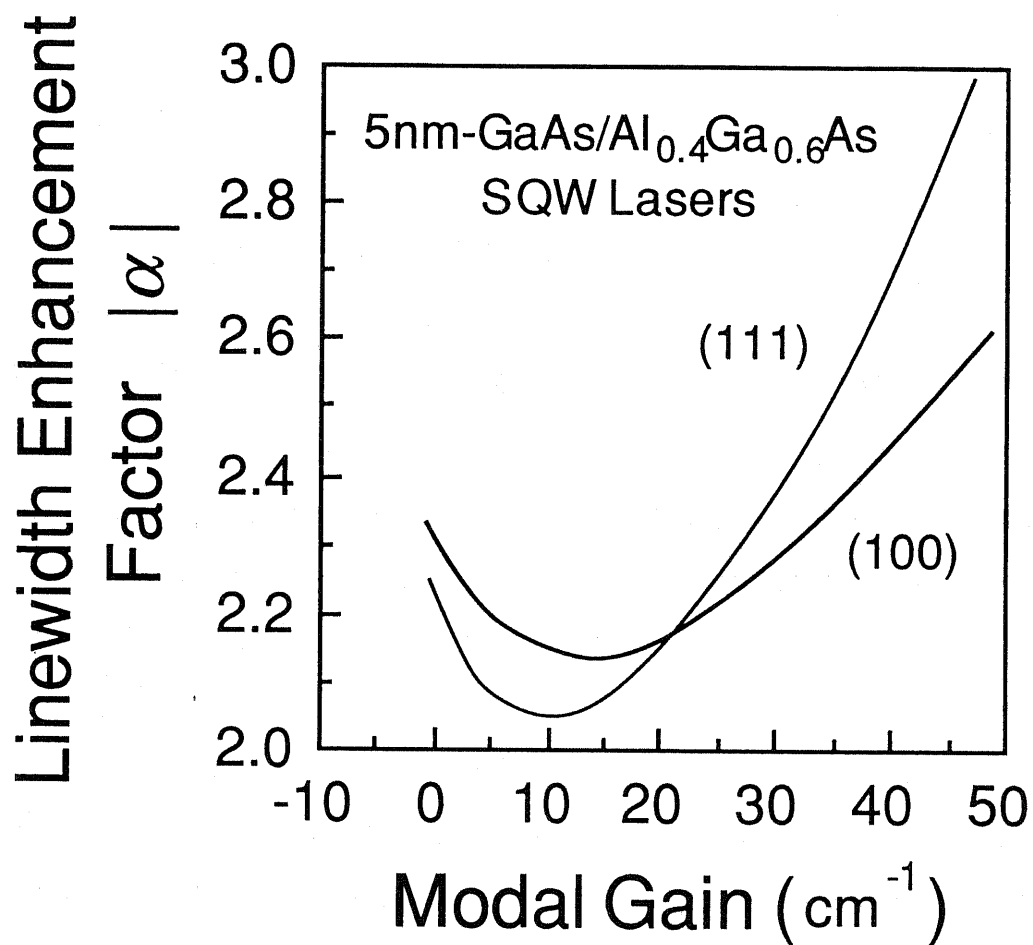
Fig. 8. 6   Linewidth enhancement factor α as a function of the modal gain of (100)- and (111)-SQW lasers.

8. 7. Effective Masses

In this section, we discuss the well thickness dependence of the normal effective masses $m_\perp$ and the in-plane effective masses $m_{//}$, in the (100)- and (111)-planes. Fig. 8. 7 shows the $m_\perp$'s of (a) electron and (b) heavy-hole in the (100)- and (111)-planes as a function of quantum well thickness. In this figure, all masses are normalized by the (100) bulk electron effective mass $m_\perp^{(100)}$. As shown in this figure, $m_\perp$'s of both electron and heavy-hole increase with the increase of the quantum well thickness. Though the difference of the normal effective masses affect the quantized energy levels, that is, lasing wavelengths, it is not important for the lasing dynamics.

Fig. 8. 8 shows the $m_{//}$'s of (a) electron and (b) heavy-hole in the (100)- and (111)-planes as a function of the quantum well thickness. As is shown in this figure, all of the $m_{//}$'s increase with decreasing well thickness. However, it is indicated that the $m_{//}$ of the heavy-hole in the (100)-plane has a strong dependence on well thickness, but that in the (111)-plane, the $m_{//}$ of the heavy-hole hardly depends on the well thickness.

The ratio of in-plane effective masses of electron and heavy-hole plotted as a function of the quantum well thickness is shown in Fig. 8. 9. In (111)-plane the ratio gets near 1 with decrease of the quantum well thickness in contrast to the ratio in (100)-plane. In general, heavy in-plane effective mass leads to the increase of carrier density at the transparency and threshold current and also leads to the suppression of the gain flattening

effect. On the other hand, the balance of effective masses of electron and heavy-hole leads to the reduction of carrier density at the transparency and threshold current. The gain properties in (100) and (111) SQW lasers are plotted as a function of the injected current density in Figs. 8. 10 (a) and (b), which indicate that the gain property is improved in thin SQW lasers and that this improvement is more remarkable in (111) SQW lasers because the less dependence of $m_{//}^{h.h.}$ (111) on the quantum well thickness and the good balance of electron and heavy-hole masses. Thus, the orientation dependence of the lasing properties caused by the asymmetry of the in-plane effective masses should be more enhanced in thinner quantum well structures.
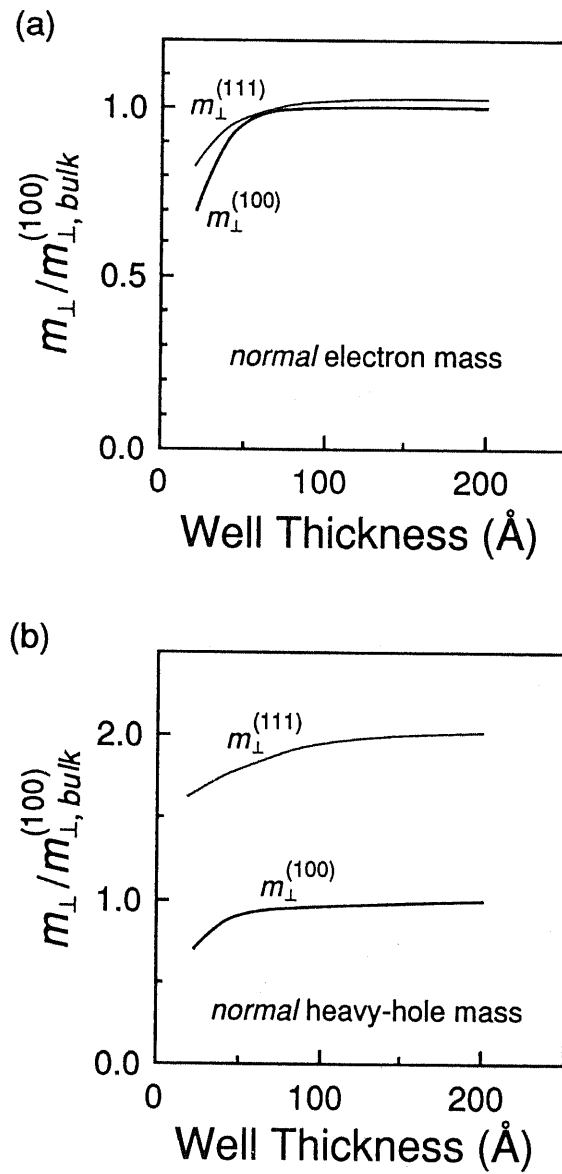
Fig. 8. 7 Normal effective masses $m_\perp$'s of (a) electron and (b) heavy-hole in the (100)- and (111)-planes as a function of quantum well thickness.
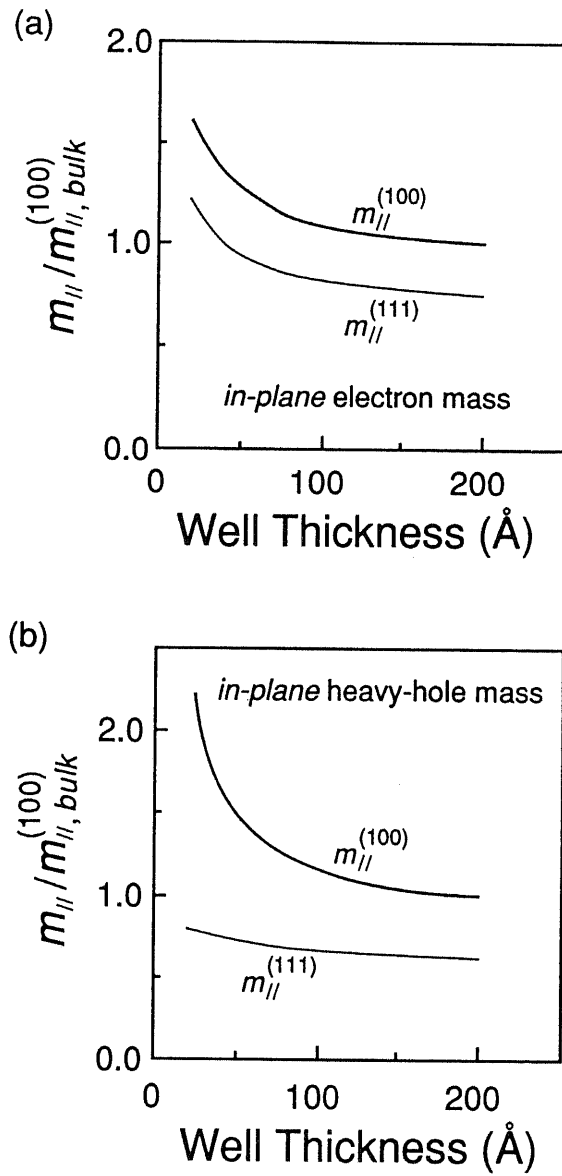
Fig. 8. 8   In-plane effective masses of (a) electron and (b) heavy-hole as a function of quantum well thickness.
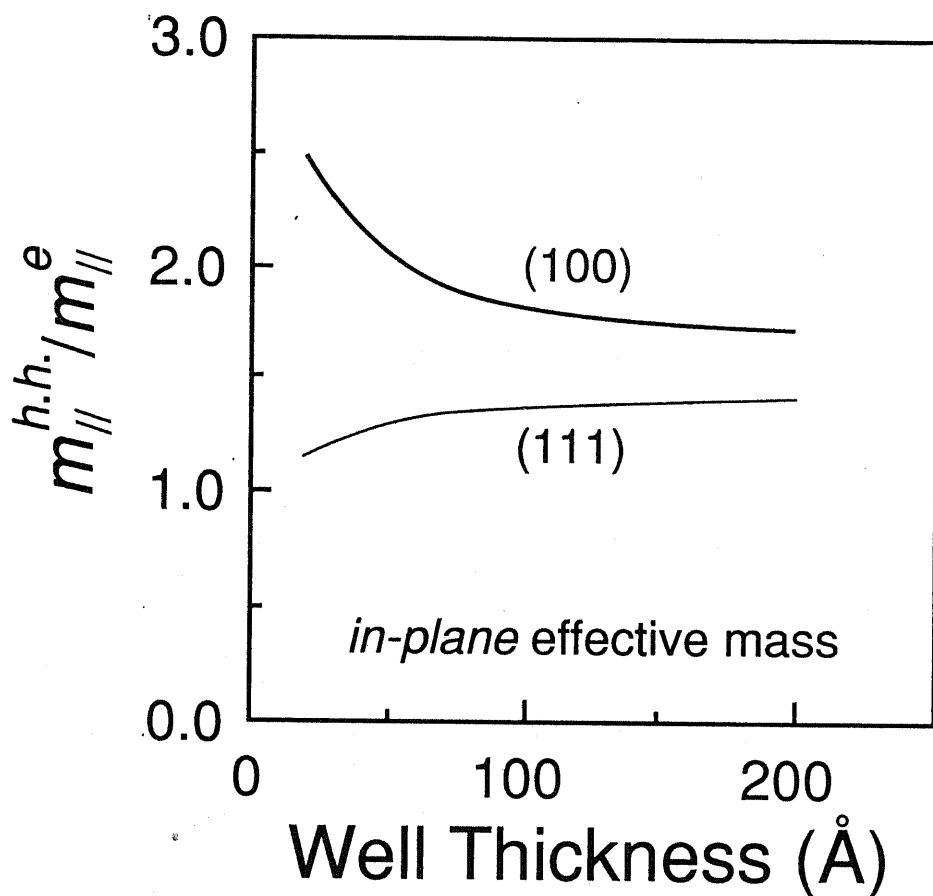
Fig. 8. 9   The ratio of in-plane effective masses of electron and heavy-hole plotted as a function of the quantum well thickness.

(a)

(b)
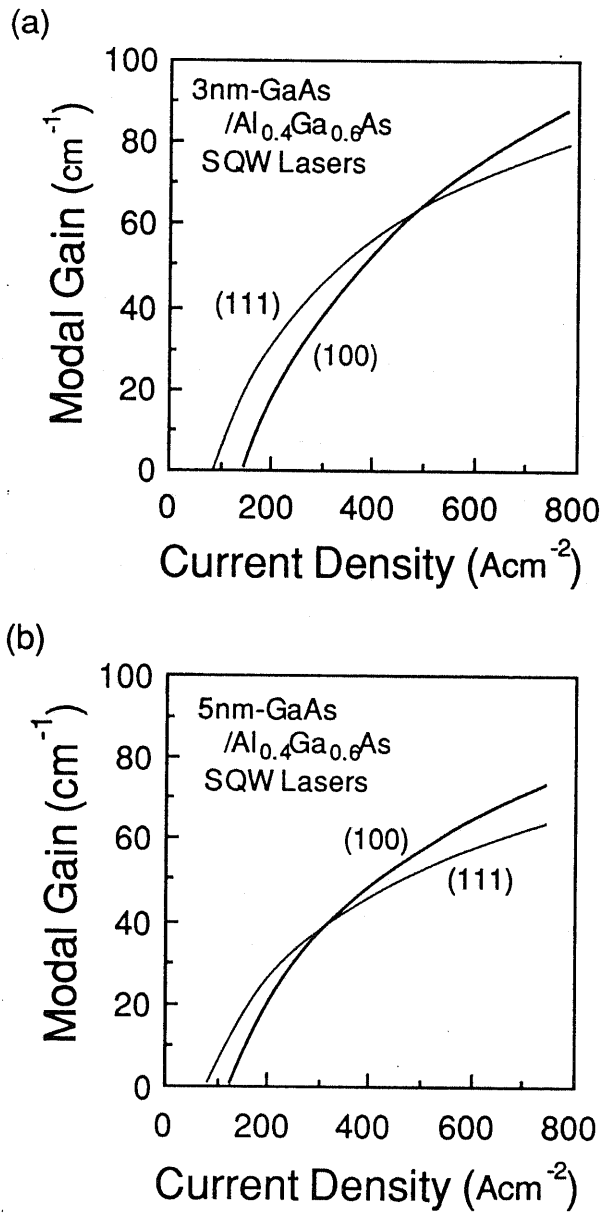
Fig. 8. 10 The gain properties in (100) and (111) SQW lasers are
plotted as a function of the injected current density
with two kinds of quantum well thickness ((a): 3 nm
and (b): 5 nm).

8. 8. Concluding Remarks

In Chapter VIII, we have investigated the effects of the substrate-orientation on lasing properties of QW lasers using the tight binding method to calculate the band structures. As a result, the threshold current density in (111)-QW lasers can be reduced compared to (100)-QW lasers. On the other hand, the modulation dynamics and spectral properties are degraded in (111)-QW lasers. These results are due to the reduction of the in-plane effective masses of the QWs grown on (111)-orientated substrate. It is important to choose the substrate-orientation while considering which lasing property is to be improved for a given application.

Chapter IX Lasing Characteristics in Quantum Well Box Lasers

9. 1. Introduction

Recent progress of direct write lithograph technology combined with epitaxial growth technology for quantum well materials leads to the possibility of realizing quantum well wire (QWW) and quantum well box (QWB) structures. In 1982, Arakawa and Sakaki proposed use of arrays of QWW and QWB as the active layer of a semiconductor laser [10]. Preliminary theoretical studies have discussed threshold current characteristics [70], [71], modulation bandwidth [11] and spectral properties [131] in QWB lasers, noise characteristics in QWB amplifiers [72] and line shape functions in QWB structures [73]. The QWB effects in the semiconductor lasers are also experimentally demonstrated by placing a quantum well laser in a high magnetic field in which the QWB structures are simulated [131]-[133]. However, achievable limits of those characteristics due to the QWB effect have not been clarified sufficiently [134].

The purpose of this chapter is to discuss the achievable limits of the lasing characteristics due to the QWB effects quantitatively, emphasizing the importance of controlling the number of QWBs in the active layer. The results indicate the possibility of achieving threshold current as low as 1 µA, wider modulation bandwidth and higher coherency than those of

double heterostructure (DH), QW and QWW lasers. In addition, the modulation doping effects in the QWB lasers is investigated, which leads to further improvements of lasing characteristics. Lastly, influence of the size fluctuation of the QWB structures on the lasing characteristics is discussed.

9. 2. Concept and Modeling of Quantum Well Box Lasers

With reduction of dimensionality of electron-motion freedom in QW, QWW, and QWB structures, the density of states changes from a parabolic function to a step-like function, a reciprocal of square-root function, and a delta-function, respectively, having less broadened density of states. Fig. 9. 1 shows a simple illustration of those structures together with the configurations of the density of states.

In a QWB structure, the density of states (per unit energy and box) of electrons is given by

$$\rho_c(E) = 2 \sum_{k,m,n}^{\infty} \delta(E - E_k - E_m - E_n), \qquad (9\text{-}1)$$

where E_k, E_m, and E_n are the quantized energy levels of a QWB structure in x, y, and z directions, respectively. If we assume a structure consisting of cubic GaAs/AlGaAs QWBs with a dimension of L_z, energy levels $\{E_i\}_{i=k,m,n}$ are expressed by the following equation, where the barrier height in the potential profile is assumed to be infinite:

$$E_i = \frac{h^2}{2m_{c,i}} (\frac{\pi}{L_z})^2 \qquad (9\text{-}2)$$

where $m_{c,i}$ is the effective mass of electrons along the i-axis. When higher subband energy levels in both conduction band and

valence band are ignored, the electronic state is equivalent to that of two-levels atomic systems. Therefore, the basic properties of the QWB lasers should be coincide with those of gas lasers.

In the actual devices, injection efficiency of carriers is important. If the QWBs are completely isolated, the injection of carriers into each QWB is difficult. Therefore, in order to realize high injection efficiency of carriers, the tunneling effect between each QWB should be utilized, while keeping the QWB effects. For this purpose, the barrier thickness is designed carefully so that the tunneling time τ_T satisfies following relations:

$$\tau_r \gg \tau_T \gg \tau_{in}, \qquad (9\text{-}3)$$

where τ_r and τ_{in} are the recombination lifetime and the intraband relaxation time, respectively. The first unequal relation implies that the tunneling time should be short compared to the recombination time so that carrier injection occurs sufficiently before the carrier recombination. On the other hand, the second unequal relation implies that the tunneling time should be long enough so that the broadening effect in the gain profile due to this tunneling effect can be negligibly small compared to the intraband relaxation effect.
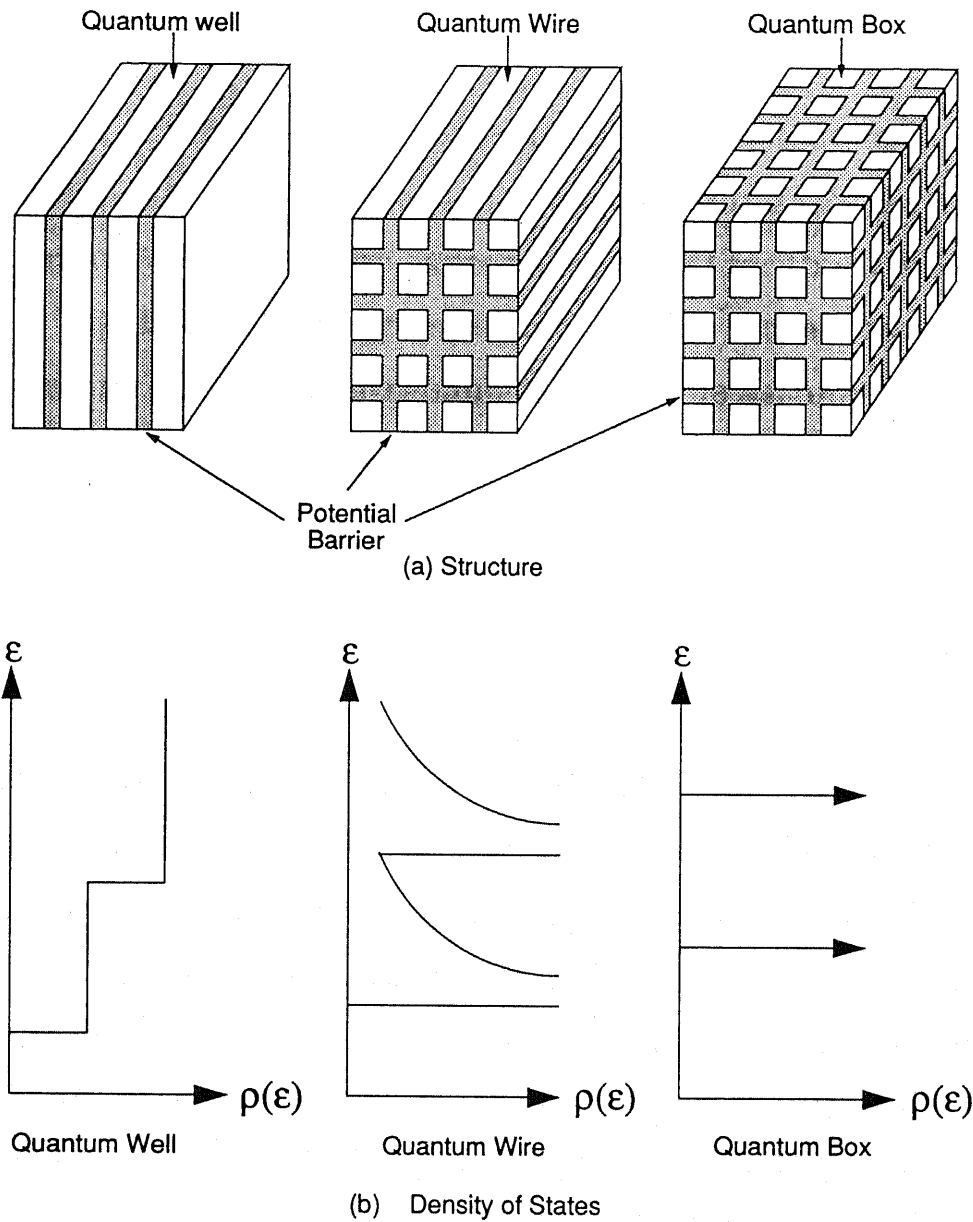
Fig. 9. 1 A simple illustration of those structures together with
the configurations of the density of states.

9. 3. Gain Properties and Threshold Current

Since the density of states has a peaked structure, the gain profile $g(E)$ of the semiconductor lasers having QWB structures is extremely narrow. The expression of $g(E)$ for the QWB laser is given by the following equation if the Lorentzian energy broadening due to the intraband relaxation is assumed:

$$g(E) = 2 \sum_{k,m,n}^{\infty} A \frac{\hbar/\tau_{in}}{(\hbar/\tau_{in})^2 + (E - E_k - E_m - E_n)^2}$$

$$(9\text{-}4)$$

where A is a constant proportional to the matrix element. If higher subbands can be ignored, the gain profile of this laser is very narrow. Therefore, importance of Fermi statics in shaping the gain profile is reduced in the QWB structures. This property results in extremely low threshold current and extremely wide modulation bandwidth. Note that the dipole matrix element of the electron-hole pairs in the QWBs is equal to that in the DH structures since both structures are isotropic structures.

Fig. 9. 2 shows the modal gain (i. e., the bulk gain multiplied by the optical confinement factor Γ), plotted as a function of the injected current for various numbers of QWBs. In the calculation, it is assumed that the QWB structure has GaAs cubic active layers of 50 Å, sandwiched by AlGaAs barriers of 50 Å. Since higher subbands effects are almost suppressed in QWB structures with 50 Å, the lasing characteristics in this laser

exhibit achievable limit. In fact, the lasing characteristics of the QWB lasers with larger dimension are inferior to those with 50 Å dimensions. The cavity length of the laser is 300 µm and τ_{in} is 0.2 psec. It is assumed that all carriers are injected into the active region, ignoring non-radiative effects such as the carrier leakage effect. For simplicity, in the direction of the cavity length, the active layer is filled with the QWBs sandwiched by the barriers. Therefore, the controllable parameter concerning the total number of QWBs is the number of two-dimensional QWB arrays N in the plane which is perpendicular to the direction of the cavity length. It is also assumed that the laser has a separate confinement structure in which optical confinement regions surround the QWB active region, so that Γ can be assumed to be proportional to N.

Since the gain saturates with the increase of the injected current, as shown in Fig. 9. 2, there exists an optimum N for minimizing the threshold current. If, for instance, the modal gain is 100 cm^{-1}, the optimum N is about 10, which results in a threshold current of about 25 µA. Note that the value of the threshold current strongly depends on the intraband relaxation time and the configuration of the broadening function. If the broadening function is a Gaussian function, the gain value is enhanced, leading to lower threshold current.

Fig. 9. 3 shows the threshold current plotted as a function of the cavity length for various reflection coefficients R on the basis of the gain properties in Fig. 9. 2. As shown in the figure, there

exists the optimum cavity length to minimize threshold current for each R. The results indicate that an extremely low threshold current, as low as 1 µA, might be obtained with ~ 1 µm cavity length for $R = 0.9$. This value is much smaller than in QW lasers, in which the expected lowest threshold current is about 100 µA.
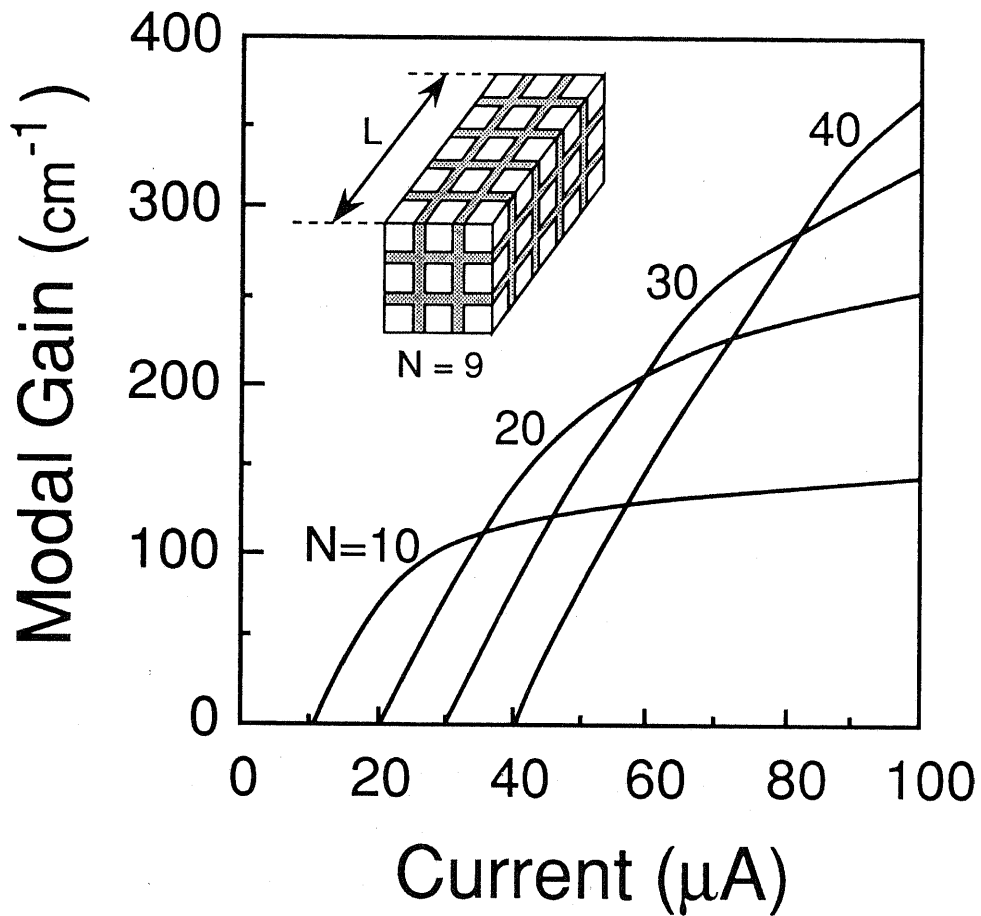
Fig. 9. 2 Modal gain (i. e., the bulk gain multiplied by the optical confinement factor Γ), plotted as a function of the injected current for various numbers of QWBs.
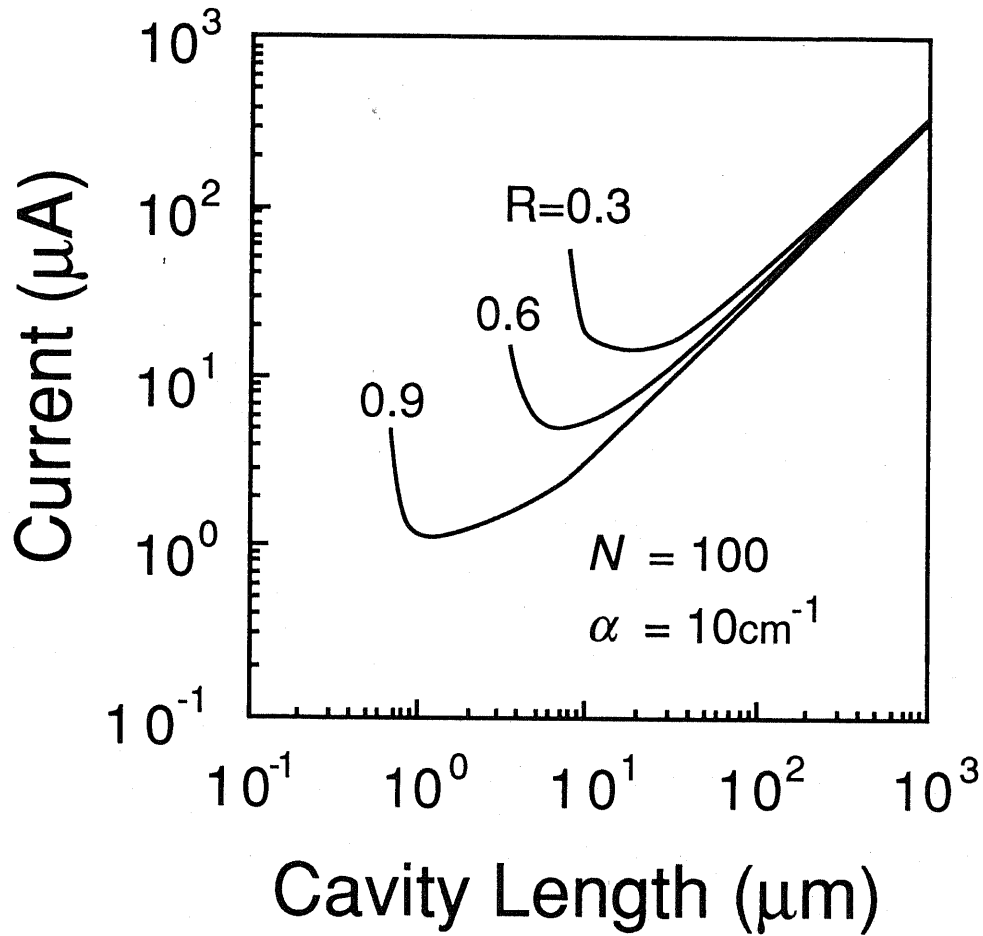
Fig. 9. 3   Threshold current plotted as a function of the cavity
length for various reflection coefficients R on the basis
of the gain properties in Fig. 9. 1.

9. 4. Modulation Dynamics

Modulation characteristics are very important for practical application of semiconductor lasers to high-speed optical communication systems. The important parameter for the modulation bandwidth is the relaxation resonant frequency f_r, which can be derived by conventional rate equations. The result is

$$f_r = \sqrt{\frac{g' P_0}{\tau_p}} \qquad (9\text{-}5)$$

where P_0, τ_p, and g' are the stationary photon density in the cavity, the photon lifetime, and the differential gain (i. e., $g' = \partial g/\partial n$, where n is the carrier density), respectively. Eq. (9-5) indicates that increase of g' or P_0, and decrease of τ_p leads to enhancement of f_r. In the QWB laser, we can expect that g' is greatly enhanced compared to DH lasers since the gain profile is extremely narrow. Therefore, use of the QWB structure in the semiconductor lasers leads to ultra high-speed modulation.

Fig. 9. 4 shows g' of the QWB laser plotted as a function of the quasi-Fermi energy level ε_{fc} which is measured on the basis of the quasi-Fermi energy level ε_{trans} at which the transparent condition is satisfied. For comparison, g's of the QW laser and the QWW laser are also plotted. The results indicate two important features. The first one is that g' is enhanced in QWB lasers compared to QWW lasers by a factor of three and to QW lasers by a factor of ten, if low quasi-Fermi energy level is chosen by

increasing the number of QWBs. In this case, the maximum value of g' in a QWB lasers reached over 7×10^{-5} cm^{3}s^{-1}. The second one is that g' is strongly dependent on the quasi-Fermi energy level, which is more pronounced with the decrease of the dimension of electron motion freedom. Owing to this fact, the wide modulation bandwidth can be achieved by increasing N, since the quasi-Fermi energy at the lasing conditions becomes lower with larger N. As a result, the modulation bandwidth f_r of the QWB laser is about three times as high as that of the QW laser and six times as high as that of a DH laser.
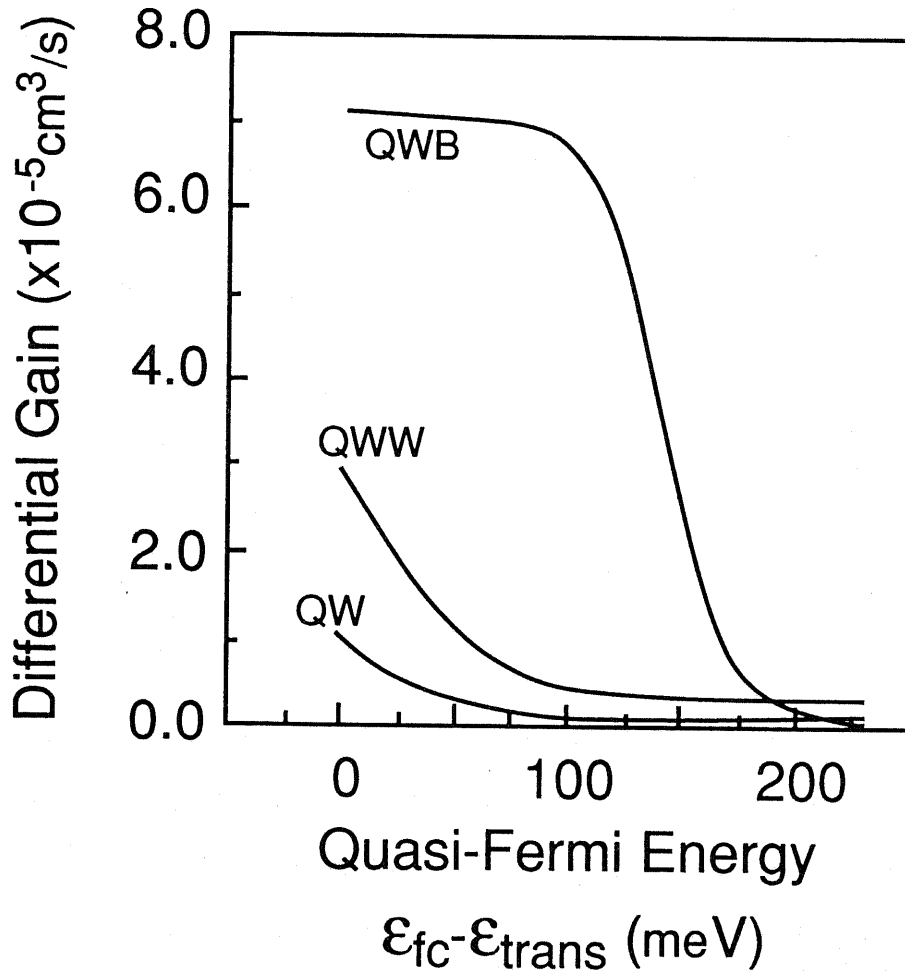
Fig. 9. 4   Differential gain g' of the QWB laser plotted as a function of the quasi-Fermi energy level ε_{fc} which is measured on the basis of the quasi-Fermi energy level ε_{trans} at which the transparent condition is satisfied.

9.5. Spectral Properties

Coherency is one of important characteristics in laser properties. In semiconductor lasers spectral linewidth $\Delta \nu$ is broadened by a factor of $(1+\alpha^2)$ compared to well-known Schawlow-Townes spectral linewidth $\Delta \nu_{ST}$ as followings;

$$\Delta \nu = \Delta \nu_{ST}\,(1+\alpha^2)\,, \qquad\qquad (9\text{-}6)$$

$$\Delta \nu_{ST} = \frac{V_g^{\,2}\, h\nu\, \Gamma g\, R_m\, n_{sp}}{\pi P_0}\,, \qquad\qquad (9\text{-}7)$$

$$\alpha = \frac{\partial \chi_R / \partial n}{\partial \chi_I / \partial n}\,, \qquad\qquad (9\text{-}8)$$

where V_g, $h\nu$, Γ, g, R_m, P_0 and n_{sp} are the group velocity, photon energy, optical confinement factor, bulk gain coefficient, mirror loss, output power intensity and spontaneous emission factor, respectively. χ_R and χ_I are the real and imaginary part of the complex susceptibility, respectively, and n is the carrier density. This α is called as the linewidth enhancement factor. Denominator of Eq. (9-8) corresponds to differential gain discussed in Section 9.4. In DH lasers the wavelength that gives the maximum of denominator of Eq. (9-8) does not coincide the wavelength that gives the minimum of numerator of Eq. (9-8). Actually, measured $|\alpha|$ in DH laser is 2~7. On the other hand, QWB lasers can be considered to be two-levels lasers if higher subbands can be neglected. In the two-levels lasers the

wavelength which gives the maximum of denominator of Eq. (9-8) completely coincides the wavelength that gives the minimum of numerator of Eq. (9-8). Therefore, it is expected that α in QWB lasers becomes almost zero and that Δv is narrowed to Δv_{ST}.

Fig. 9. 5 shows calculated $|\alpha|$'s in QW, QWW and QWB lasers as a function of the quasi-Fermi energy level $\varepsilon_{fc} - \varepsilon_{trans}$. As shown in this figure, $|\alpha|$ in QWB lasers is almost zero when $\varepsilon_{fc} - \varepsilon_{trans}$ is low, which indicates the high coherency of QWB lasers. On the other hand, $|\alpha|$ in QWB lasers drastically increases with the increase of $\varepsilon_{fc} - \varepsilon_{trans}$ above 150 meV. This is due to the higher subbands effects in QWB lasers. These results indicate that quasi-Fermi energy at the operating point of QWB lasers should be low, and that, therefore, it is needed to increase the number of QWB's.

As indicated in Eqs. (9-6) and (9-7), spectral linewidth Δv is proportional to $n_{sp} (1+\alpha^2)$. Fig. 9. 6 shows α, n_{sp} and $n_{sp} (1+\alpha^2)$ in QWB lasers as a function of quasi-Fermi energy level $\varepsilon_{fc} - \varepsilon_{trans}$. As shown in this figure, there exists an optimal point to minimize the spectral linewidth, which indicates that it is important to design the number of QWB's in order to realize the narrowest spectral linewidth.
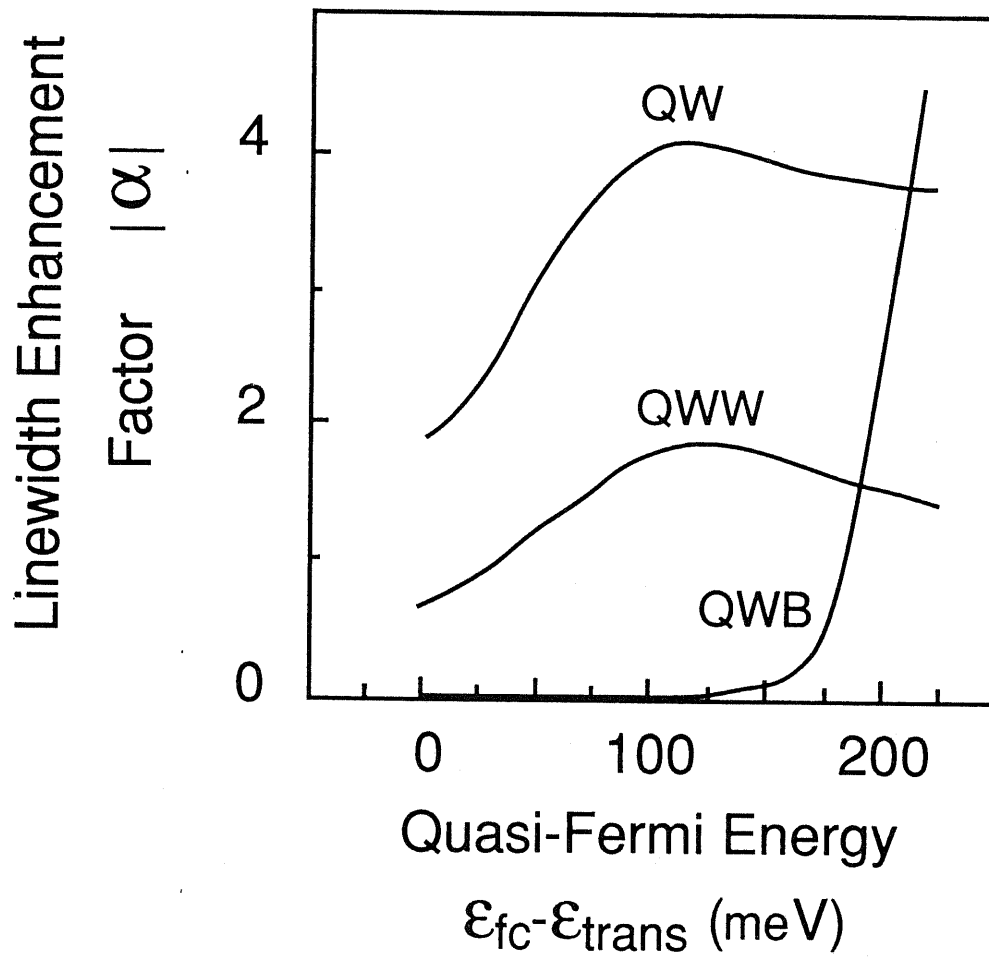
Fig. 9. 5 Calculated $|\alpha|$'s in QW, QWW and QWB lasers as a function of the quasi-Fermi energy level $\varepsilon_{fc}-\varepsilon_{trans}$.
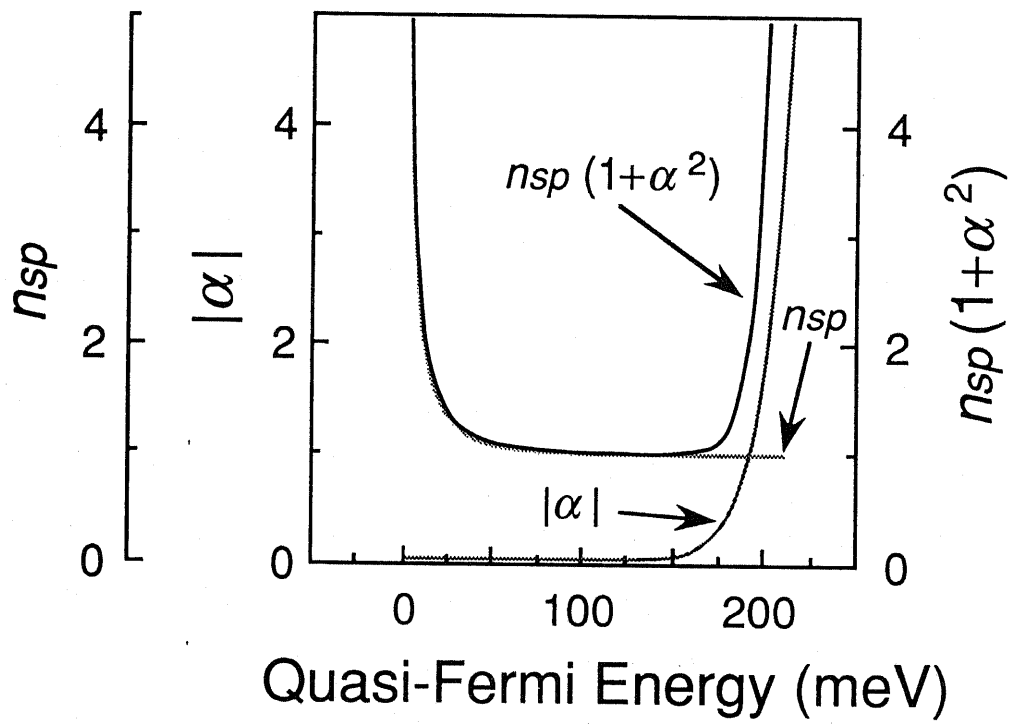
Fig. 9. 6 Calculated α, n_{sp} and n_{sp} $(1+\alpha^2)$ in QWB lasers as a function of quasi-Fermi energy level $\varepsilon_{fc}-\varepsilon_{trans}$.

9. 6. Modulation Doping Effects

Recently use of the modulation dopes structures in QW lasers has been proposed and demonstrated experimentally [135]. It is predicted that lasing properties are improved by using p-modulation doped structures. In these modulation doped structures, the acceptors are doped in the barrier layers so that the hole density can be changed without causing broadening if the energy levels of electrons in the QWBs on the basis a simple model. In this section, we discuss briefly the modulation doping effect on the modulation characteristics of QWB lasers.

Fig. 9. 7 shows the differential gain plotted as a function of the doping level, where the doping level is normalized by the number of QWBs. As shown in this figure, the differential gain strongly depends on the doping level, where the threshold modal gain and N are assumed to be 85 cm^{-1} and 10, respectively. The result indicates that the modulation doping of acceptors in QWBs leads to further improvement in the lasing characteristics, showing that g' is enhanced by a factor of three in the highly doped QWB laser compared to undoped QWB lasers.

However, the calculated results also indicate that the maximal value of the differential gain which is given by the quasi-Fermi energy level with the transparency condition is not dependent in the doping levels. Consequently, if the necessary gain is much smaller and large number QWBs is prepared in the active layer, the advantage of the modulation doping effects

disappears. In addition, more careful discussion might be required for utilizing the modulation effects in the QWB lasers.
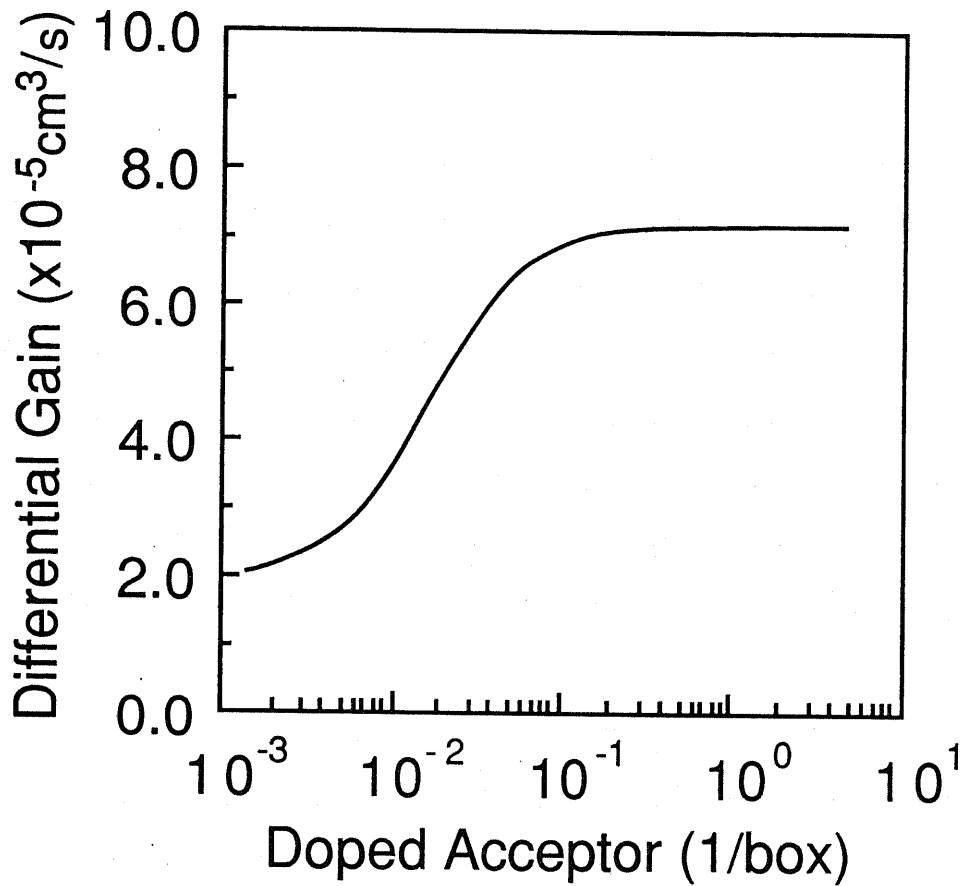
Fig. 9. 7 Differential gain plotted as a function of the doping level, where the doping level is normalized by the number of QWBs.

9. 7. Size Fluctuation Effects on Lasing Characteristics

There have been some reports on the fabrication of the QWW structures and QWB structures. However, at the present stage, this fabrication still involves difficult problems to be solved. The first one is to fabricate fine structures with smaller size. In fact, fabrication of smaller structures with less than 300 Å are very difficult at present. In addition, even if this problem is overcome, the size fluctuation problems still exists. With the decrease of cubic dimensions, this factor becomes mire important. The size fluctuation is equivalent to inhomogeneous broadening in the gain profile which reduces high gain effects. In fact, the size fluctuation leads to the energy broadening of the quantized levels.

Fig. 9. 8 shows g' plotted as a function of $\xi = \Delta L_z / L_z$ for $L_z = 50$ Å, where L_z is the average dimension of the cubic QWBs and ΔL_z is the standard deviation of L_z due to the size fluctuation. In this calculation the size fluctuation effects are included by considering the Lorentzian broadening in the gain profile due to both the intraband relaxation time and this size fluctuation. The result indicates that g' decreases drastically with the increase of ξ, demonstrating the importance of fabricating uniform QWB structures.
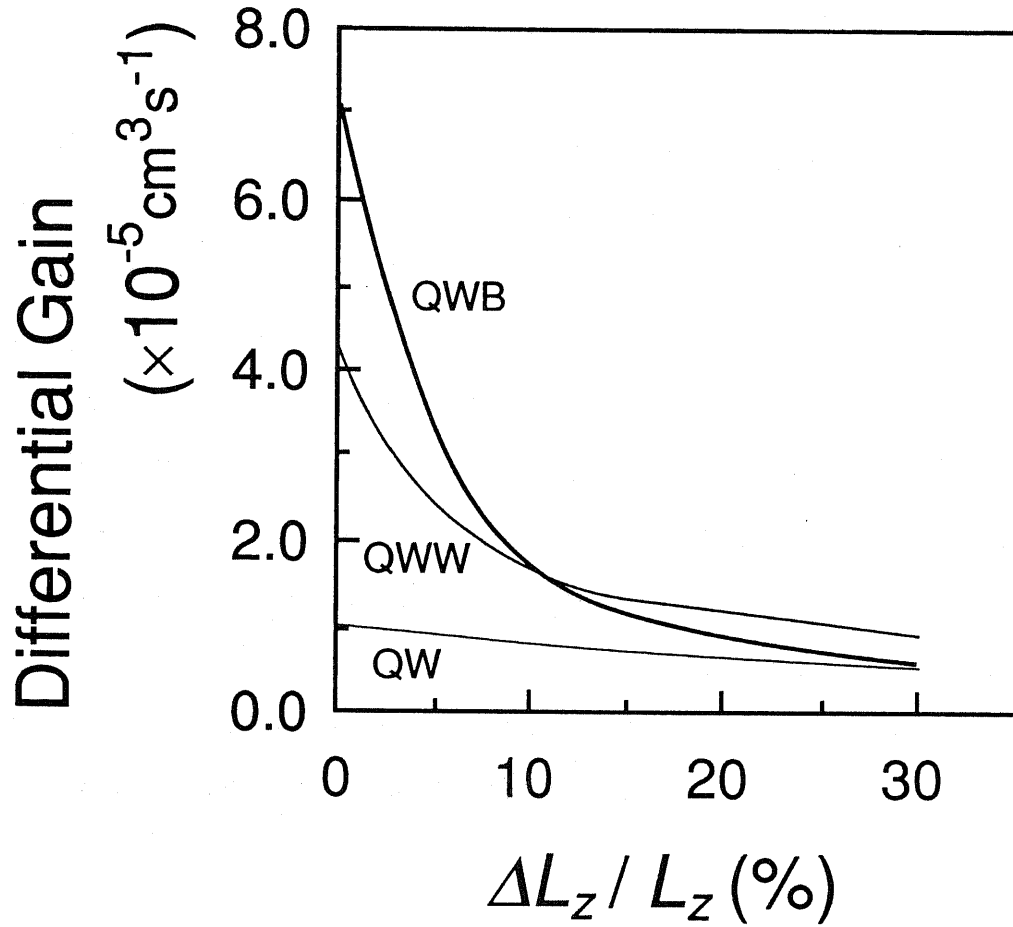
Fig. 9. 8   Differential gain g' plotted as a function of $\xi = \Delta L_z/L_z$
for L_z = 50 Å, where L_z is the average dimension of the
QW, QWW or QWB, and ΔL_z is the standard deviation
of L_z due to the size fluctuation.

9. 8. Concluding Remarks

In Chapter IX, we investigated lasing characteristics of GaAs/AlGaAs semiconductor lasers having QWB structures theoretically. The results indicate that threshold current, modulation dynamics and spectral properties are significantly improved by carefully controlling the total number of QWBs as well as quantum box dimensions. Furthermore, effects of the modulation doping and the size fluctuation on the lasing characteristics are also discussed. At present it is still difficult to realize these QWB lasers. However, in the near future we might achieve such fine-structure lasers since the fabrication technology is progressing very rapidly. For more careful discussion of those lasing characteristics, we have to clarify several parameters such as the intraband relaxation time and the configuration of the gain broadening function.

Chapter X   Optical Nonlinear Effects in Quantum Microstructure Lasers

10. 1. Introduction

Investigation of nonlinear gain in semiconductor lasers is important since those properties play important roles in certain laser characteristics such as modulation dynamics [57], [136]-[139], laser amplification [58], and phase conjugate wave generation [140]. Recently, the nonlinear gain effects in semiconductor lasers were experimentally discussed [141]-[143] As the main mechanisms for the gain nonlinearity, the spectral hole burning, spatial hole burning, and carrier heating have been so far discussed [144]-[152]. Among these mechanisms, the spectral hole burning is the most intrinsic mechanism which directly reflects the quantum confinement effect of electrons.

In this chapter, we present the nonlinear gain effects due to the spectral hole burning in QW, quantum well wire (QWW), and quantum well box (QWB) lasers theoretically. As a result, it is found that the gain nonlinearity is enhanced by the quantum-confinement of carriers and is further enhanced in the QWW and QWB lasers. These nonlinear gain effects significantly affect the modulation dynamics of the semiconductor lasers under high photon density condition. It should be emphasized here that not only the damping rate but also the resonant relaxation frequency is degraded through reduction of the differential gain. We also discuss the effects of nonlinear gain on the spectral dynamics.

The result indicates that the gain nonlinearity causes enhancement of the linewidth enhancement factor α with the increase of the photon density, which leads to the spectral re-broadening under high photon density conditions.

In Section 10. 2, formulation of the nonlinear gain in the semiconductor lasers is summarized. In Section 10. 3, the nonlinear gain properties in QW lasers are discussed including modulation dynamics and spectral properties. In Section 10. 4, the nonlinear gain in QWW and QWB lasers are investigated.

10.2. Theory of Nonlinear Gain Effects

The gain coefficient including the nonlinear gain effects is calculated using the third order perturbation theory of the density matrix equations [146], [149]. In our analysis the nonlinear gain is assumed to be due to the spectral hole burning. The diagonal elements of the density matrix ρ_{xx} ($x = c, v$) with the consideration of the single mode spectral hole burning is expressed as

$$\rho_{xx} = f_{xx} + \delta\rho_{xx} , \qquad (10\text{-}1)$$

where f_{xx} is a quasi-Fermi distribution and $\delta\rho_{xx}$ is a local deviation of the carrier population from f_{xx} due to the spectral hole burning. Here, c and v mean the conduction band and valence band, respectively. On the other hand, the off-diagonal element of the density matrix $\rho_{cv}(t)$ is expressed as

$$\rho_{cv}(t) = \rho_{cv}(\omega) \exp(-i\omega t) . \qquad (10\text{-}2)$$

Substituting Eqs. (10-1) and (10-2) into the rate equations of the density matrix in the saturation state we obtain the following approximate solutions:

$$\rho_{cv}(\omega) = \hbar^{-1} M_{cv} (f_{cc} + \delta\rho_{cc} - f_{vv} - \delta\rho_{vv})$$
$$\times \mathcal{L}(\omega - \omega_{cv}) \, \mathcal{E}(\omega) \, U , \qquad (10\text{-}3)$$

$$\delta\rho_{xx} = \pm T_{1y}\, \hbar^{-2}\, |M_{cv}|^2\, (f_{cc} - f_{vv})\, \mathcal{L}_I(\omega - \omega_{cv})$$
$$\times |\mathcal{E}(\omega)|^2\, |U|^2\, , (x, y = c, v), \qquad (10\text{-}4)$$

where M_{cv}, $\mathcal{L}(\omega - \omega_{cv})$, $\mathcal{L}_I(\omega - \omega_{cv})$, $\mathcal{E}(\omega)$, and U are the transition dipole moment, the complex lineshape function, its imaginary part, mode amplitude, and normalized spatial distribution function, respectively. By substituting Eqs. (10-1)-(10-4) into the rate equations of density matrix again, the complex susceptibility χ is obtained. By considering linear dependence of χ on $|\mathcal{E}|^2$, the nonlinear gain $g\,(E, n, P)$ of the semiconductor lasers at the photon energy $E\,(=\hbar\,\omega)$ can be approximately obtained as follows:

$$g\,(E, n, P) = g_l\,(E, n)\,(1 - \varepsilon\,(E, n)\,P)\,, \qquad (10\text{-}5)$$

where $g_l\,(E, n)$, n, and $\varepsilon\,(E, n)$ are the linear gain coefficient, carrier density, and the nonlinear coefficient, respectively. P is the photon density which is equal to $|\mathcal{E}(\omega)|^2$. The nonlinear gain coefficient $\varepsilon\,(E, n)$ is given by:

$$\varepsilon\,(E, n) = \frac{A}{g_l} \sum_{n=1}^{\infty} \sum_{j=l,\,h} \int |M_{n,\,j}\,(E_{cv})|^4\, D_n^{\,j}(E_{cv})$$
$$\times (f_{cc} - f_{vv})\, \mathcal{L}_I^2\,(E - E_{cv})\, dE_{cv}\,, \qquad (10\text{-}6)$$

where E, $D_n^{\,j}\,(E)$, and $M_{n,\,j}\,(E)$ are the photon energy, the reduced density of states for n_{th} subband with light hole ($j = l$) or

heavy hole ($j = h$), and the matrix element, respectively. A is a constant. As shown in this equation, $\varepsilon(E, n)$ includes the density of states $D(E)$. Therefore, the increase of the quantum confinement of carriers in QW, QWW, and QWB lasers leads to the change in the nonlinear gain compared with conventional doublehetero (DH) lasers.

There have been many discussions on the shape of $\mathcal{L}_I(E - E_{cv})$. If we assume Markovian Process in the carrier dephasing effect, the $\mathcal{L}_I(E - E_{cv})$ can be expressed by the Lorentzian Function as follows:

$$\mathcal{L}_I(E - E_{cv}) = \frac{1}{\pi} \frac{\hbar/\tau_{in}}{(E - E_{cv})^2 + (\hbar/\tau_{in})^2}, \qquad (10\text{-}7)$$

where τ_{in} is the intraband relaxation time. As discussed in separate papers, the lineshape function becomes Gaussian-like function if the effect of nonmarkovian process is considered [153], [154]. In the discussion of this chapter, however, we will assume $\mathcal{L}_I(E - E_{cv})$ can be expressed by this Lorentzian Function.

10.3. Nonlinear Gain Effects in Quantum Well Lasers

10. 3. 1. Gain Properties

Since Eq. (10-6) includes the density of states, the nonlinear gain should be strongly affected by the quantum confinement effect. Fig. 10. 1 shows the nonlinear gain coefficient ε as a function of quantum well thickness in GaAs/AlGaAs and InGaAsP/InP quantum well lasers at modal gain of 50 cm^{-1}. This figure indicates that the nonlinear gain effect is enhanced with the decrease of quantum well thickness, which means the quantum confinement effect enhances the gain nonlinearity. This figure also indicates that the nonlinear gain effect in GaAs/AlGaAs quantum well lasers is slightly stronger than that in InGaAsP/InP quantum well lasers, which results from the difference of band parameters summarized in Table X. I. In this calculation the intraband relaxation time τ_{in} is assumed to be 0.1 psec.

The gain nonlinearity can be controlled by designing the number of QWs to some extent. Fig. 10. 2 shows the nonlinear gain coefficient ε as a function of linear bulk gain coefficient g_l in InGaAsP/InP QW lasers with QW thickness L_z of 50, 100, and 1000Å. As indicated in Fig. 10. 2, the nonlinear gain coefficient becomes larger with the decrease of the bulk gain (i.e., the Fermi-energy level). At the lasing condition the total loss is equal to the modal gain which is defined by the bulk gain multiplied by optical confinement factor Γ. Since Γ is proportional to the number of

QWs, we can control the Fermi-energy level (i.e., the carrier concentration or the bulk gain) by designing the number of QWs through the change in Γ. Therefore, multi-QW (MQW) lasers need lower bulk gain at the lasing condition than single-QW (SQW) lasers, because the value of gain which is required in each well is lower in the MQW lasers. Therefore, the nonlinearity in the MQW lasers is stronger than that in the SQW laser. Thus, we can control the nonlinear gain effects by designing the number of QWs. Note that it is due to the limitation of the perturbation theory used in this discussion that $\varepsilon\,(E,\,n)$ seems to increase towards infinity with the decrease of the linear bulk gain coefficient .
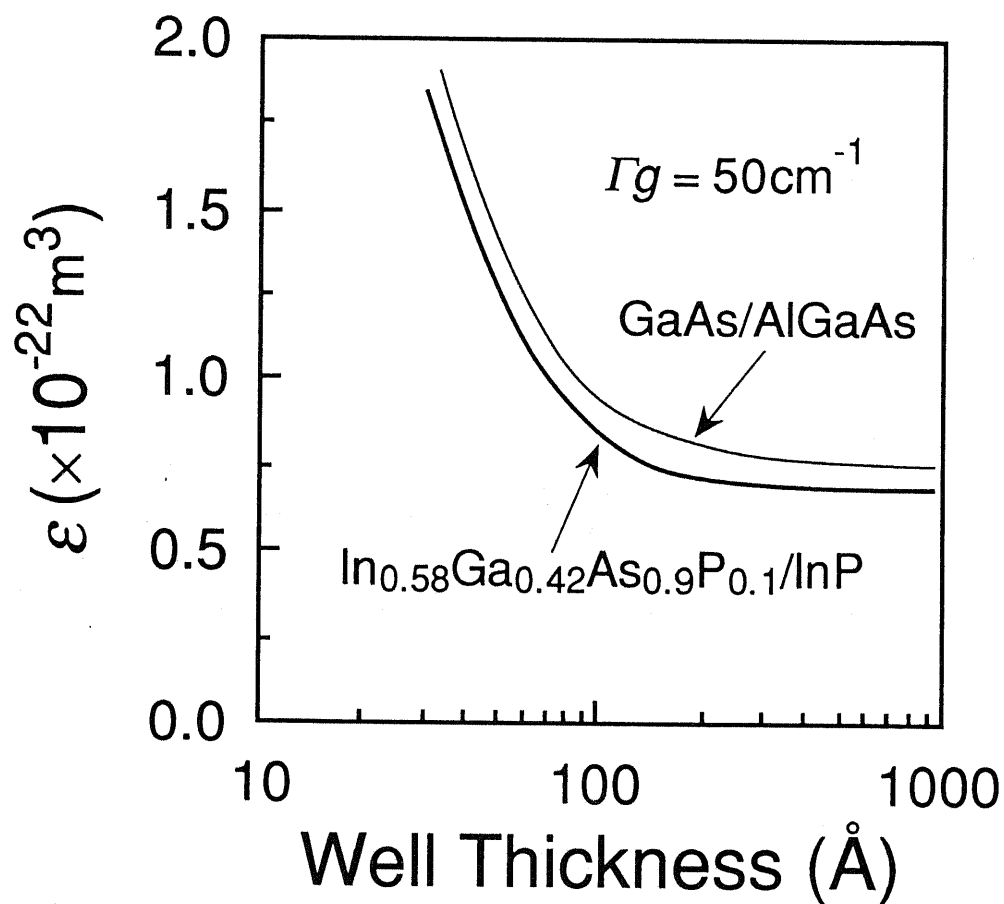
Fig. 10. 1 Nonlinear gain coefficient e as a function of quantum
well thickness in GaAs/AlGaAs and InGaAsP/InP
QW lasers.

	m_e^*/m_0	m_{hh}^*/m_0	m_{lh}^*/m_0	ΔE_c (meV)	ΔE_v (meV)
$Al_{0.3}Ga_{0.7}As/GaAs$	0.067	0.45	0.082	240	160
$In_{0.58}Ga_{0.42}As_{0.9}P_{0.1}/InP$	0.045	0.44	0.057	210	340

Table X. I   Material parameters used in this calculation in GaAs/AlGaAs and InGaAsP/InP heterostructures.
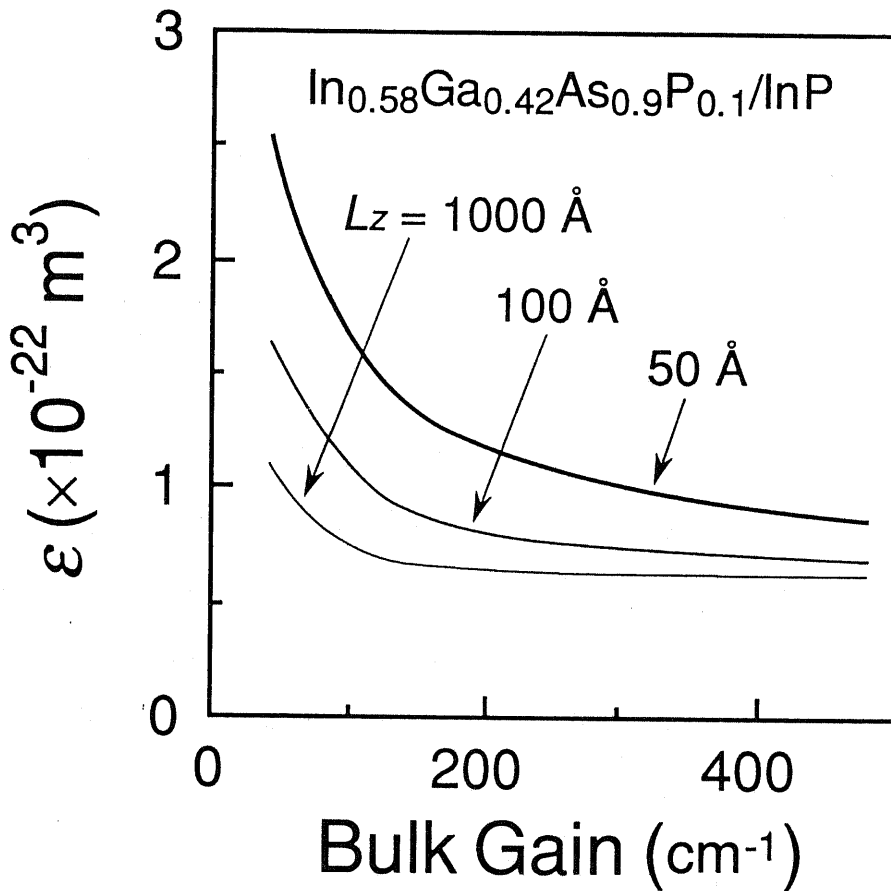
Fig. 10. 2 Nonlinear gain coefficient ε as a function of linear bulk gain coefficient g_l in InGaAsP/InP QW lasers with quantum well thickness Lz equal to 50, 100, and 1000 Å.

10. 3. 2. Modulation Dynamics

In this section, we discuss the modulation dynamics using the following rate equations:

$$\frac{dP}{dt} = (\Gamma g - \alpha_{loss}) P + R_{sp}, \tag{10-8}$$

$$\frac{dn}{dt} = \frac{J}{e\,d} - \frac{n}{\tau_s} - g P, \tag{10-9}$$

where Γ, α_{loss}, R_{sp}, J, e, d and τ_s are the optical confinement factor, the cavity loss, the rate of spontaneous emission into the lasing mode, the injection current density, the elementary charge, the active layer thickness, and the carrier life time, respectively. In the small signal analysis the resonant relaxation frequency f_r and the damping rate Γ_R are calculated as follows [151];

$$f_r^2 = \frac{1}{(2\pi)^2}\left\{ \left(\frac{1}{\tau_p} + \Gamma \frac{\partial g}{\partial P} P_0 \right) \frac{\partial g}{\partial n} P_0 + \Gamma_N \Gamma_P \right\}, \tag{10-10}$$

$$\Gamma_R = \Gamma_N + \Gamma_P, \tag{10-11}$$

$$\Gamma_N = \frac{1}{\tau_{s0}} + \frac{\partial (1/\tau_s)}{\partial n} n_0 + \frac{\partial g}{\partial n} P_0, \tag{10-12}$$

$$\Gamma_P = \frac{R_{sp}}{P_0} - \Gamma \frac{\partial g}{\partial P} P_0, \tag{10-13}$$

111

where τ_p is the photon life time. In Eqs. (10-10)-(10-13), suffix 0 means the value in the steady states. As shown in Eqs. (10-10) and (10-13), the differential gain g' ($\equiv \partial g / \partial n$) is very important parameter to determine the resonant relaxation frequency and the damping rate. If we neglect the term of damping effects such as Γ_N and Γ_P, the resonant relaxation frequency f_r can be rewritten from Eq. (10-10) as the generally used form $f_r = 1/2\pi \sqrt{g' \times P_0 / \tau_p}$. Eqs. (10-10)-(10-13) indicates that, even if the gain nonlinearity is included, higher differential gain g' still leads to higher resonant relaxation frequency f_r.

It is now well known that the differential gain g' is enhanced with the decrease of QW thickness, if the nonlinear gain effects is ignored [11]. However, we should note that the nonlinear gain effect also causes reduction of the differential gain itself. Fig. 10. 3 shows g' as a function of the photon density P in a InGaAsP/InP 50 Å-QW laser compared with a doublehetero (DH) laser. In this calculation the intraband relaxation time τ_{in} is assumed to be 0.1 psec. Here, the photon density of 1×10^{16} cm^{-3}, for instance, corresponds to the output power of about 200 mW from a semiconductor laser with 1 μm^2 beam at the facet. This result clearly indicates that the differential gain g' in each laser is suppressed with the increase of P_0 due to the nonlinear gain effects. In addition, the degree of the suppression is larger in the 50 Å-QW laser compared with the DH laser, which results from enhanced gain nonlinearity with the increase of the quantum

confinement of carriers. As a result, the modulation dynamics in QW lasers would be more suppressed than that in DH lasers.

Fig. 10. 4 shows the resonant relaxation frequency f_r in the 50 Å-InGaAsP/InP QW laser as a function of the square root of the photon density $\sqrt{P}$ calculated using Eqs. (10-10)-(10-13). As shown in this figure, f_r has a saturation tendency with the increase of the photon density due to the nonlinear gain effects. On the other hand, 3dB bandwidth f_{3dB}, which is very important on the discussion of the modulation bandwidth of the semiconductor lasers, f_{3dB} is also affected by the nonlinear gain effects. In Fig. 10. 4, f_{3dB} estimated from the calculated frequency response is additionally plotted. As shown in Fig. 10. 4, f_{3dB} is suppressed with the increase of the photon density as same as f_r but f_{3dB} is always slightly higher than f_r, which indicates that the modulation bandwidth discussed based on f_{3dB} is wider than based on f_r. The damping rate Γ_R also increases according to the increase of the photon density as shown in Fig. 10. 5. This result is consistent with the previous reported results [141], [143], [152]. In Fig. 10. 5, K-factor defined by $K = \Gamma_R/f_r^2$ is also plotted. The result shows that K-factor becomes almost constant regardless to the photon density. Therefore, the widely-used assumption that K is a constant is proved to be almost correct.

Next, the QW thickness dependence of f_r is discussed. Fig. 10. 6 shows f_r in 50 Å, 100 Å, and 600 Å InGaAsP/InP QW lasers. In general, the thin QW lasers have higher differential gain. However, the nonlinear gain is also enhanced in thinner

QW lasers. The calculation results including these effect shown in Fig. 10. 6 indicates that f_r in 50 Å QW laser is still the highest of all, which indicates that the effect of the high differential gain is dominant compared with the nonlinearity in this case. Fig. 10. 7 shows the damping rates in the same lasers in Fig. 10. 6. As shown in this figure, the damping rate in thinner quantum well laser is higher than that in thick quantum well lasers, which indicates that the nonlinearity is enhanced in thinner quantum well lasers.

Then dependence of f_r on the optical confinement factor Γ is discussed. Fig. 10. 8 shows f_r in 50 Å InGaAsP/InP QW lasers with various number of QWs. Since larger Γ leads to lower threshold bulk gain, the differential gain is higher and the nonlinearity is stronger with large number of QW's, that is, large Γ. Fig. 10. 8 shows that f_r increases with the increase of Γ, which indicates again that the effect of the high differential gain is dominant compared with the nonlinear gain effect.

In these calculations, the intraband relaxation time τ_{in} is assumed to be constant. Therefore, dependence of f_r on τ_{in} should be also notified. Longer τ_{in} enhances both the differential gain and the gain nonlinearity under the single mode operation because the gain broadening is suppressed. Fig. 10. 9 shows f_r with various τ_{in} for 50 Å QW lasers. This result shows that f_r is reduced with the increase of τ_{in}, which indicates that the effect of the nonlinearity is more dominant compared with the the enhanced enhanced differential gain in this case. For more

rigorous discussion, dependence of τ_{in} on the QW structure should be considered.

Fig. 10. 10 (a) and (b) show frequency responses in 200 Å and 50 Å QW lasers, respectively, with two kinds of photon density. As shown in these figures, in both lasers the frequency response is damped at high photon density condition.
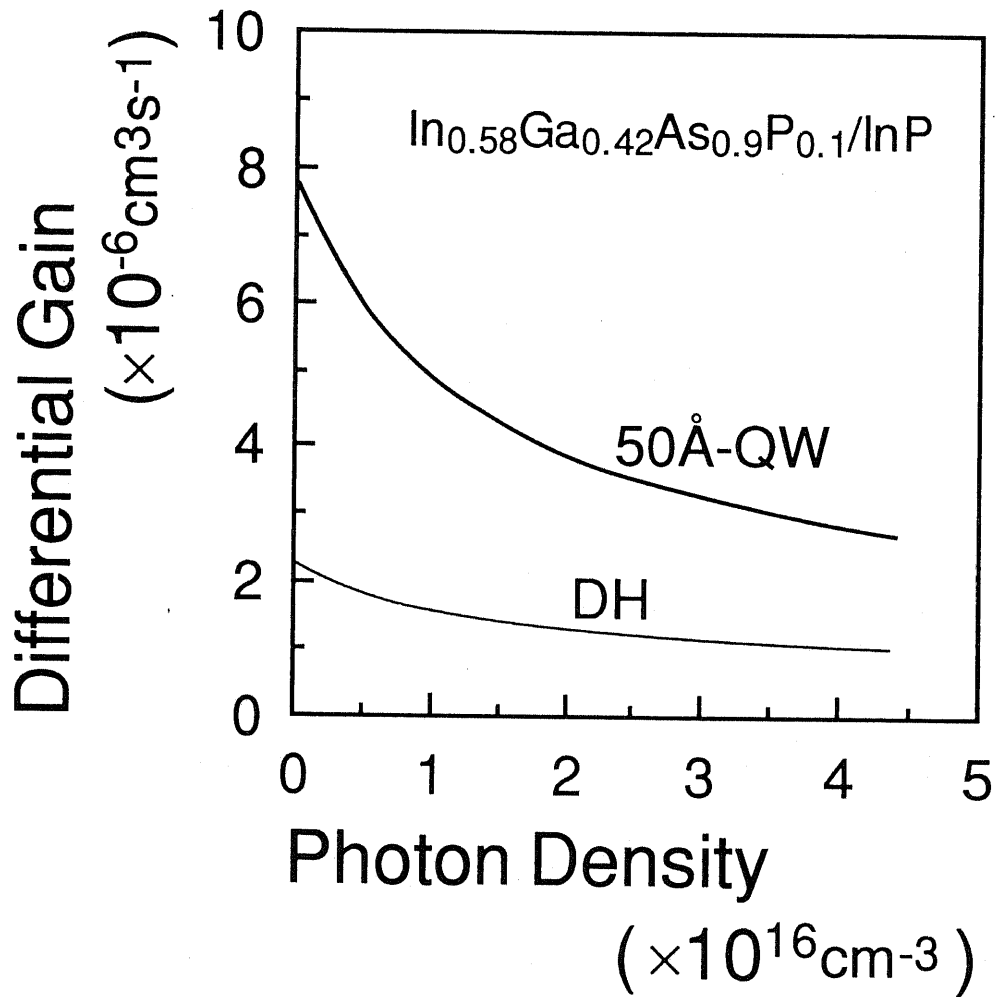
Fig. 10. 3 Calculated differential gain g' as a function of photon
density P in a InGaAsP/InP 50 Å-QW laser
compared with a doublehetero (DH) laser.
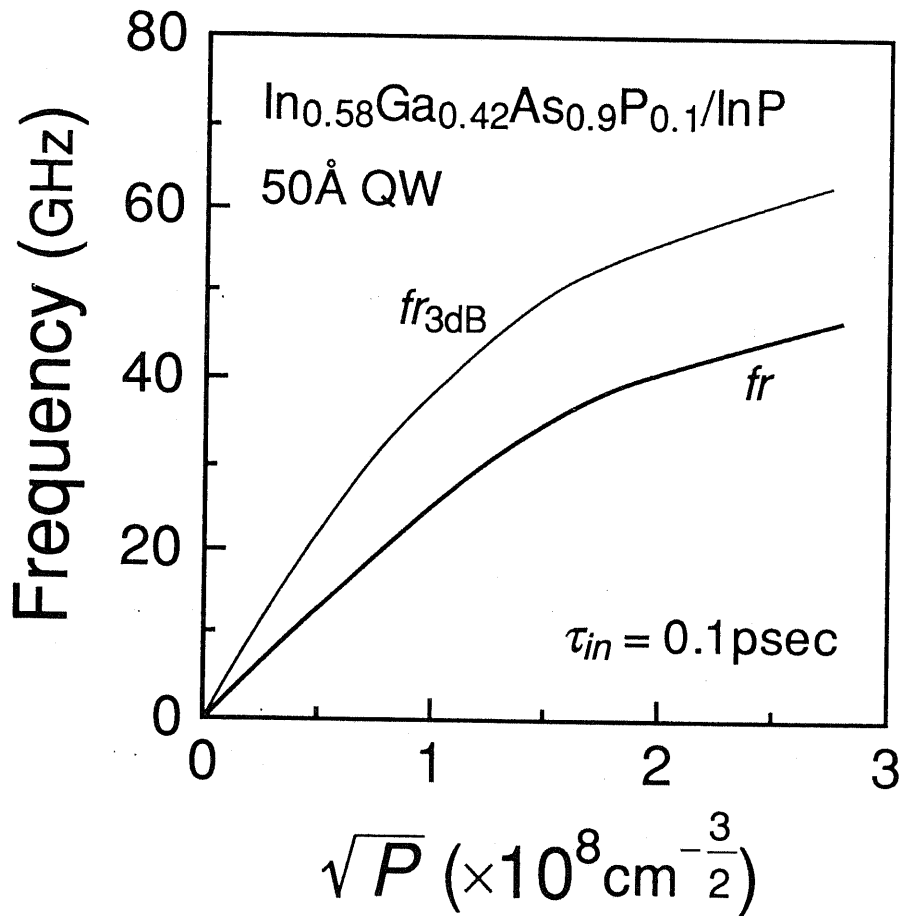
Fig. 10. 4 Calculated resonant relaxation frequency f_r and 3dB bandwidth f_{3dB} in the 50 Å-InGaAsP/InP QW laser as a function of square root of photon density $\sqrt{P}$.
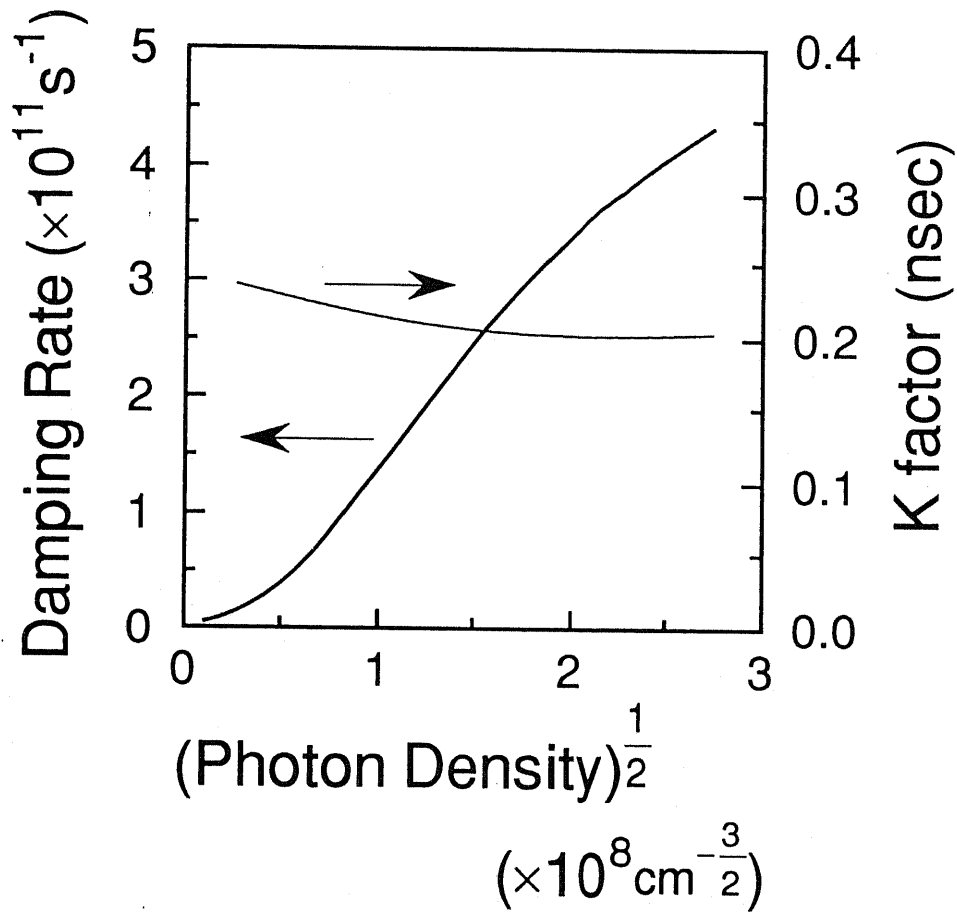
Fig. 10. 5 Damping rate Γ_R and K-factor in 50 Å-InGaAsP/InP QW laser as a function of square root of photon density $\sqrt{P}$.
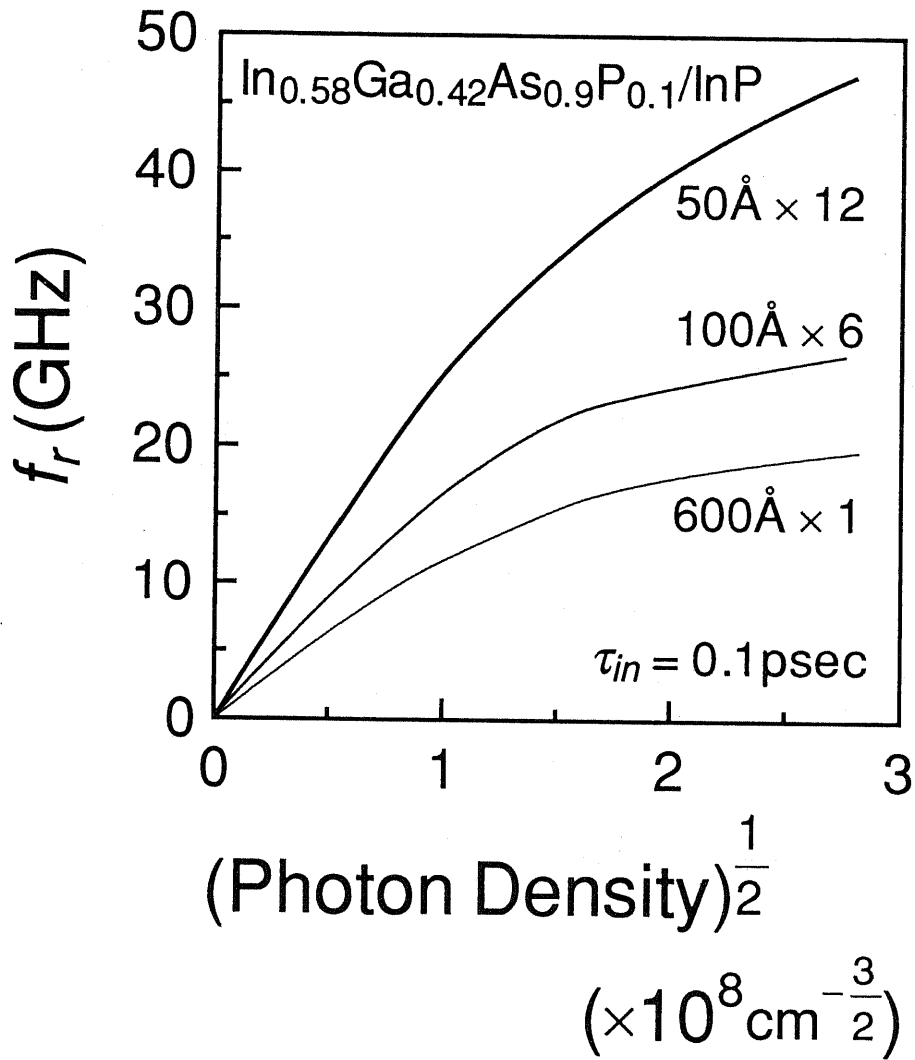
Fig. 10. 6 Calculated f_r as a function of square root of photon density $\sqrt{P}$ in InGaAsP/InP lasers with various well thickness.
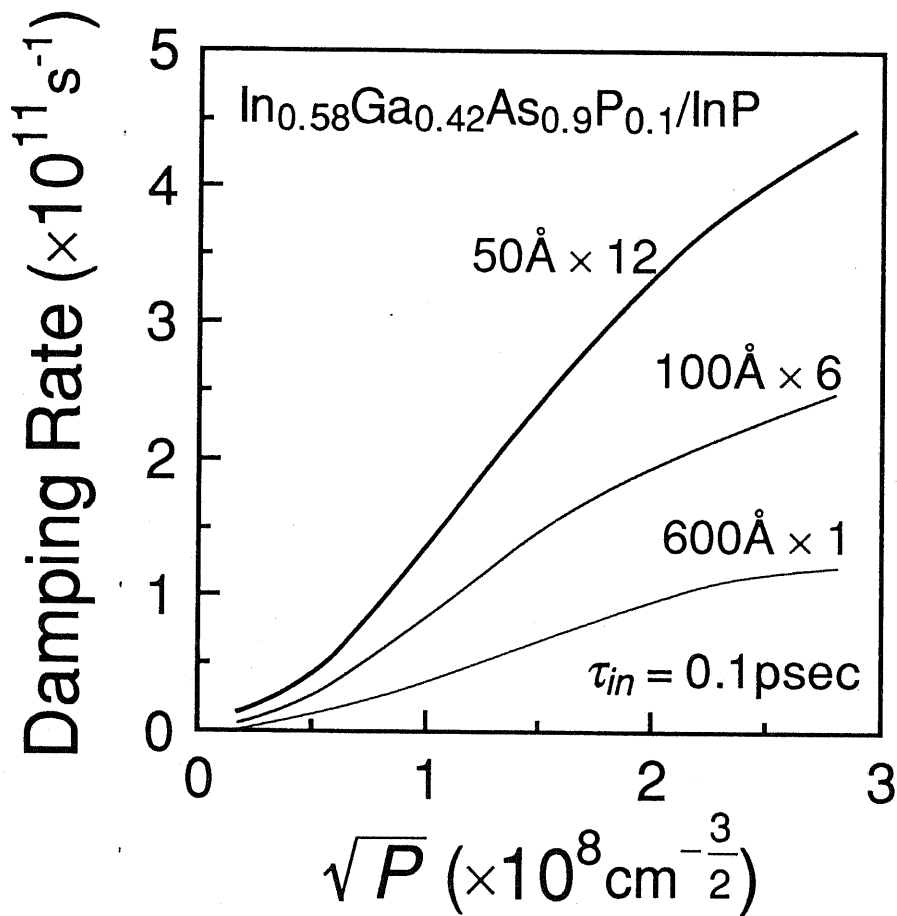
Fig. 10. 7 Damping rates as a function of square root of photon density $\sqrt{P}$ in InGaAsP/InP lasers with various well thickness.
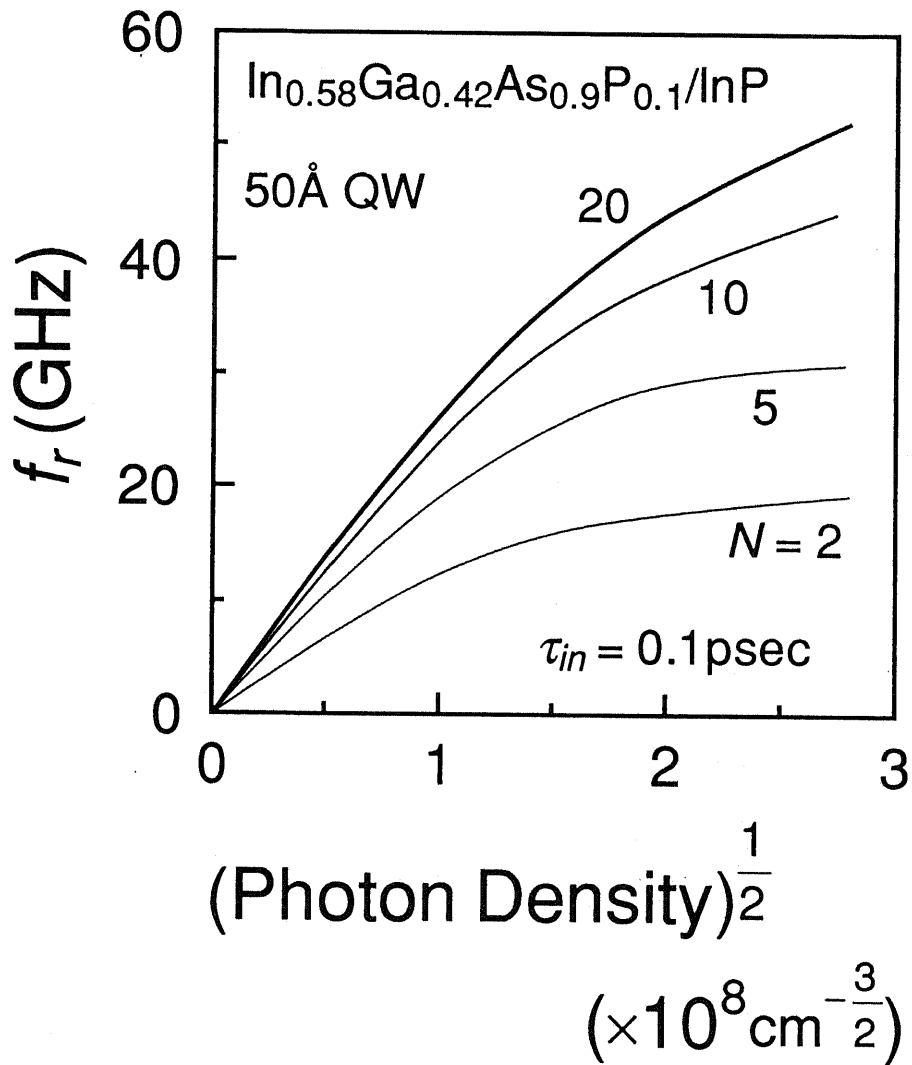
Fig. 10. 8 f_r as a function of square root of photon density $\sqrt{P}$ in 50 Å-InGaAsP/InP QW lasers with various number of wells, that is, various optical confinement factor.
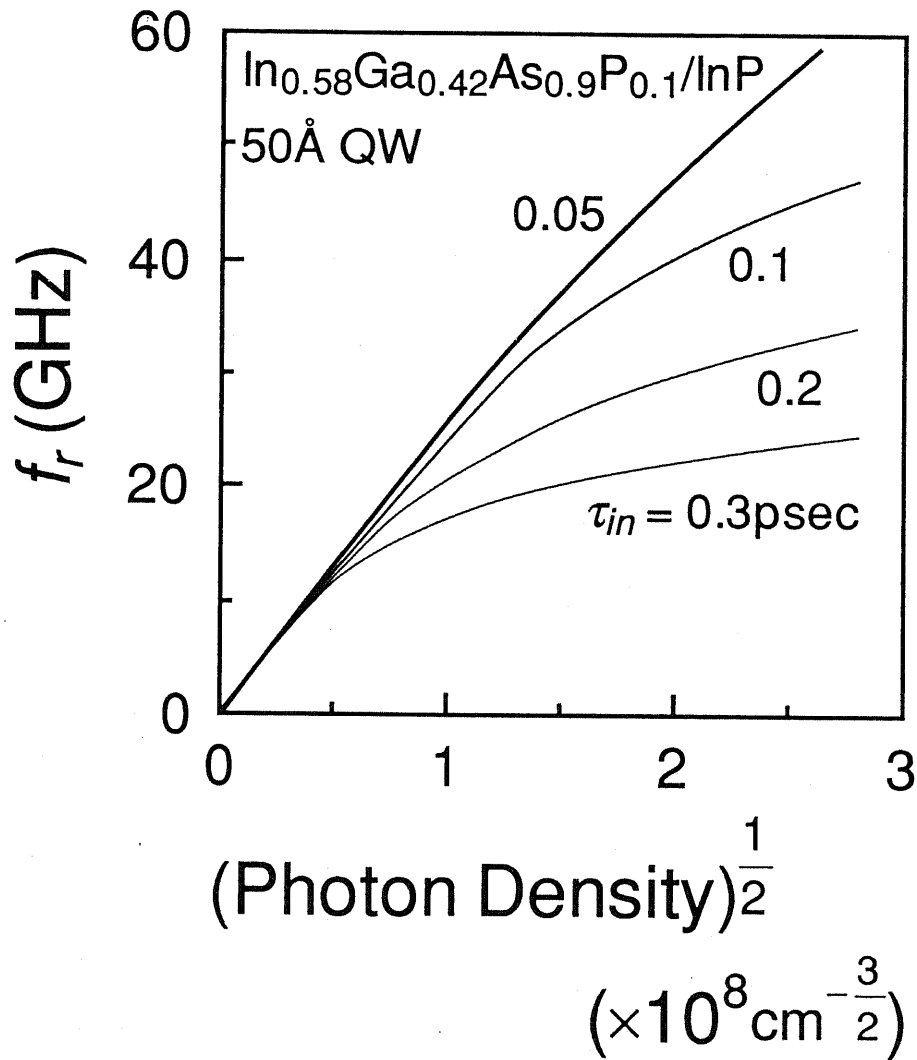
Fig. 10. 9 f_r as a function of square root of photon density $\sqrt{P}$ in 50 Å-InGaAsP/InP QW lasers with various intraband relaxation time τ_{in}.
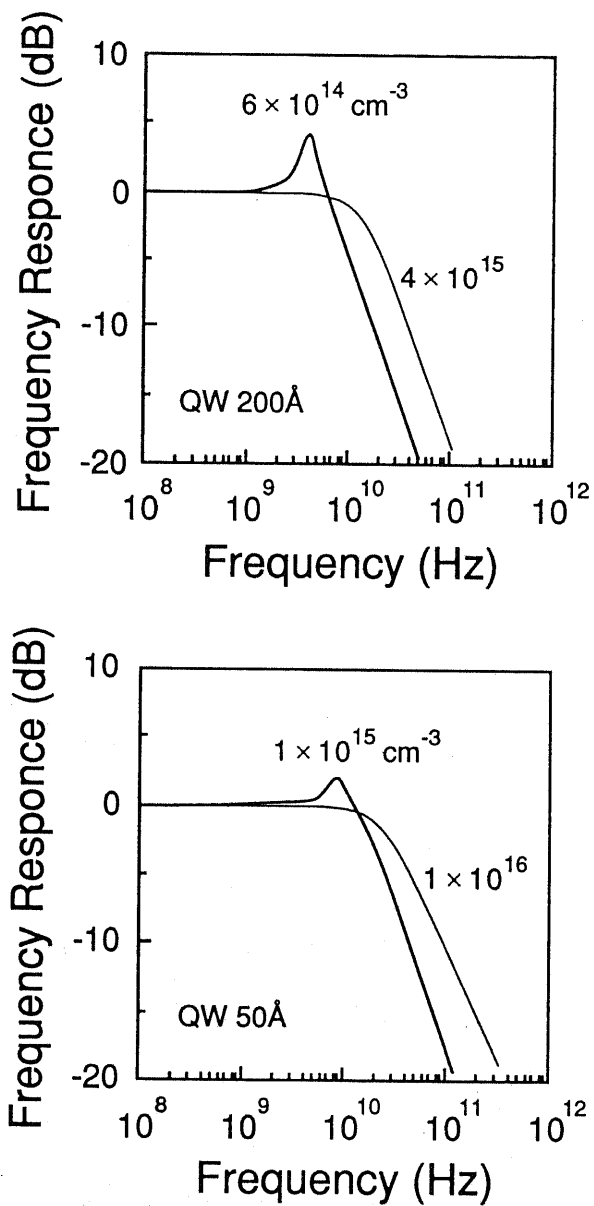
Fig. 10. 10 Frequency responses in 200 Å and 50 Å QW lasers, respectively, with two kinds of photon density.

10. 3. 3. Spectral Properties

The nonlinear gain effect also affects the spectral dynamics of the semiconductor lasers. In the semiconductor lasers, the spectral linewidth Δv is enhanced by a factor of $(1+\alpha^2)$ compared to the well-known Schawlow-Townes linewidth Δv_{ST}:

$$\Delta v = \Delta v_{ST} \, (1+\alpha^2) \, , \qquad\qquad (10\text{-}14)$$

$$\Delta v_{ST} = \frac{V_g{}^2 \, h v \, \Gamma g \, R_m \, n_{sp}}{\pi P_0} \, , \qquad\qquad (10\text{-}15)$$

$$\alpha = \frac{\partial \chi_R / \partial n}{\partial \chi_I / \partial n} \, , \qquad\qquad (10\text{-}16)$$

where V_g, hv, Γ, g, R_m, P_0 and n_{sp} are the group velocity, photon energy, optical confinement factor, bulk gain coefficient, mirror loss, output power intensity and spontaneous emission factor, respectively. χ_R and χ_I are the real and imaginary part of the complex susceptibility, respectively, and n is the carrier density. This α is called as the linewidth enhancement factor.

Reduction of α due to the quantum confinement effect has been theoretically predicted [11] and experimentally demonstrated. It should be noted, however, α is also affected by the nonlinear gain effect since α includes the complex susceptibility as indicated in Eq. (10-16) [150]. Therefore, the gain nonlinearity enhanced by the quantum confinement suppresses the improvement of α in the QW lasers. Fig. 10. 11 shows

calculated α as a function of the photon density at the fixed carrier density in a InGaAsP/InP QW laser whose well thickness is 50 Å. The results shown in Fig. 10. 11 indicate that α increases with the increase of photon density, which is caused by the nonlinear gain effect. The increase of α is mainly due to the reduction of $\partial\chi_I/\partial n$ which is a denominator of Eq. (10-16). Since the gain coefficient is proportional to χ_I, this reduction of $\partial\chi_I/\partial n$ corresponds to the reduction of differential gain due to the nonlinear gain effect discussed above (in Fig. 10. 3).

The increase of α due to the nonlinear gain effect leads to the degradation of lasing properties such as frequency chirping and spectral linewidth. If α is a constant regardless of the photon density P, the spectral linewidth Δv should be inversely proportional to P. However, since α depends on P due to the gain nonlinearity, Δv under a high photon density condition should be larger than Δv without considering the nonlinear gain effect. Fig. 10. 12 shows $\Delta\omega = n_{sp}(1+\alpha^2)/P$, which is proportional to the spectral linewidth Δv , as a function of inverse output power in 50 Å-InGaAsP/InP QW lasers. For comparison, $\Delta\omega$ of a conventional DH laser is also indicated. As shown in this figure, the broadening of spectral linewidth under the high power output condition occurs in both lasers. Though the nonlinear gain effect is enhanced in the QW laser, its effect on the spectral broadening effect is still stronger in the DH laser. This is due to the fact that the spectral linewidth depends on α^2 which is much larger in the DH laser than that in the QW laser.
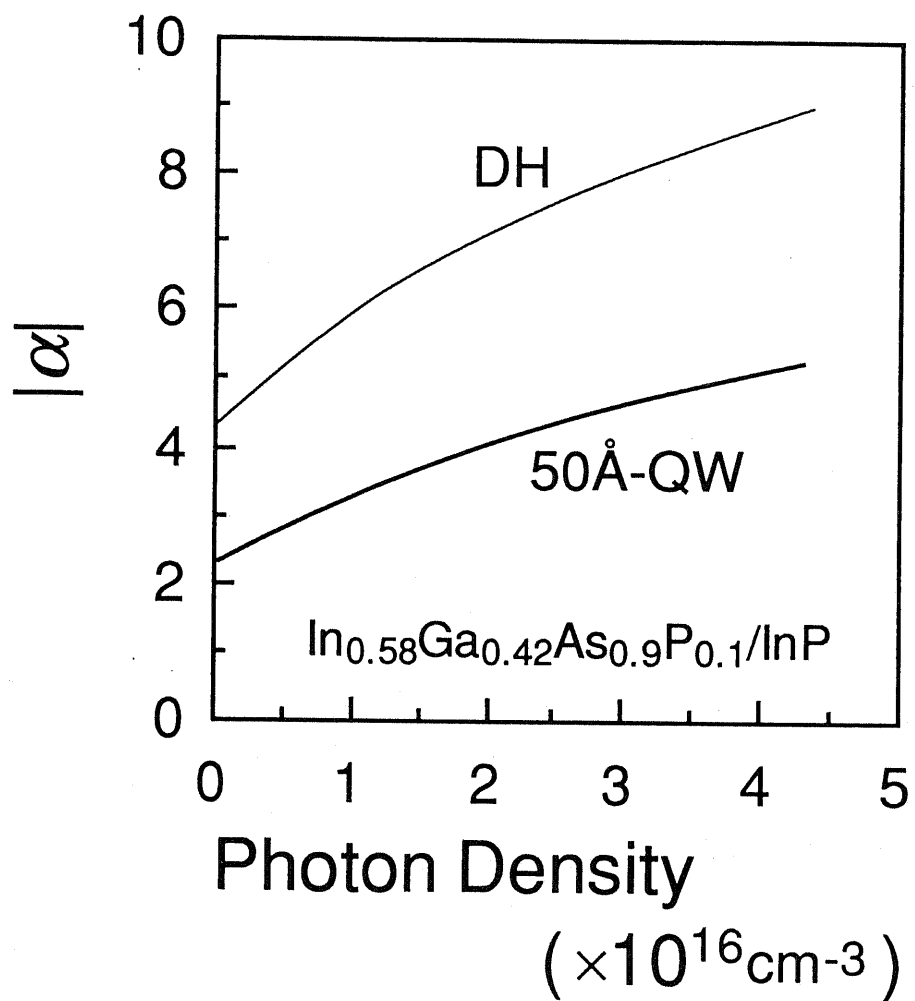
Fig. 10. 11 Calculated linewidth enhancement factor $|\alpha|$ as a function of photon density P in a InGaAsP/InP 50 Å-QW laser compared with a doublehetero (DH) laser.
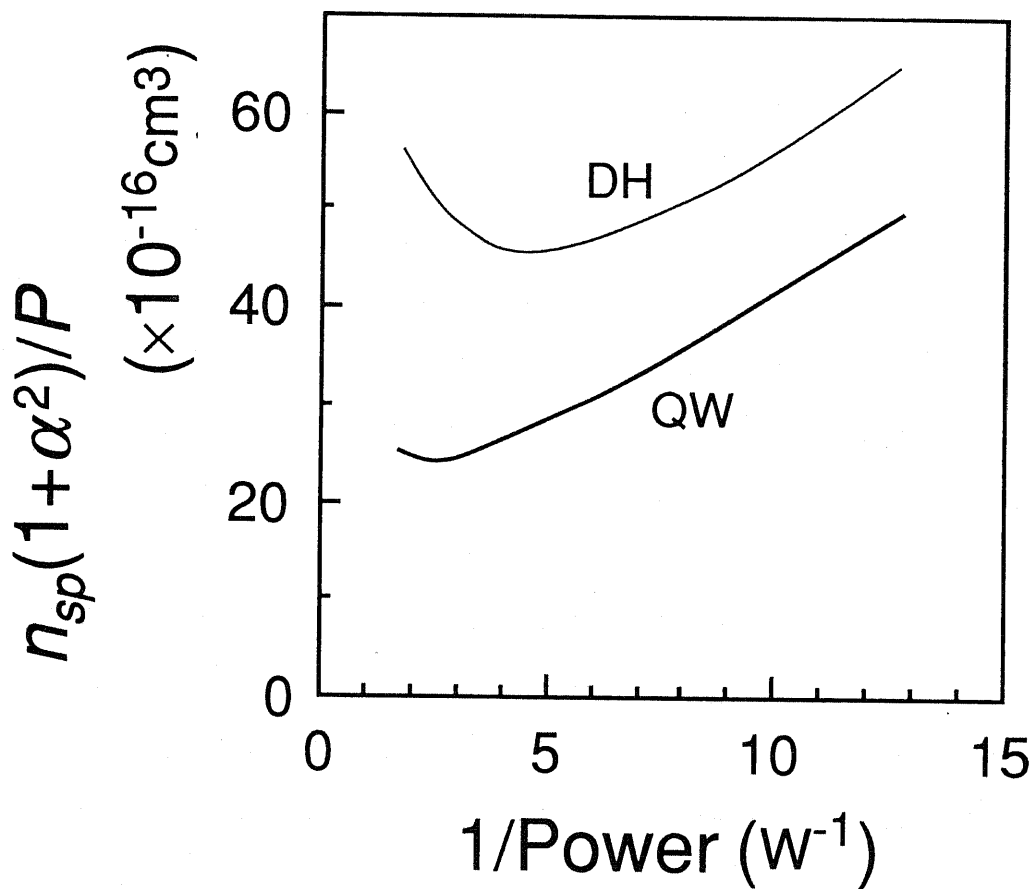
Fig. 10. 12 $\Delta\omega = n_{sp}\,(1+\alpha^2)/P$ as a function of inverse of output power in InGaAsP/InP 50 Å-QW and DH lasers.

10.4. Nonlinear Gain Effects in Quantum Well Wire and Quantum Well Box

10. 4. 1. Nonlinear Gain Coefficients

In this section, the nonlinear gain effects in QWW and QWB are discussed. Here, we assume the GaAs/AlGaAs QWW and QWB lasers. Table X. I shows the band parameters of GaAs/AlGaAs heterostructures used in this calculation compared with InGaAsP/InP heterostructures. In spite of the difference of the band parameters, the calculated results indicate that the nonlinear gain coefficient $\varepsilon (E, n)$ in GaAs/AlGaAs lasers is almost same as in InGaAsP/InP lasers. Fig. 10. 13 shows the nonlinear gain coefficient ε as a function of quantum well thickness in QW, QWW, and QWB lasers. As shown in this figure, the gain nonlinearity is enhanced with the decrease of quantum well thickness and the increase of the dimensionality of quantum confinements. Fig. 10. 14 shows the nonlinear gain coefficient ε plotted as a function of linear bulk gain coefficient g_l of GaAs/AlGaAs QW, QWW, and QWB lasers. The nonlinear gain effect which results from reduction of the inverted carrier population is enhanced in the QWW and QWB lasers compared to the QW lasers. This is due to the fact that the nonlinear gain effect is enhanced with the increase of the degree to which the homogeneous broadening nature is pronounced in the laser systems. In the QWB structures, as well known, the δ-function-like density of states leads to complete homogeneous broadening,

which results in enhancement of the gain nonlinearity. As shown in both Fig. 10. 13 and Fig. 10. 14, the QWB lasers have the largest value of ε, which demonstrates the nonlinear gain effect is enhanced with the increase of the dimensionality of the quantum confinement. Such dependence on the dimensionality of quantum confinement can be explained as follows: In the single mode theory, the width of spectral hole burning is determined by a factor $\hbar / \tau_{in}$. In the QW lasers, the carrier distribution width is much wider than this factor $\hbar / \tau_{in}$ and in the QWW lasers, the carrier distribution width is rather wider than $\hbar / \tau_{in}$. On the other hand, in the QWB lasers, the carrier distribution is δ-function-like. Therefore, the gain spectral width is the exact same as $\hbar / \tau_{in}$. As a result, in the QWB lasers, the spectral hole burning directly affects the saturation of gain properties.

Fig. 10. 14 also indicates that the nonlinearity in the QWW and QWB lasers becomes stronger owing to the decrease of the bulk gain, which is as same as in the QW lasers. Therefore, we can also control the nonlinear gain effects by designing the number of quantum well wires or boxes.
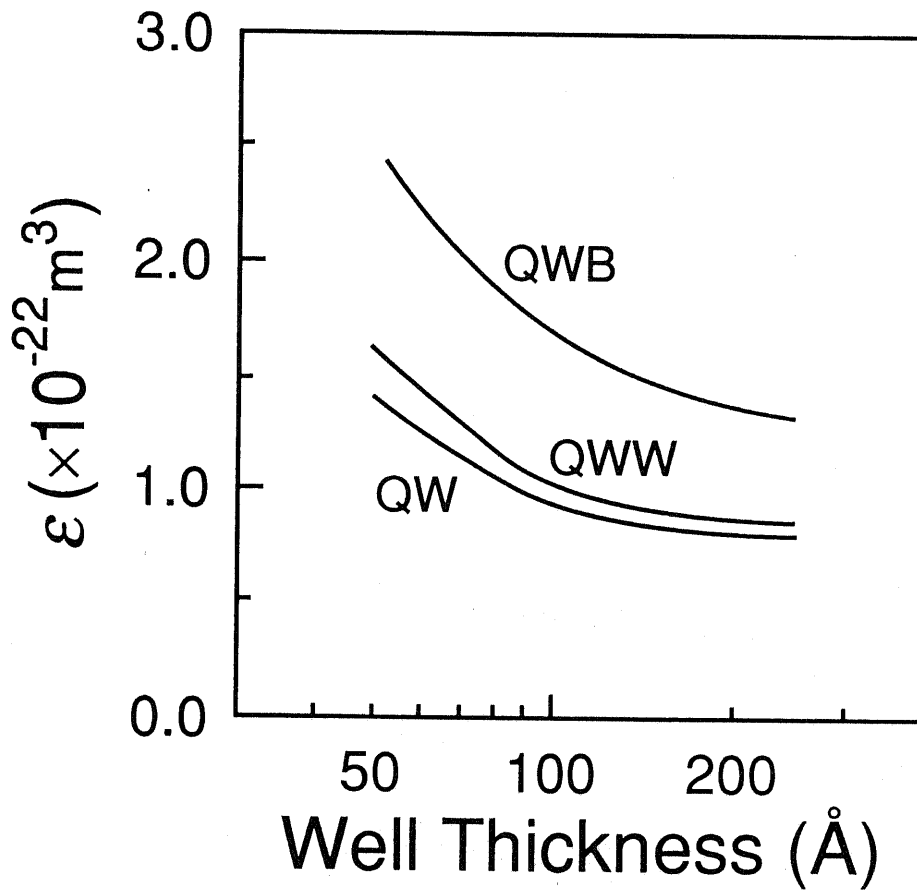
Fig. 10. 13 Nonlinear gain coefficient ε as a function of quantum well thickness in QW, QWW, and QWB lasers.
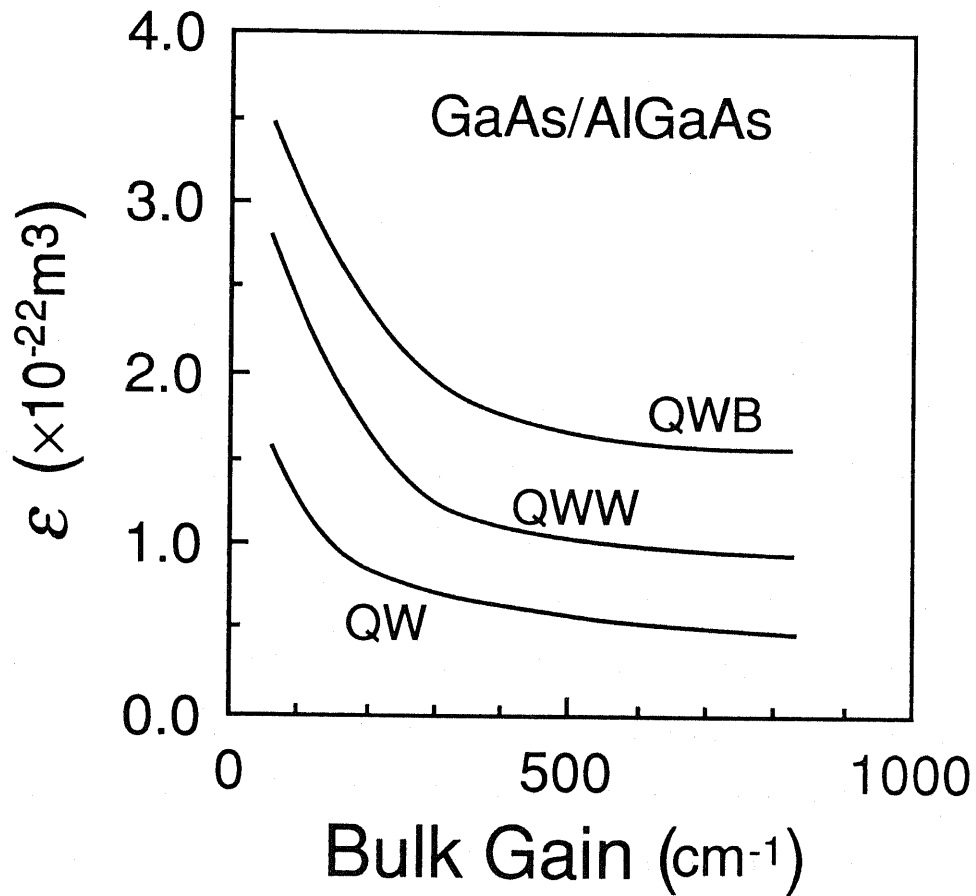
Fig. 10. 14 Nonlinear gain coefficient ε as a function of linear bulk gain coefficient g_l of GaAs/AlGaAs QW, QWW, and QWB lasers.

10. 4. 2. Modulation Dynamics and Spectral Properties

Fig. 10. 15 shows the differential gain as a function of photon density in QW, QWW and QWB lasers, which indicates that the suppression of the differential gain due to the nonlinear gain effects is most remarkable in QWB laser but the differential gain in QWB laser is still higher than those in QW and QWW lasers. The calculated resonant relaxation frequency f_r using Eq. (10-10) in the GaAs/AlGaAs QW, QWW, and QWB lasers as a function of square root of the photon density with considering the nonlinear gain effects is shown in Fig. 10. 16. The well thickness of each laser is assumed to be 50 Å. The results indicate that f_r in the QWB laser is still higher than those in QW and QWW lasers though the QWB laser has the strongest nonlinear gain effects of all. Therefore, the enhancement of the differential gain due to the multi-quantum confinement is still dominant for the modulation dynamics compared with the enhancement of the nonlinear gain effect.

It has been expected that α-parameter of 50 Å-GaAs/AlGaAs QWB lasers is almost zero, because the QWB lasers can be considered as two-energy levels lasers. However, if the nonlinear gain effect is included, α-parameter increases with the increases of the photon density, which significantly degrades the spectral properties under high photon density condition as shown in Fig. 10. 17. It is indicated that the increase of α due to the nonlinear gain effects is most remarkable in the QWB lasers.
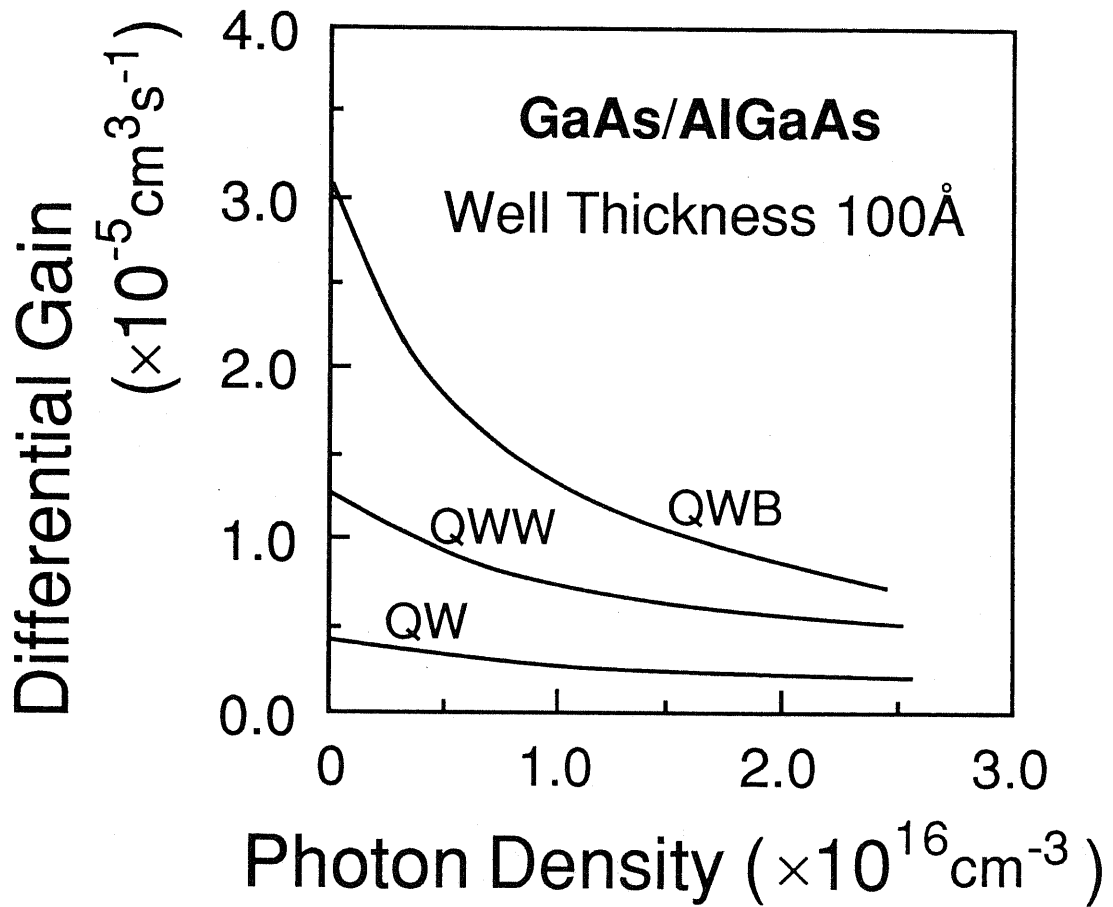
Fig. 10. 15 Differential gain as a function of photon density in
QW, QWW and QWB lasers
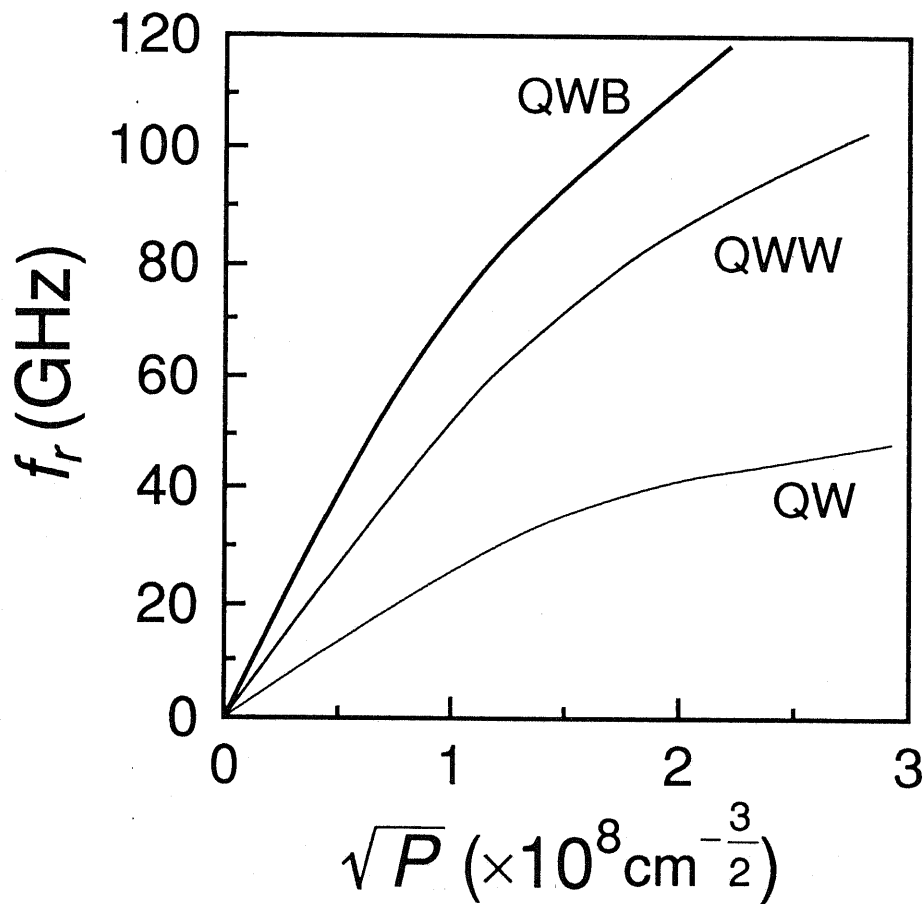
Fig. 10. 16 Calculated resonant relaxation frequency f_r as a function of square root of photon density $\sqrt{P}$ in GaAs/AlGaAs QW, QWW, and QWB lasers. The well thickness of each laser is assumed to be 50 Å.
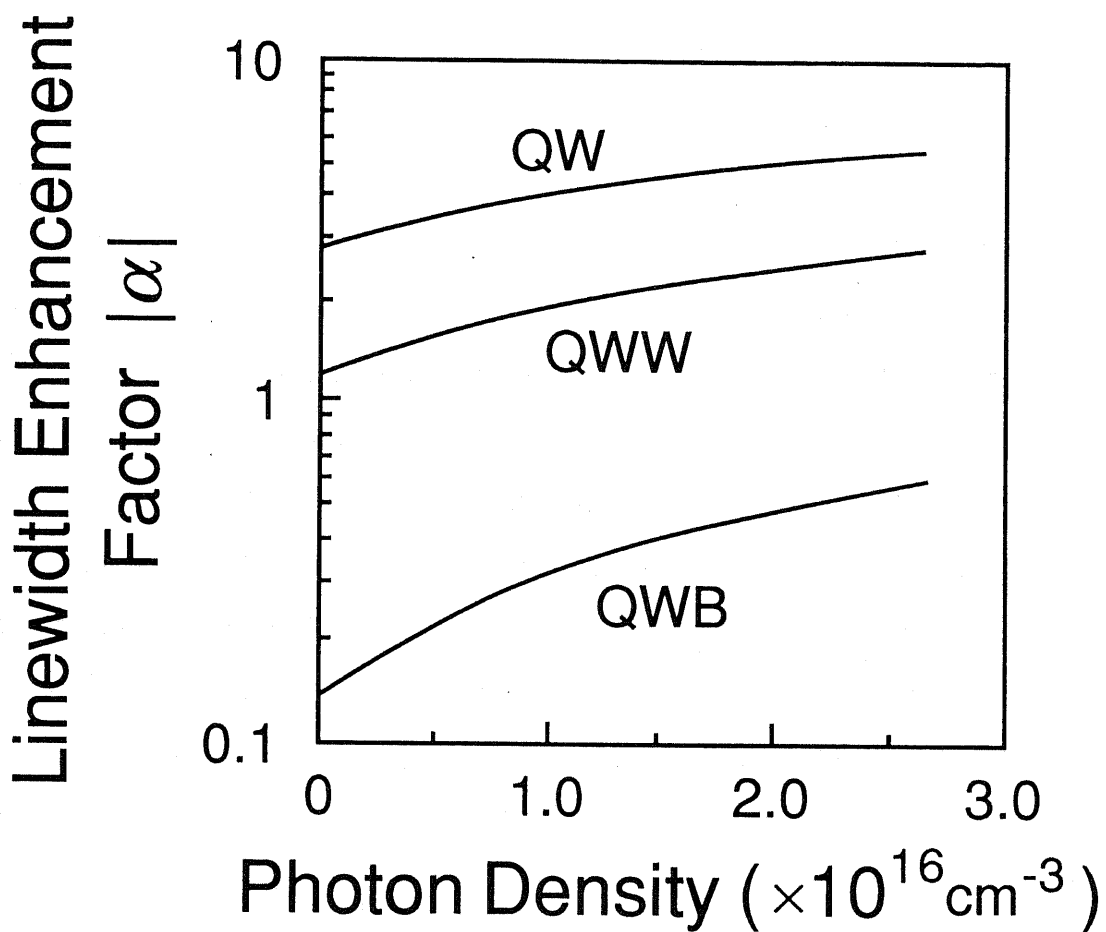
Fig. 10. 17 Calculated linewidth enhancement factor $|\alpha|$ as a
function of photon density in 50 Å-GaAs/AlGaAs
QW, QWW, and QWB lasers.

10. 4. 3. Intraband Relaxation Time Dependence

In the discussion above of this section the intraband relaxation time τ_{in} is assumed to be 0.1 psec. However, in the QWB structures, since the energy levels are completely discrete because of three dimensional quantum confinement, an intraband relaxation process becomes just same as an inter-subbands transition process. Therefore, the intraband relaxation time τ_{in} in QWB structures can be expected to become longer than in other structures. We investigate τ_{in} dependence of the nonlinear gain coefficient in the QWB lasers. As shown in Fig. 10. 18, the nonlinear gain coefficient drastically increases, that is, the nonlinearity is enhanced with the increase of τ_{in}. Thus, in the QWB lasers the nonlinear gain effect may be more enhanced than discussed above caused by the increase of the intraband relaxation time.
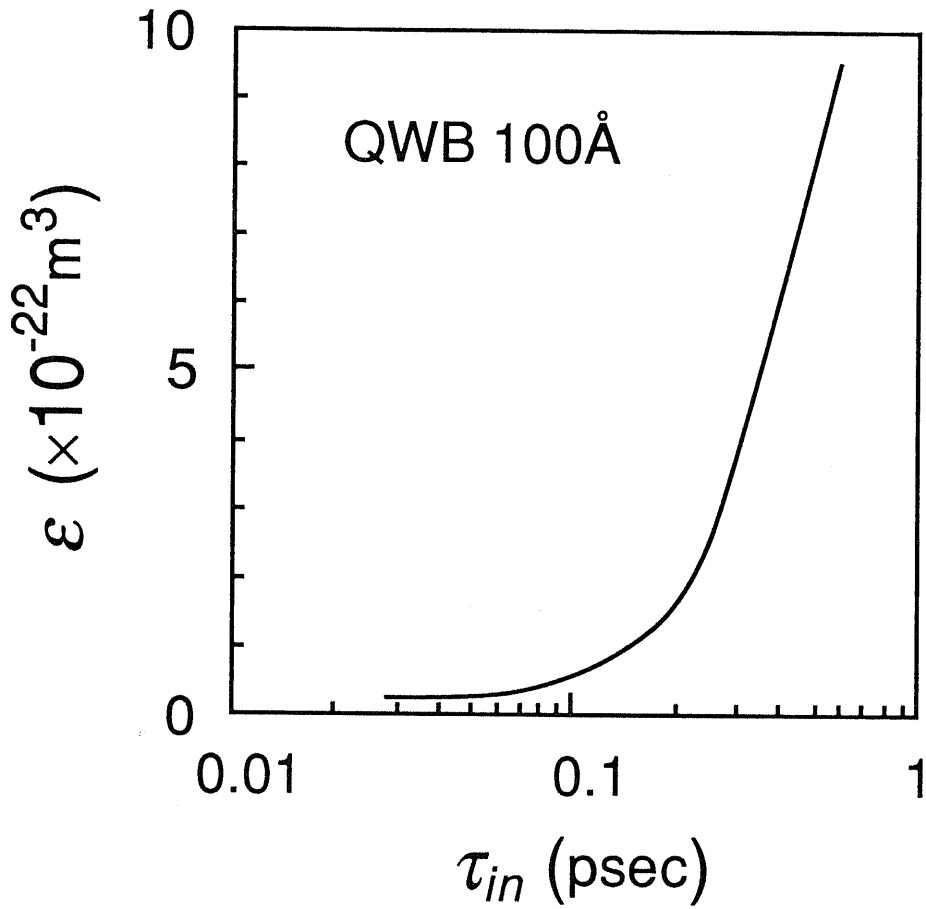
Fig. 10. 18 Nonlinear gain coefficient ε as a function of
intraband relaxation time τ_{in} in a 50 Å-
GaAs/AlGaAs QWB laser.

10. 5. Concluding Remarks

We investigate the nonlinear gain effect in GaAs/AlGaAs and InGaAsP/InP QW, QWW, and QWB lasers theoretically, considering design of QW structures for improving lasing characteristics. The results indicate that the nonlinear gain is enhanced with the increase of the quantum confinement effect and its dimensionality. It is also shown that the gain nonlinearity can be controlled by choosing the number of QWs. Using these result, modulation dynamics and spectral properties are discussed, indicating that the nonlinear gain significantly affects these lasing characteristics.

Chapter XI   Summary of Part II

In Part II, we reported the theoretical analysis of lasing characteristics in quantum microstructure lasers such as quantum well (QW), quantum well wire (QWW), and quantum well box (QWB) lasers.

We investigated effects of the substrate-orientation on lasing properties of QW lasers using the tight binding method. As a result, the threshold current density in (111)-QW lasers can be reduced compared to (100)-QW lasers. On the other hand, the modulation dynamics and spectral properties are degraded in (111)-QW lasers. These results are due to the reduction of the in-plane effective masses of the QWs grown on (111)-orientated substrate. It is important to choose the substrate-orientation while considering which lasing property should be improved for a given application.

We also investigated lasing characteristics of GaAs/AlGaAs semiconductor lasers having QWB structures theoretically. The results indicate that threshold current, modulation dynamics and spectral properties are significantly improved by carefully controlling the total number of QWBs as well as quantum box dimensions. Furthermore, effects of the modulation doping and the size fluctuation on the lasing characteristics are also discussed.

In addition, we investigated nonlinear gain effects in GaAs/AlGaAs and InGaAsP/InP QW, QWW, and QWB lasers

theoretically, considering design of QW structures for improving lasing characteristics. The results indicate the nonlinear gain is enhanced with the increase of the quantum confinement. It is also shown that the gain nonlinearity can be controlled by choosing the number of QWs. Using these result, modulation dynamics and spectral properties are discussed indicating that the nonlinear gain significantly affects these lasing characteristics.

Chapter XII Conclusions

In this thesis, the author has studied fabrication technologies and device physics of quantum microstructure lasers.

In Part I, the successful fabrication of GaAs wire structures by an electron beam induced selective growth technique in a metalorganic chemical vapor deposition (MOCVD) system is reported.

In Chapter IV, a novel selective growth technique using *in situ* irradiation of the electron beam in the EBI-MOCVD system for the purpose to fabricate the quantum microstructures is demonstrated. The results show successful fabrication of GaAs quasi-quantum wire structures whose width is as narrow as 300 nm and GaAs dot structures. In addition, we discuss the growth mechanisms of this selective growth, showing that the electron beam irradiation affects the decomposition of TMG adsorbed onto the substrate surface.

In Chapter V, an *in situ* processes for the fabrication technology of semiconductor microstructures combining the contamination resists formed by the electron beam irradiation and MOCVD method is demonstrated. The results show successful fabrication of GaAs quasi-quantum wire structures whose width is as narrow as 700 nm.

Although our results are still at preliminary stage, these techniques lead to potential applications to the fabrication of

semiconductor quantum microstructures with real multi-confinements effects.

In Part II, the theoretical analysis of lasing characteristics in quantum microstructure lasers such as quantum well (QW), quantum well wire (QWW), and quantum well box (QWB) lasers are reported.

In Chapter VIII, effects of the substrate-orientation on lasing properties of QW lasers using the tight binding method is theoretically analyzed. As a result, the threshold current density in (111)-QW lasers can be reduced compared to (100)-QW lasers. On the other hand, the modulation dynamics and spectral properties are degraded in (111)-QW lasers. These results are due to the reduction of the in-plane effective masses of the QWs grown on (111)-orientated substrate. It is important to choose the substrate-orientation while considering which lasing property should be improved for a given application.

In Chapter IX, lasing characteristics of GaAs/AlGaAs semiconductor lasers having QWB structures are theoretically analyzed. The results indicate that threshold current, modulation dynamics and spectral properties are significantly improved by carefully controlling the total number of QWBs as well as quantum box dimensions. Furthermore, effects of the modulation doping and the size fluctuation on the lasing characteristics are also discussed.

In Chapter X, nonlinear gain effects in GaAs/AlGaAs and InGaAsP/InP QW, QWW, and QWB lasers are theoretically

analyzed, considering design of QW structures for improving lasing characteristics. The results indicate the nonlinear gain is enhanced with the increase of the quantum confinement. It is also shown that the gain nonlinearity can be controlled by choosing the number of QWs. Using these result, modulation dynamics and spectral properties are discussed indicating that the nonlinear gain significantly affects these lasing characteristics.

The author hopes that the present study contributes to the applications to the fabrication technologies of quantum microstructures and the fundamental understanding of the physics in quantum microstructure lasers.

References

[1] T. Mimura, S. Hiyamizu, T. Fujii and K. Nambu, "A new field-effect transistor with selectively doped GaAs/ n-$Al_xGa_{1-x}As$ heterojunctions," *Jpn. J. Appl. Phys.* **19**, L225 (1980).

[2] H. Sakaki, "Scattering suppression and high-mobility effect of size-quantized electrons in ultrafine semiconductor wire structures," *Jpn. J. Appl. Phys.* **19**, L735 (1980).

[3] R. Dingle, A. C. Gossard and W. Wiegmann, "Direct observation of super lattice formation in a semiconductor heterostructure," *Phys. Rev. Lett.* **34**, 1327 (1975).

[4] J. P. van der Ziel, R. Dingle, R. C. Miller, W. Wiegmann and W. A. Nordland, Jr., "Laser oscillation from quantum well states in very thin GaAl-$Al_{0.2}Ga_{0.8}As$ multilayer structures," *Appl. Phys. Lett.* **26**, 463 (1975).

[5] N. Holonyak, Jr., R. M. Kolbas, R. D. Dupuis and P. D. Dapkus, "Quantum-well heterostructure lasers," *IEEE J. Quantum Electron.* **QE-16**, 170 (1980).

[6] W. T. Tsang, "Extremely low threshold (AlGa)As modified multiquantum well heterostructure lasers grown by molecular beam epitaxy," *Appl. Phys. Lett.* **39**, 786 (1981).

[7] T. Fujii, S. Yamakoshi, K. Nambu, O. Wada and S. Hiyamizu, "MBE growth of extremely high-quality GaAs-

AlGaAs GRIN-SCH lasers with a superlattice buffer layer," *J. Vac. Sci. Technol.* **2**, 259 (1984).

[8] R. Chin, N. Holonyak, Jr., B. A. Bojak, K. Hess, R. D. Dupuis and P. D. Dapkus, "Temperature dependence of threshold current for quantum well $Al_x Ga_{1-x} As - GaAs$ heterostructure laser diodes," *Appl. Phys. Lett.* **36**, 19 (1979).

[9] K. Hess, B. A. Bojak, N. Holonyak, Jr., R.Chin and P. D. Dapkus, "Temperature dependence of threshold current for a quantum-well heterostructure laser," *Solid-State Electron.* **23**, 585 (1980).

[10] Y. Arakawa and H. Sakaki, "Multiquantum well laser and its temperature dependence of the threshold current," *Appl. Phys. Lett.* **40**, 939 (1982).

[11] Y. Arakawa, K. Vahala and A. Yariv, "Quantum noise and dynamics in quantum well and quantum wire lasers," *Appl. Phys. Lett.* **45**, 950 (1984).

[12] Y. Arakawa and A. Yariv, "Theory of gain modulation response and spectral linewidth in AlGaAs quantum well lasers," *IEEE J. Quantum Electron.* **QE-21**, 1666 (1985).

[13] Y. Arakawa and A. Yariv, "Quantum well lasers – gain, spectra, dynamics," *IEEE J. Quantum Electron.* **QE-22**, 1887 (1986).

[14] H. M. Manasevit, "Single-crystal gallium arsenide on insulation substrates," *Appl. Phys. Lett.*, **12** 156 (1968).

[15] R. D. Dupuis, P. D. Dapkus, N. Holonyak, Jr., E. A. Rezek and R. Chin, "Room-temperature laser operation of quantum-well $Ga_{1-x}Al_xAs$-GaAs laser diodes grown by metal-organic chemical vapor deposition," *Appl. Phys. Lett.* **32**, 295 (1978).

[16] N. Holonyak, Jr., R. M. Kolbas, W. D. Laidig, B. A. Vojak, P. D. Dupuis and P. D. Dapkus, "Low-threshold continuous laser operation (300-337K) of multilayer MOCVD $Al_xGa_{1-x}As$-GaAs quantum-well heterostructures," *Appl. Phys. Lett.* **33**, 737 (1978).

[17] J. J. Coleman, P. D. Dapkus, D. E. Thompson and D. R. Clarke "The growth and characterization of metalorganic chemical vapor deposition (MOCVD) quantum well transport structures," *J. Cryst. Growth* **55**, 207 (1981).

[18] J. R. Arthur and J. J. Lepore, "GaAs, GaP, and $GaAs_xP_{1-x}$ epitaxial films grown by molecular beam deposition," *J. Vac. Sci. Technol.* **6**, 545 (1969).

[19] L. L. Chang, L. Esaki, W. E. Howard and R. Ludeke, "The growth of a GaAs-GaAlAs superlattice," *J. Vac. Sci. Technol.* **10**, 11 (1973).

[20] L. L. Chang, L. Esaki, W. E. Howard, R. Ludeke and G. Schul, "Structures grown by molecular beam epitaxy (GaAs and GaAs-$Ga_{1-x}Al_xAs$)," *J. Vac. Sci. Technol.* **10**, 655 (1973).

[21] R. Ludeke, L. L. Chang and L. Esaki, "Molecular beam epitaxy of alternating metal-semiconductor films," *Appl. Phys. Lett.* **23**, 201 (1973).

[22] L. Esaki, "Computer-controlled molecular beam epitaxy," *Jpn. J. Appl. Phys.* **2**, 821 (1974).

[23] W. E. Johnson and L. A. Schlie, "Photodeposition of Zn, Se, and ZnSe thin films," *Appl. Phys. Lett.* **40**, 798 (1982).

[24] J. Nishizawa, Y. Kokubun, H. Shimawaki and M. Koike, "Photoexcitation effects on the growth rate in the vapor phase epitaxial growth of GaAs," *J. Electrochem. Soc.* **132**, 1939 (1985).

[25] H. Ando, H. Inuzuka, M. Konagai and K. Takahashi, "Photoenhanced metalorganic chemical vapor deposition of ZnSe films using diethylzinc and dimethylselenide," *J. Appl. Phys.* **58**, 802 (1985).

[26] Sg. Fujita, A. Tanabe, T. Sakamoto, M. Isemura and Sz. Fujita, "Growth rate enhancement by xenon lamp irradiation in organometallic vapor-phase epitaxy of ZnSe," *Jpn. J. Appl. Phys.* **26**, L2000 (1987).

[27] Sg. Fujita, A. Tanabe, T. Sakamoto, M. Isemura and Sz. Fujita, "Investigations of photo-assisted mechanism for growth rate enhancement in photo-assisted OMVPE of ZnSe and ZnS," *J. Cryst. Growth* **93**, 259 (1988).

[28] V. M. Donnelly, M. Geva, J. Long and R. F. Karlicek, "Excimer laser induced deposition of InP and indium-oxide films," *Appl. Phys. Lett.* **44**, 951 (1984).

[29] V. M. Donnelly, D. Brasen, A. Appelbaum and M. Geva, "Excimer laser-induced deposition of InP: Crystallographic and mechanistic studies," *J. Appl. Phys.* **58**, 2022 (1985).

[30] B. J. Morris, "Photochemical organometal vapor phase epitaxy of mercury cadmium telluride," *Appl. Phys. Lett.* **48**, 867 (1986).

[31] C. W. Tu, V. M. Donnelly, J. C. Beggy, F. A. Baiocchi, V. R. McCrary, T. D. Harris and M. G. Lamont, "Laser-modified molecular beam epitaxial growth of (Al)GaAs on GaAs and (Ca, Sr)F$_2$/GaAs substrates," *Appl. Phys. Lett.* **52**, 966 (1988).

[32] V. M. Donnelly, C. W. Tu, J. C. Beggy, V. R. McCrary, M. G. Lamont, T. D. Harris, F. A. Baiocchi and R. C. Farrow, "Laser-assisted metalorganic molecular beam epitaxy of GaAs," *Appl. Phys. Lett.* **52**, 1065 (1988).

[33] Shirley S. Chu, T. L. Chu, C. L. Chang and H. Firouzi, "Laser-induced homoepitaxial growth of gallium arsenide films," *Appl. Phys. Lett.* **52**, 1243 (1988).

[34] J. J. Zinck, P. D. Brewer, J. E. Jensen, G. L. Olson and L. W. Tutt, "Excimer laser-assisted metalorganic vapor phase epitaxy of CdTe on GaAs," *Appl. Phys. Lett.* **52**, 1434 (1988).

[35] V. M. Donnelly and J. A. McCaulley, "Selected area growth of GaAs by laser-induced pyrolysis of adsorbed triethylgallium," *Appl. Phys. Lett.* **54**, 2458 (1989).

[36] Y. Aoyagi, S. Masuda, S. Namba and A. Doi, "Laser enhanced metalorganic vapor deposition crystal growth in GaAs," *Appl. Phys. Lett.* **47**, 95 (1985).

[37] Y. Aoyagi, M. Kanazawa, A. Doi, S. Iwai and S. Namba, "Characteristics of laser metalorganic vapor-phase epitaxy in GaAs," *J. Appl. Phys.* **60**, 3131 (1986).

[38] S. M. Bedair, J. K. Whisnant, N. H. Karam, M. A. Tischler and T. Katsuyama, "Laser selective deposition of GaAs on Si," *Appl. Phys. Lett.* **48**, 174 (1986).

[39] S. M. Bedair, J. K. Whisnant, N. H. Karam, D. Griffis, N. A. El-Masry and H. H. Standelmaier, "Laser selective deposition of III-V compounds on GaAs and Si substrates," *J. Cryst. Growth* **77**, 229 (1986).

[40] N. H. Karam, N. A. El-Masry and S. M. Bedair, "Laser direct writing of single-crystal III-V compounds on GaAs," *Appl. Phys. Lett.* **49**, 880 (1986).

[41] N. H. Karam, H. Liu, I. Yoshida, B. -L. Jiang and S. M. Bedair, "Low temperature selective epitaxy of III-V Compounds by laser assisted chemical vapor deposition," *J. Cryst. Growth* **93**, 254 (1988).

[42] A. Doi, Y. Aoyagi and S. Namba, "Growth of GaAs by switched laser metalorganic vapor phase epitaxy," *Appl. Phys. Lett.* **48**, 1787 (1986).

[43] A. Doi, Y. Aoyagi and S. Namba, "Stepwise monolayer growth of GaAs by switched laser metalorganic chemical phase epitaxy," *Appl. Phys. Lett.* **49**, 785 (1986).

[44] Y. Aoyagi, A. Doi, S. Iwai and S. Namba, "Atomic-layer growth of GaAs by modulated-continuous-wave laser metalorganic vapor-phase epitaxy," *J. Vac. Sci. Technol.* **B 5**, 1460 (1987).

[45] T. Meguro, T. Suzuki, K. Ozaki, Y. Okano, A. Hirata, Y. Yamamoto, S. Iwai, Y. Aoyagi and S. Namba, "Surface processes in laser-atomic layer epitaxy (Laser ALE) of GaAs," *J. Cryst. Growth* **93**, 190 (1988).

[46] N. H. Karam, H. Liu, I. Yoshida and S. M. Bedair, "Direct writing of GaAs monolayers by laser-assisted atomic layer epitaxy," *Appl. Phys. Lett.* **52**, 1144 (1988).

[47] S. Iwai, T. Meguro, Y. Aoyagi and T. Miyoshi, "Patterned crystal growth of GaAs using laser scanning with atomic layer epitaxy," *J. Cryst. Growth* **107**, 136 (1991).

[48] K. Nagata, Y. Iimura, Y. Aoyagi, S. Namba and S. Den, "Photo-assisted chemical beam epitaxy of GaAs," *J. Cryst. growth* **95**, 142 (1989).

[49] H. Sugiura, R. Iga, T. Yamada and M. Yamaguchi, "Ar ion laser-assisted metalorganic molecular beam epitaxy of GaAs," *Appl. Phys. Lett.* **54**, 335 (1989).

[50] R. Iga, H. Sugiura, T. Yamada and K. Wada, "Carbon reduction in GaAs films grown by laser-assisted metalorganic molecular beam epitaxy," *Appl. Phys. Lett.* **55**, 451 (1989).

[51] R. Iga, H. Sugiura and T. Yamada, "Ar ion laser-assisted metalorganic molecular beam epitaxy of InP," *Jpn. J. Appl. Phys.* **29**, 475 (1990).

[52] K. Nagata, Y. Iimura, Y. Aoyagi and S. Namba, "Laser assisted chemical beam epitaxy," *J. Cryst. Growth* **105**, 52 (1990).

[53] T. Hiroshima and R. Lang, "Effect of conduction-band nonparabolicity on quantized energy levels of a quantum well," *Appl. Phys. Lett.* **49**, 456 (1986).

[54] U, Ekenberg, "Enhancement of nonparabolicity effects in a quantum well," *Phys. Rev.* **B 36**,6152 (1987).

[55] D. F. Nelson, R. C. Miller and D. A. Kleinman, "Band nonparabolicity effects in semiconductor quantum wells," *Phys. Rev.* **B 35**, 7770 (1987).

[56] U. Ekenberg, "Nonparabolicity effects in a quantum well: sublevel shift, parallel mass, and Landau levels," *Phys. Rev.* **B 40**, 7714 (1989).

[57] R. Olshansky, P. Hill, V. Lanzisera, and W. Powazinik, "Frequency response of 1.3 µm InGaAsP high speed semiconductor lasers," *IEEE J. Quantum Electron.* **QE-23**, 1410 (1987).

[58] J. C. Simon, "Polarization characteristics of a travelling-wave-type semiconductor laser amplifier," *Electron. Lett.* **18**, 438 (1982).

[59] P. M. Petroff, A. C. Gossard, R. A. Logan and W. Wiegmann, "Toward quantum well wires: Fabrication and optical properties," *Appl. Phys. Lett.* **41**, 635 (1982).

[60] K. Kash, A. Scherer, J. M. Worlock, H. G. Craighead and M. C. Tamargo, "Optical spectroscopy of ultrasmall structures etched from quantum wells," *Appl. Phys. Lett.* **49**, 1043 (1986).

[61] Y. Miyamoto, M. Cao, Y. Shingai, K. Furuta, Y. Suematsu, K. G. Ravikumar and S. Arai, "Light emission from quantum-box structure by current injection," *Jpn. J. Appl. Phys.* **26**, L225 (1987).

[62] M. A. Reed, R. T. Bate, K. Bradshaw, W. M. Duncan, W. R. Frensley, J. W. Lee and H. D. Shih, "Spatial quantization in GaAs-AlGaAs multiple quantum dots," *J. Vac. Sci. Technol.* **B 4**, 358 (1986).

[63] J. Cibert, P. M. Petroff, G. J. Dolan, S. J. Pearton, A. C. Gossard and J. H. English, "Optically detected carrier confinement to one and zero dimension in GaAs quantum well wires and boxes," *Appl. Phys. Lett.* **49**, 1275 (1986).

[64] H. Temkin, G. J. Dolan, M. B. Panish and S. N. G. Chu, "Low-temperature photoluminescence from InGaAs/InP quantum wires and boxes," *Appl. Phys. Lett.* **50**, 413 (1987).

[65] Y. Hirayama, S. Tarucha, Y. Suzuki and H. Okamoto, "Fabrication of a GaAs quantum-well-wire structure by Ga focused-ion-beam implantation and its optical properties," *Phys. Rev.* **B 37**, 2774 (1988).

[66] Y. Hirayama, Y. Suzuki, S. Tarucha and H. Okamoto, "Compositional disordering of GaAs-Al$_x$Ga$_{1-x}$As superlattice by Ga focused ion beam implantation ands its application to submicron structure fabrication," *Jpn. J. Appl. Phys.* **24**, L516 (1985).

[67] Y. Arakawa, K. Vahala, A. Yariv and K. Lau, "Enhanced modulation bandwidth of GaAlAs double heterostructure lasers in high magnetic fields: dynamic response with quantum wire effects," *Appl. Phys. Lett.* **47**, 1142 (1985).

[68] Y. Arakawa, K. Vahala, A. Yariv and K. Lau, "Reduction of the spectral linewidth of semiconductor lasers with quantum wire effects – Spectral properties of GaAlAs double heterostructure lasers in high magnetic fields," *Appl. Phys. Lett.* **48**, 384 (1986).

[69] M. Asada, Y. Miyamoto and Y. Suematsu, "Theoretical gain of quantum-well wire lasers," *Jpn. J. Appl. Phys.* **24**, L95 (1985).

[70] M. Asada, Y. Miyamoto and Y. Suematsu, "Gain and the threshold of three-dimensional quantum-box lasers," *IEEE J. Quantum Electron.* **QE-22**, 1915 (1986).

[71] Y. Miyamoto, Y. Miyake, M. Asada and Y. Suematsu, "Threshold current density of GaInAsP/InP quantum-box lasers," *IEEE J. Quantum Electron.* **25**, 2001 (1989).

[72] K. Komori, S. Arai and Y. Suematsu, "Noise in semiconductor laser amplifiers with quantum box structure," *IEEE Photonics Technol. Lett.* **3**, 39 (1991).

[73] T. Ohtoshi and M. Yamanishi, "Line shape functions of quantum-box lasers," *Jpn. J. Appl. Phys.* **30**, L1406 (1991).

[74] P. M. Petroff, A. C. Gossard and W. Wiegmann, "Structure of AlAs-GaAs interfaces grown on (100) vicinal surfaces by molecular beam epitaxy," *Appl. Phys. Lett.* **45**, 620 (1984).

[75] T. Fukui and H. Saito, "$(AlAs)_{0.5}(GaAs)_{0.5}$ fractional-layer superlattices grown on (001) vicinal surfaces by metalorganic chemical vapor deposition," *Appl. Phys. Lett.* **50**, 824 (1987).

[76] T. Fukui, H. Saito and Y. Tokura, "Superlattice structure observation for $(AlAs)_{1/2}(GaAs)_{1/2}$ grown on (001) vicinal GaAs substrates," *Jpn. J. Appl. Phys.* **27**, L1320 (1988).

[77] T. Fukui and H. Saito, "$(AlAs)_{1/2}(GaAs)_{1/2}$ fractional-layer superlattices grown on (001) vicinal GaAs substrates by metal-organic chemical vapor deposition," *J. Vac. Sci. Technol.* **B 6**, 1373 (1988).

[78] J. M. Gaines, P. M. Petroff, H. Kroemer, R. J. Simes, R. S. Geels and J. H. English, "Molecular-beam epitaxy growth of tilted GaAs/AlAs superlattices by deposition of fractional monolayers on vicinal (001) substrates," *J. Vac. Sci. Technol.* **B 6**, 1378 (1988).

[79] M. Tsuchiya, P. M. Petroff and L. A. Coldren, "Spontaneous growth of coherent tilted superlattice on vicinal (100) GaAs substrates," *Appl. Phys. Lett.* **54**, 1690 (1989).

[80] H. Yamaguchi and Y. Horikoshi, "Step-flow growth on vicinal GaAs surfaces by migration-enhanced epitaxy," *Jpn. J. Appl. Phys.* **28**, L1456 (1989).

[81] H. Saito and T. Fukui, "Impurity-induced disordering in fractional-layer growth on a (001) vicinal surface by metalorganic chemical vapor deposition," *Appl. Phys. Lett.* **56**, 87 (1990).

[82] T. Fukui, H. Saito, Y. Tokura K. Tsubaki and N. Susa, "$(AlAs)_{1/2}(GaAs)_{1/2}$ fractional-layer superlattices grown on (001) vicinal GaAs substrates by MOCVD," *Surf. Sci.* **228**, 20 (1990).

[83] T. Fukui and H. Saito, "Ideal crystal growth from kink sites on a GaAs vicinal surface by metalorganic chemical vapor deposition," *Jpn. J. Appl. Phys.* **29**, L731 (1990).

[84] S. A. Chalmers, H. Kroemer, A. C. Gossard, "(Al, Ga)Sb tilted superlattices," *Appl. Phys. Lett.* **57**, 1751 (1990).

[85] T. Fukui and H. Saito, "Step-flow growth and fractional-layer superlattices on (111)B GaAs vicinal surfaces," *J. Cryst. Growth* **107**, 231 (1991).

[86] M. S. Miller, C. E. Pryor, H. Weman, L. A. Samoska, H. Kroemer and P. M. Petroff, "Serpentine superlattice: concept and first results," *J. Cryst. Growth* **111**, 323 (1991).

[87] P. M. Petroff, M. S. Miller, Y. T. Lu, S. A. Chalmers, H. Metiu, H. Kroemer and A. C. Gossard, "MBE growth of tilted superlattices: advances and novel structures," *J. Cryst. Growth* **111**, 360 (1991).

[88] S. A. Chalmers, H. Kroemer and A. C. Gossard, "The growth of (Al, Ga)Sb tilted superlattices and their heteroepitaxy with InAs to form corrugated-barrier quantum wells," *J. Cryst. Growth* **111**, 647 (1991).

[89] H. Kanbe, A. Chavez-Pirson, H. Ando, H. Saito and T. Fukui, "Direct observation of optical anisotropy in a GaAs/AlAs quantum well wire array," *Appl. Phys. Lett.* **58**, 2969 (1991).

[90] H. Asai, S. Yamada and T. Fukui, "Narrow two-dimensional electron gas channels in GaAs/AlGaAs sidewall interfaces by selective growth," *Appl. Phys. Lett.* **51**, 1518 (1987).

[91] T. Fukui, S. Ando, Y. Tokura and T. Toriyama, "GaAs tetrahedral quantum dot structures fabricated using selective area metalorganic chemical vapor deposition," *Appl. Phys. Lett.* **58**, 2018 (1991).

[92] A. Doi, S. Iwai, T. Meguro and S. Namba, "A growth analysis for metalorganic vapor phase epitaxy of GaAs," *Jpn. J. Appl. Phys.* **27**, 795 (1988).

[93] M. Tsuda, M. Morishita, S. Oikawa and M. Mashita, "Epitaxial growth mechanism of the (100) As surface of GaAs – The effect of positive holes –," *Jpn. J. Appl. Phys.* **27**, L960 (1988).

[94] H. Sugiura, T. Yamada and R. Iga, "Mechanism of GaAs selective growth in Ar+ laser-assisted metalorganic molecular beam epitaxy," *Jpn. J. Appl. Phys.* **29**, L1 (1990).

[95] S. A. Hussien, A. A. Fahmy, N. A. El-Masry and S. M. Bedair, "A criterion for the suppression of plastic deformation in laser-assisted chemical vapor deposition of GaAs," *J. Appl. Phys.* **67**, 3853 (1990).

[96] A. N. Broers, W. W. Molzen, J. J. Cuomo, and N. D. Wittels, "Electron-beam fabrication of 80-Å metal structures," *Appl. Phys. Lett.* **29**, 596 (1976).

[97] S. Matsui and K. Mori, "New selective deposition technology by electron beam induced surface reaction," *J. Vac. Sci. Technol.* **B 4**, 299 (1986).

[98] L. Esaki and R. Tsu, "Superlattice and negative differential conductivity in semiconductor lasers," *IBM. J. Res. Develop.* **14**, 61 (1970).

[99] K. Uomi, N. Chinone, T. Ohtoshi and T. Kajimura, "High relaxation oscillation frequency (beyond 10 GHz) of GaAlAs multiplequantum well lasers," *Jpn. J. Appl. Phys.* **24**, L539 (1985).

[100] T. P. Pearsall, F. H. Pollak, J. C. Bean and R. Hull, "Electroreflectance spectroscopy of Si-Ge$_x$Si$_{1-x}$ quantum-well structures," *Phys. Rev.* **B 33**, 6821 (1986).

[101] M. -H. Meynadier, J. -L. Miguel, M. C. Tamargo and R. E. Nahory, "Optical investigations of the band structure of strained InAs/AlInAs quantum wells," *Appl. Phys. Lett.* **52**, 302 (1988).

[102] D. C. Bertolet, H. Jung-Kuei, S. H. Jones and Kei May Lau, "Pseudomorphic GaAs/InGaAs single quantum wells by

atmospheric pressure organometalic chemical vapor deposition," *Appl. Phys. Lett.* **52**, 293 (1988).

[103] M. -E. Pistol, M. R. Leys and L. Samuelson, "Properties of tin strained Ga(As, P) layers," *Phys. Rev.* **B 37**, 4664 (1988).

[104] E. Yablonovitch and E. O. Kane, "Band structure engineering of semiconductor lasers for optical communications," *J. Lightwave Technol.* **6**, 1292 (1988).

[105] M. -P. Houng and Y. -C. Chang, "Electronic structres of $In_{1-x}Ga_xAs$-InP strained-layer quantum wells," *J. Appl. Phys.* **65**, 3096 (1989).

[106] R. P. Schneider, Jr. and B. W. Wessels, "Optical properties of InAs/InP strained single quantum wells grown by organometallic vapor-phase epitaxy," *J. Appl. Phys.* **70**, 405 (1991).

[107] R. J. Warburton, R. J. Nicholas, L. K. Howard and M. T. Emeny, "Intraband and interband magneto-optics of p-type $In_{0.18}Ga_{0.82}As$/GaAs quantum wells," *Phys. Rev.* **B 43**, 14124 (1991).

[108] H. Banvillet, E. Gil, R. Cadoret, P. Disseix, K. Ferdjani, A. Vasson, A. M. Vasson, A. Tabata, T. Benyattou and G. Guillot, "Optical investigation in ultrathin InAs/InP quantum wells grown by hydride vapor-phase epitaxy," *J. Appl. Phys.* **70**, 1638 (1991).

[109] T. Hayakawa, M. Kondo, T. Suyama, K. Takahashi, S. Yamamoto and T. Hijikata, "Reduction in threshold

current density of quantum well lasers grown by molecular beam epitaxy on 0.5° misoriented (111)B substrates," *Jpn. J. Appl. Phys.* **26**, L302 (1987).

[110] T. Suyama, T. Hayakawa, M. Kondo, K. Takahashi, S. Yamamoto and T. Hijikata, "Near-ideal low-threshold current in (111)-oriented GaAs/AlGaAs quantum well lasers," *IEEE Electron Devices* **ED-34**, 2378 (1987).

[111] T. Hayakawa, M. Kondo, K. Morita, K. Takahashi, T. Suyama, S. Yamamoto and T. Hijikata, "Interface disorder in GaAs/AlGaAs quantum wells grown by molecular beam epitaxy on 0.5°-misoriented (111)B substrates," *Appl. Phys. Lett.* **51**, 1705 (1987).

[112] T. Hayakawa, T. Suyama, K. Takahashi, M. Kondo, S. Yamamoto and T. Hijikata, "Near-ideal low-threshold behavior in (111) oriented GaAs/AlGaAs quantum well lasers," *Appl. Phys. Lett.* **52**, 339 (1988).

[113] T. Hayakawa, K. Takahashi, M. Kondo, T. Suyama, S. Yamamoto and T. Hijikata, "Enhancement in optical transition in (111)-oriented GaAs-AlGaAs quantum well structures," *Phys. Rev. Lett.* **60**, 349 (1988).

[114] T. Hayakawa, K. Takahashi, T. Suyama, M. Kondo, S. Yamamoto and T. Hijikata, "Enhancement of heavy-hole-related excitonic optical transitions in (111)-oriented quantum wells," *Jpn. J. Appl. Phys.* **27**, L300 (1988).

[115] T. Hayakawa, M. Kondo, T. Suyama, K. Takahashi, S. Yamamoto and T. Hijikata, "Enhancement of the capture

rate of carriers in (111)-oriented GaAs/ AlGaAs quantum well structures," *Jpn. J. Appl. Phys.* **27**, L762 (1988).

[116] T. Hayakawa, K. Takahashi, T. Suyama, M. Kondo, S. Yamamoto and T. Hijikata, "High reliability in AlGaAs laser diodes prepared by molecular beam epitaxy on 0.5°-misoriented (111)B substrates," *Jpn. J. Appl. Phys.* **27**, L889 (1988).

[117] T. Hayakawa, K. Takahashi, S. Yamamoto and T. Hijikata, "Temperature dependence of photoluminescence properties in (111)- and (100)-oriented GaAs/AlGaAs quantum well structures," *Jpn. J. Appl. Phys.* **27**, L979 (1988).

[118] T. Hayakawa, K. Takahashi, M. Kondo, T. Suyama, S. Yamamoto and T. Hijikata, "Observation of the $2s$ state excitons in (111)-oriented GaAs/Al$_x$Ga$_{1-x}$As quantum-well structures," *Phys. Rev.* **B 38**, 1526 (1988).

[119] T. Hayakawa, T. Suyama, K. Takahashi, M. Kondo, S. Yamamoto and T. Hijikata, "Polarization-dependent gain-current relationship in (111)-oriented GaAs/AlGaAs quantum-well lasers," *J. Appl. Phys.* **64**, 297 (1988).

[120] W. Batty, U. Ekenberg, A. Ghiti, and E. P. O'Reilly, "Valence subband structure and optical gain of GaAs-AlGaAs (111) quantum wells," *Semicond. Sci. Technol.* **4**, 904 (1989).

[121] M. -P. Houng, Y. -C. Chang and W. I. Wang, "Orientation dependence of valence-subband structures in GaAs-

$Ga_{1-x}Al_xAs$ quantum-well structures," *J. Appl. Phys.* **64**, 4609 (1988).

[122] J. N. Schulman and T. C. Mcgill, "Electronic properties of the AlAs-GaAs (001) interface and superlattice," *Phys. Rev.* **B 19**, 6341 (1971).

[123] J. N. Schulman and Y. -C. Chang, "New method for calculating electronic properties of superlattices using complex band structures," *Phys. Rev.* **B 24**, 4445 (1981).

[124] Y. -C. Chang and J. N. Schulman, "Modification of optical properties of $GaAs$-$Ga_{1-x}Al_xAs$ superlattice due to band mixing," *Appl. Phys. Lett.* **43**, 536 (1983).

[125] J. N. Schulman and Y. -C. Chang, "Reduced Hamiltonian method for soling the tight-binding model of interface," *Phys. Rev.* **B 27**, 2346 (1983).

[126] J. N. Schulman and Y. -C. Chang, "Band mixing in semiconductor superlattices," *Phys. Rev.* **B 31**, 2056 (1985).

[127] Y. -C. Chang and J. N. Schulman, "Interband optical transitions in $GaAs$-$Ga_{1-x}Al_xAs$ and InAs-GaSb superlattices," *Phys. Rev.* **B 31**, 2069 (1985).

[128] J. N. Schulman and Y. -C. Chang, "HgTe-CdTe superlattice subband dispersion," *Phys. Rev.* **B 33**, 2594 (1986).

[129] J. N. Schulman, "$Ga_{1-x}Al_xAs$-$Ga_{1-y}Al_yAs$-GaAs double-barrier structures," *J. Appl. Phys.* **60**, 3954 (1986).

[130] M. Kumagai, T. Takagahara and E. Hanamura, "Optical properties and indirect-to-direct transition of GaP/AlP (001) superlattices," *Phys. Rev.* **B 37**, 989 (1988).

[131] Y. Arakawa, M. Nishioka, H. Sakaki, and H. Okamoto, "Spontaneous emission characteristics of quantum well lasers in string magnetic fields. An approach to quantum-well-box light source," *Jpn. J. Appl. Phys.* **22**, L804 (1983).

[132] K. Vahala, Y. Arakawa, and A. Yariv, "Reduction of the field spectrum linewidth of a multiple quantum well laser in a high magnetic field – spectral properties of quantum dot lasers," *Appl. Phys. Lett.* **50**, 365 (1987).

[133] T. T. J. M. Berendschot, H. A. J. M. Reinen, H. J. A. Bluyssen, C. Harder and H. P. Meier, "Wavelength and threshold current of a quantum well laser in a strong magnetic field," *Appl. Phys. Lett.* **54**, 1827 (1989).

[134] K. Uomi, T. Mishima and N. Chinone, "Ultrahigh relaxation oscillation frequency (up to 30 GHz) of highly p-doped GaAs/GaAlAs multiple quantum well lasers," *Appl. Phys. Lett.* **51**, 78 (1987).

[135] K. Vahala, "Quantum box fabrication torelance and size limits in semiconductors and their effect on optical gain," *IEEE J. Quantum Electron.* **24**, 523 (1988).

[136] D. J. Channin, "Effect of gain saturation on injection laser switching," *J. Appl. Phys.* **50**, 3858 (1979).

[137] M. J. Adams and M. Osinski, "Influence of spectral hole-burning on quanternary laser transients," *Electron. Lett.* **19**, 627 (1973).

[138] R. Olshansky, D. M. Fye, J. Manning and C. B. Su, "Effect of nonlinear gain on the bandwidth of semiconductor lasers," *Electron. Lett.* **21**, 721 (1985).

[139] G. P. Agrawal, "Effect of nonlinear gain on single-frequency behaviour of semiconductor lasers," *Electron. Lett.* **22**, 696 (1986).

[140] H. Nakajima and R. Frey, "Observation of bistable reflectivity of a phase-conjugated signal through intracavity nearly degenerate four-wave mixing," *Phys. Rev. Lett.* **54**, 1798 (1985).

[141] L. D. Westbrook, N. C. Fletcher, D. M. Cooper, M. Stevenson and P. C. Spurdens, "Intensity noise in 1.5 μm GaInAs quantum well buried heterostructure lasers," *Electron. Lett.* **25**, 1183 (1989).

[142] C. B. Su, V. Lanzisera and R. Olshansky, "Measurement of nonlinear gain from FM modulation index of InGaAsP lasers," *Electron. Lett.* **21**, 893 (1985).

[143] S. Tsuji, R. S. Vodhanel and M. M. Choy, "Measurements of the nonlinear damping factor in 1.5 μm distributed feedback lasers," *Appl. Phys. Lett.* **54**, 90 (1989).

[144] T. L. Koch and R. A. Linke, "Effect of nonlinear gain reduction on semiconductor laser wavelength chirping," *Appl. Phys. Lett.* **48**, 613 (1986).

[145] J. E. Bowers, B. R. Hemenway, A. L. Gnauck and D. P. Wilt, "High-speed InGaAsP Constricted-mesa lasers," *IEEE J. Quantum Electron.* **QE-22**, 833 (1986).

[146] G. P. Agrawal, "Gain nonlinearities in semiconductor lasers: Theory and aaplication to distributed feedback lasers," *IEEE J. Quantum Electron.* **QE-23**, 860 (1987)

[147] G. P. Agrawal, "Population pulsations and nondegenerate four-wave mixing in semiconductor lasers and amplifiers," *J. Opt. Soc. Am.* **B 5**, 147 (1988).

[148] G. P. Agrawal, "Spectral hole-burning and gain saturation in semiconductor lasers: Strong-signal theory," *J. Appl. Phys.* **63**, 1232 (1988).

[149] N. Ogasawara and R. Ito, "Longitudinal mode competition and asymmetric gain saturation in semiconductor injection lasers. II. Theory," *Jpn. J. Appl. Phys.* **27**, 615 (1988).

[150] G. P. Agrawal, "Intensity dependence of the linewidth enhancement factor and its implication for semiconductor lasers," *IEEE Photonics Technol. Lett.* **1**, 212 (1989).

[151] G. P. Agrawal, "Effect of gain nonlinearities on the dynamic response of single-mode semiconductor lasers," *IEEE Photonics Technol. Lett.* **1**, 419 (1989).

[152] K. Uomi and N. Chinone, "Proposal on reducing constant in semiconductor lasers by using quantum well structures," *Jpn. J. Appl. Phys.* **28**, L1424 (1989).

[153] M. Yamanishi and Y. Lee, "Phase dampings of optical dipole moments and gain spectra in semiconductor lasers," *IEEE J. Quantum Electron.* **QE-23**, 367 (1987).

[154] M. Asada, "Intraband relaxation time in quantum-well lasers," *IEEE J. Quantum Electron.* **25**, 2019 (1989).

Publication List

I. Technical Journals

[1] <u>T. Takahashi</u> and Y. Arakawa
"Theoretical Analysis of Gain and Dynamic Properties of Quantum-Well Box Lasers"
Optoelectronics -Devices and Technologies-, vol. 3, pp. 155-162, 1988.

[2] Y. Arakawa and <u>T. Takahashi</u>
"Effect of Nonlinear Gain on Modulation Dynamics in Quantum Well Lasers"
Electron. Lett., vol. 25, pp. 169-170, 1989.

[3] <u>T. Takahashi</u>, M. Nishioka and Y. Arakawa
"Differential Gain of GaAs/AlGaAs Quantum Well and Modulation-Doped Quantum Well Lasers"
Appl. Phys. Lett., vol. 58, pp. 4-6, 1991.

[4] <u>T. Takahashi</u> and Y. Arakawa
"Nonlinear Gain Effects on Spectral Dynamics in Quantum Well Lasers"
IEEE Photonics Technology Lett., vol. 3, pp. 106-107, 1991.

[5] <u>T. Takahashi</u>, J. N. Schulman and Y.Arakawa
"Dependence of Lasing Characteristics of Quantum Well Lasers on Substrate Orientation: Tight-Binding Theory"
Appl. Phys. Lett., vol. 58, pp. 881-883, 1991.

[6] T. Takahashi, Y. Arakawa and M. Nishioka

"*In-situ* Patterning of Contamination Resists in Metalorganic Chemical Vapor Deposition for Fabrication of Quantum Wires"

Appl. Phys. Lett., vol. 58, pp. 2372-2374, 1991.

[7] T. Takahashi and Y. Arakawa

"Nonlinear Gain Effects in Quantum Well, Quantum Well Wire, and Quantum Well Box Lasers"

IEEE J. Quantum Electron., vol. 27, pp. 1824-1829, 1991.

[8] T. Yamauchi, T. Takahashi and Y. Arakawa

"Tight-Binding Analysis for Quantum Wire Lasers and Quantum Wire Infrared Detectors"

IEEE J. Quantum Electron., vol. 27, pp. 1817-1823, 1991.

[9] Y. Arakawa and T. Takahashi

"Nonlinear Optical Effect in Quantum Well Lasers"

J. of Nonlinear Optics, vol. 1, pp. 141-148, 1991.

[10] T. Takahashi, Y. Arakawa, M. Nishioka and T. Ikoma

"Selective Growth of GaAs Wire Structures Using Electron Beam Induced Metalorganic Chemical Vapor Deposition"

Appl. Phys. Lett., vol. 60, January Issue, 1992.

II. Presentations

A. *International Conferences*

[1] Y. Arakawa, <u>T. Takahashi</u> and K. Vahala

"Lasing Properties of Semiconductor Lasers with Quantum-Well Box Structures"

XVI International Conference on Quantum Electronics, Tokyo, July 1988.

[2] Y. Arakawa and <u>T. Takahashi</u>

"Nonlinear Gain Effect and Modulation Dynamics in Quantum Well Lasers"

Conference on Lasers and Electro-Optics, Baltimore, April 1989.

[3] <u>T. Takahashi</u> and Y. Arakawa

"Lasing Properties of Quantum Box Lasers"

Second Regional Symposium on Optoelectronics, Jakarta, 1989.

[4] <u>T. Takahashi</u>, J. N. Schulman and Y. Arakawa

"Orientation Dependence of Lasing Properties in Quantum Well Lasers: Theoretical Analysis"

Advanced Processing and Characterization Technologies, Tokyo, October 1989.

[5] T. Takahashi and Y. Arakawa

"Nonlinear Gain Effects in Quantum Well Wire and Box Lasers"

Conference on Lasers and Electro-optics, Anaheim, May 1990.

[6] T. Takahashi, J. N. Schulman and Y. Arakawa

"Substrate-Orientation Dependence of Lasing Properties in Quantum Well Lasers"

International Quantum Electronics Conference, Anaheim, May 1990.

[7] T. Takahashi, Y. Arakawa, M. Nishioka and T. Ikoma

"Selective growth by Electron Beam Induced MOCVD for Quantum Microstructures"

International Conference on Solid State Devices and Materials, Sendai, August 1990.

[8] T. Takahashi and Y. Arakawa

"Theoretical Analysis of Nonlinear Gain Effects in InGaAsP/InP Quantum Well Lasers"

International Semiconductor Laser Conference, Davos, September 1990.

[9] T. Takahashi, Y. Arakawa, M. Nishioka and T. Ikoma

"A Novel Selective Growth Technology for Quantum Microstructure Fabrication: Electron Beam Induced MOCVD"

Fall Meeting of Materials Research Society, Boston, November 1990.

[10] T. Takahashi, Y. Arakawa, M. Nishioka and T. Ikoma
"Electron Beam Induced Selective Growth for GaAs Wires
and Dots"
*International Workshop on Science and Technology for
Surface Reaction Process*, Tokyo, January 1992.

B. Domestic Conferences (in Japanese)

[1] <u>T. Takahashi</u> and Y. Arakawa

"Analysis of Dynamics and Spectral Properties of Quantum Well Box Lasers"

The 48th Autumn Meeting, 1987; The Japan Society of Applied Physics, Nagoya, October 1987.

[2] <u>T. Takahashi</u>, Y. Arakawa and M. Nishioka

"Differential Gain Properties of Quantum Well Lasers"

The 49th Autumn Meeting, 1988; The Japan Society of Applied Physics, Toyama, October 1988.

[3] <u>T. Takahashi</u> and Y. Arakawa

"Nonlinear Gain Properties of Quantum Well Lasers"

The 49th Autumn Meeting, 1988; The Japan Society of Applied Physics, Toyama, October 1988.

[4] <u>T. Takahashi</u> and Y. Arakawa

"Nonlinear Gain Properties of Quantum Well Wire and Box Lasers"

The 36th Spring Meeting, 1989; The Japan Society of Applied Physics and Related Societies, Chiba, April 1989.

[5] <u>T. Takahashi</u>, J. N. Schulman and Y. Arakawa

"Orientation Dependence of Lasing Properties in Quantum Well Lasers"

The 50th Autumn Meeting, 1989; The Japan Society of Applied Physics, Fukuoka, September 1989.

[6] T. Takahashi, Y. Arakawa, M. Nishioka and T. Ikoma
"Fabrication of Semiconductor Microstructures by Electron Beam Induced MOCVD System"
The 37th Spring Meeting, 1990; The Japan Society of Applied Physics and Related Societies, Asaka, May 1990.

[7] T. Takahashi and Y. Arakawa
"Nonlinear Gain Properties in InGaAsP/InP Quantum Well Lasers"
The 51st Autumn Meeting, 1990; The Japan Society of Applied Physics, Morioka, September 1990.

[8] T. Takahashi, Y. Arakawa, M. Nishioka and T. Ikoma
"Selective Growth by EBI-MOCVD for Semiconductor Microstructures"
The 51st Autumn Meeting, 1990; The Japan Society of Applied Physics, Morioka, September 1990.

[9] T. Takahashi, Y. Arakawa, M. Nishioka and T. Ikoma
"Selective Growth of a GaAs Wire Structure Using EBI-MOCVD"
The 52nd Autumn Meeting, 1991; The Japan Society of Applied Physics, Okayama, October 1991.